# The study of lignin valorization by Lipomyces starkeyi as a microbial platform for the production of value-added biochemicals

PUTRA, FILEMON JALU NUSANTARA

(Degree)
博士（工学）

(Date of Degree)
2024-09-25

(Date of Publication)
2025-09-01

(Resource Type)
doctoral thesis

(Report Number)
甲第9024号

(URL)
https://hdl.handle.net/20.500.14094/0100492533

# Doctoral Dissertation

## The study of lignin valorization by *Lipomyces starkeyi* as a microbial platform for the production of value-added biochemicals

付加価値のある生化学物質の生産のための微生物プラットフォームとしてのリポミセス・スターケイによるリグニンの価値化の研究

July 2024

Department of Chemical Science and Engineering

Graduate School of Engineering

Kobe University

FILEMON JALU NUSANTARA PUTRA

## Preface

This dissertation represents the culmination of two and half years of research, exploration, and dedication. Throughout this journey, I have been fortunate to receive guidance, support, and inspiration from a multitude of sources, without which this work would not have been possible. The inception of this dissertation can be traced back to the motivation to be a better individual for others and the environment. From that moment, I embarked on a quest to delve deeper into the realms of biorefinery and biomass valorization. What ensued was an intellectually stimulating journey filled with challenges, breakthroughs, and moments of enlightenment. I am deeply indebted to my supervisor, Professor Chiaki Ogino, Professor Prihardi Kahar, and Professor Akihiko Kondo whose unwavering guidance, encouragement, and expertise have been instrumental in shaping the direction of this research. Their insightful feedback, constructive criticism, and invaluable support have pushed me to strive for excellence and to explore new avenues of inquiry. Furthermore, I am grateful to The Ministry of Education, Culture, Sports, Science and Technology for supporting my study. Their support provided me with the necessary resources and infrastructure to conduct my research effectively. I also extend my heartfelt appreciation to my committee members, Professor Takashi Nishino and Professor Hideki Yamaji, for their invaluable feedback, suggestions, and scholarly insights throughout the dissertation and evaluation process. Their expertise and constructive criticism have greatly enriched the quality of this work. I would also like to acknowledge the contributions of my family, friends, and all of the lab members who

have supported me emotionally and intellectually throughout this journey. Their encouragement, understanding, and belief in my abilities have been a constant source of motivation. Finally, I dedicate this dissertation to my beloved wife, Manti, and my son, Sena, whose influence, support, and inspiration have played a significant role in shaping my academic journey. This dissertation represents not only the culmination of years of dedicated research but also the beginning of a new chapter in my academic and professional journey. It is my sincere hope that this work contributes meaningfully to the field of lignin valorization or even biomass utilization in the biorefinery field and inspires future generations of researchers to continue pushing the boundaries of knowledge.

Filemon Jalu Nusantara Putra

May 28th, 2024

# TABLE OF CONTENTS

## List of abbreviations

| | |
|---|---|
| ALE: | Adaptive laboratory evolution. |
| ATR-FTIR: | Attenuated total reflectance fourier transform infrared spectrometry. |
| C:N: | Carbon to nitrogen. |
| DCW: | Dry cell weight. |
| GC/MS: | Gas chromatography coupled mass spectrometry. |
| HPLC/RID: | High-performance liquid chromatography refractive index detector. |
| HPLC/UV-Vis: | High-performance liquid chromatography ultraviolet-visible spectrometry. |
| M/Z: | Mass to charge. |
| NMM-: | Nitrogen-limited mineral media. |
| OD: | Optical density. |
| OPEFB: | Oil palm empty fruit bunch. |

## List of tables and figures

**Fig. 7** Tolerance of *L. starkeyi* NBRC 10381 to lignin derivative aldehydes. Closed bars represent 4-hydroxybenzaldehyde, shaded bars represent vanillin, and open bars represent syringaldehyde. The results showed the average of three replicates of the biological samples with error bars representing the standard deviation from the mean value. *Statistical analysis was performed using Student's t test ($p$ value <0.05).

**Fig. 8** Different lignin derivative fermentation profiles of *L. starkeyi* NBRC 10831. (a) Time courses for carbon source consumption (closed circles) and cell growth (closed triangles) in YMPG medium with different lignin aldehydes. (b) Biodegradation of lignin aldehydes (closed squares) into their alcohol (opened circles) and acid derivatives (opened triangles). (c) Growth, glucose consumption, and lignin depletion rates in the fermentation of 4-hydroxybenzaldehyde (closed bars), vanillin (shaded bars), and syringaldehyde (opened bars) at the logarithmic phase. The results show the average of three replicates of the biological samples with error bars representing the standard deviation from the mean value.

**Fig. 9** ATR-FTIR spectra analysis of lignin derivative alcohols. FTIR spectra were recorded on a Bruker Alpha with ATR (attenuated total reflectance) attachment and reported in wavenumbers ($cm^{-1}$).

**Fig. 10** Different lignin derivative alcohols fermentation profiles of *L. starkeyi* NBRC 10831. (a) Time courses for carbon source consumption (closed circles) and cell growth (closed triangles) in YMPG medium with different lignin alcohols. (b) Lignin aldehydes (closed squares), lignin alcohol (opened circles), and acid derivatives (opened triangles). The results show the average of three replicates of the biological samples with error bars representing the standard deviation from the mean value.

**Fig. 11** Metabolic pathway for lignin monomers and their gene expression. (a) Metabolic pathway for lignin derivative aldehydes into derivative alcohols via *L. starkeyi* NBRC 10381. (b) Quantitative gene expression of *L. starkeyi* NBRC 10381 in the cultivation in lignin derivative aldehydes, namely, 4-hydroxybenzaldehyde (closed bars), vanillin (shaded bars), and syringaldehyde (opened bars). ADH, alcohol dehydrogenase; AKR, aldehyde-ketone reductase; ALDH, aldehyde dehydrogenase. $Log_2$ FC (fold change) represents transcriptional genes compared to the expression level of the TUB1 gene as a housekeeping gene. The results show the average of three replicates of the biological samples with error bars representing the standard deviation from the mean value. *Statistical analysis was performed using Student's t test ($p$ value <0.05).

**Fig. 12** Profiles of fatty acids produced during fermentation of different lignin derivative aldehydes. 4-hydroxybenzaldehyde (closed bars), vanillin (shaded bars), syringaldehyde (opened bars), and control (dotted bars). The results show the average of three replicates of the biological samples with error bars representing the standard deviation from the mean value.

**Fig. 13** Mixed lignin derivative aldehyde fermentation profile of *L. starkeyi* NBRC 10831. (a) Time courses for carbon source consumption (closed circles) and cell growth (closed triangles) under different fermentation conditions. (b) Biodegradation of mixed lignin aldehydes (4-hydroxybenzaldehyde (closed squares), vanillin (closed circles), syringaldehyde (closed triangles)) into their alcohol (4-hydroxybenzyl alcohol (shaded squares), vanillyl alcohol (shaded circles), syringyl alcohol (shaded triangles)), and acid derivative ((4-hydroxybenzoic acid (opened squares), vanillic acid (opened circles), syringic acid (opened triangles)). The results show the average of three replicates of the

biological samples with error bars representing the standard deviation from the mean value.

**Fig. 14** Profiles of fatty acids produced on mixed lignin derivative aldehydes and single-cell oil visualization. (a) Fatty acid profiles under different fermentation conditions. Low $OD_{600}$ YMPG (opened bars), high $OD_{600}$ YMPG (shaded bars), and high $OD_{600}$ NMM (closed bars). The results show the average of three replicates of the biological samples with error bars representing the standard deviation from the mean value. (b) Bodipy lipid visualization of *L. starkeyi* NBRC 10381.

**Fig. 15** Graphical abstract of study chapter 3.

**Fig. 16** Pathway of combinatory strategy for lignin monomeric alcohols and lipid production from OPEFB using alkaline nitrobenzene oxidation and bioconversion of *Lipomyces starkeyi.*

**Fig. 17** The workflow of lignin monomeric productions via alkaline nitrobenzene oxidative depolymerization from oil palm empty fruit bunch.

**Fig. 18** Effect of sodium hydroxide concentration and reaction time on the titer of (a) lignin monomeric aldehydes, (b) lignin monomeric acids, and (c) hydroxycinnamic acids productions. The results presented the mean of three biological replicate samples with error bars illustrating the standard deviation from the mean value in the dataset.

**Fig. 19** Fermentation profiles of *L. starkeyi* under different mediums. (a) Time courses for cell growth and glucose consumption in different mediums. (b) Growth and glucose consumption rates in different medium fermentation. The results presented the mean of three biological replicate samples with error bars illustrating the standard deviation from

the mean value in the dataset. *The statistical analysis employed Student's t-test, with significance set at a p-value < 0.05.

**Fig. 20** Biodegradation of lignin monomeric aldehydes into monomeric alcohols during fermentation. (a) Aldehydes (monomeric aldehydes-only). (b) Aldehydes-acids (monomeric aldehydes and monomeric acids). (c) OPEFB (all lignin monomeric derivatives from OPEFB). The results presented the mean of three biological replicate samples with error bars illustrating the standard deviation from the mean value in the dataset.

**Fig. 21** Depletion of hydroxycinnamic acids in OPEFB during fermentation. The results presented the mean of three biological replicate samples with error bars illustrating the standard deviation from the mean value in the dataset.

**Fig. 22** Fatty acids profiles produced during the fermentation of different mediums. (a) Percentage of major FAME in the lipids. (b) Percentage of minor FAME in the lipids. The results presented the mean of three biological replicate samples with error bars illustrating the standard deviation from the mean value in the dataset.

**Fig. 23** Fermentation profile of DALE-22 and WT in the 22 mM concentration of syringaldehyde. (a) Growth curve and glucose consumption. (b) Syringaldehyde conversion and syringyl alcohol production. (c) Lipid content. The results presented the mean of three biological replicate samples with error bars illustrating the standard deviation from the mean value in the dataset.

**Fig. 24** Fermentation profile of DALE-22 and WT in the 4 mM concentration of syringaldehyde. (a) Growth curve and glucose consumption. (b) Syringaldehyde

conversion and syringyl alcohol production. (c) Lipid content. The results presented the mean of three biological replicate samples with error bars illustrating the standard deviation from the mean value in the dataset.

**Fig. 25** Profiles of fatty acids produced during the fermentation of DALE-22 and WT in 4 mM concentration of syringaldehyde. (a) Major fatty acid percentage in lipids. (b) Minor fatty acid percentage in lipids. The data displayed represents the average of three biological replicate samples, with error bars showing the standard deviation from the mean.

**Fig. 26** Principal component analysis (PCA) of the DALE-22 and WT. (a) Score plot. (b) Loading plot. (c) Total metabolites detected. The results presented the mean of three biological replicate samples with error bars illustrating the standard deviation from the mean value in the dataset.

**Fig. 27** The volcano plots illustrate the distinct metabolites in DALE-22 in comparison to WT. The x-axis represents the binary logarithm of fold changes, while the y-axis represents the negative common logarithm of the p-value derived from pairwise student t-tests.

**Fig. 28** Relative quantification of significantly correlated metabolites performed by GC/MS of DALE-22 (blue) and WT (orange). (a) Stress response and protective molecules. (b) Osmolytes and cellular water balance. (c) Amino acid breakdown and by-products. The results presented the mean of three biological replicate samples with error bars illustrating the standard deviation from the mean value in the dataset.

## Synopsis

### Chapter 1

Lignin, being the third most prevalent biopolymer after cellulose and hemicellulose, has significant potential as a replacement for petroleum-based products. Nevertheless, the process of effectively and practically extracting value from lignin is still rather difficult. This review focuses on recent studies that explore the utilization of yeast to convert lignin into valuable products, including single-cell oils (SCOs), enzymes, and other chemical compounds. While previous studies have also investigated the potential of microorganisms for lignin valorization, this study specifically highlights the use of yeast in this process. Yeasts have been discovered to be a feasible option for the biological transformation of lignin and could offer useful insights for future studies aiming to create a yeast strain capable of producing additional valuable chemical compounds from lignin.

### Chapter 2

Lignin holds significant promise as a viable alternative to conventional petroleum-derived products. Recently, there has been a growing interest in the biological conversion of lignin into various value-added products, as it offers considerable potential for supporting future bioeconomic endeavors. The oleaginous yeast *Lipomyces starkeyi* is particularly noteworthy due to its inherent capability to tolerate and metabolize diverse lignin monomer derivatives, along with its capacity to produce single-cell oil (lipids) within its cells. In this investigation, we explored the concurrent abilities of lignin monomer metabolism and lipid biosynthesis in *L. starkeyi*. We successfully converted three representative lignin derivative aldehydes namely, 4-hydroxybenzaldehyde (H-lignin),

vanillin (G-lignin), and syringaldehyde (S-lignin) into their corresponding alcohol forms (4-hydroxybenzyl alcohol, vanillyl alcohol, and syringyl alcohol, respectively), without generating undesirable byproducts. Furthermore, each alcohol form was maintained throughout the cultivation process. Notably, doubling the concentration of syringaldehyde in individual lignin fermentation led to enhanced cell growth (17.01 g $L^{-1}$) and lipid accumulation (30.72% (w/w)). However, simultaneous fermentation of all lignin aldehydes resulted in significant inhibition of cell growth. Consequently, employing combined fermentation strategies involving a high initial inoculum size and utilizing a medium with a high C:N ratio proved advantageous in improving fermentation duration and increasing lipid production by up to 2.6-fold. Overall, this study offers a pioneering perspective on the production of lignin alcohols and lipids from lignin derivative aldehydes through the utilization of *L. starkeyi*.

**Chapter 3**

Efficiently transforming lignocellulosic biomass into valuable chemicals is crucial for advancing sustainable practices in the bioeconomy. This study centers on a novel two-step process aimed at converting oil palm empty fruit bunch (OPEFB) into lignin monomeric alcohols and lipids. The process involves alkaline nitrobenzene depolymerization followed by bioconversion using *Lipomyces starkeyi*. Initially, OPEFB undergoes alkaline nitrobenzene depolymerization to break down complex lignin structures into monomeric aldehydes. These derivatives then serve as substrates for bioconversion by *L. starkeyi*, which efficiently metabolizes lignin-derived compounds into higher-value lignin monomeric alcohols (syringyl, vanillyl, and 4-hydroxybenzyl

alcohol) and lipids concurrently. The study outlines the optimization of depolymerization conditions, including sodium hydroxide concentration, nitrobenzene effect, and reaction time, to maximize the yield of depolymerized lignin suitable for bioconversion. Subsequently, the bioconversion process involving cell growth, lipid production, and fatty acid profiles in various fermentations by *L. starkeyi* was investigated. The highest concentrations of syringaldehyde and vanillin obtained were up to 4.81 mM and 0.64 mM, respectively. The process successfully yielded 3.57 mM and 0.40 mM of syringyl alcohol and vanillyl alcohol, respectively, with a lipid titer of 5.86 g $L^{-1}$. This study underscores the potential of the integrated approach to convert OPEFB into valuable lignin-derived biochemicals and lipids, thereby contributing to the efficient utilization of biomass through alternative strategies.

**Chapter 4**

In this study, we employed an adaptive laboratory evolution (ALE) approach coupled with untargeted metabolomics analysis to enhance the production of lignin derivative alcohols and lipids from its monomeric aldehydes using *Lipomyces starkeyi*. Lignin, a major component of plant biomass, offers a promising feedstock for biofuel and lipid production. However, efficient conversion of lignin-derived compounds into high-value products remains a challenge. Here, we subjected *L. starkeyi* to flask serial passaging under selective pressure to adapt to syringaldehyde as lignin monomeric aldehyde. Through ALE, we achieved significant improvements in the production of lignin-derivative alcohols and lipids compared to the wild-type strain. Furthermore, untargeted metabolomics analysis revealed metabolic pathways and key metabolites associated with

enhanced lignin conversion. Our findings shed light on the adaptive mechanisms of *L. starkeyi* in utilizing lignin-derived substrates and provide valuable insights for metabolic engineering strategies aimed at enhancing lignin valorization for sustainable biorefinery applications.

**Chapter 5**

In this chapter, we share the general conclusion from this study, starting from chapter 2 to chapter 4. We pointed out the future direction of the next work regarding the lignin valorization and described the important aspects to be considered.

# Chapter 1

## Introduction

### 1.1 Lignin structure and properties

Lignin, a natural macromolecule, consists of complex arrangements of methoxy groups, phenolic hydroxyl groups, and a small number of terminal aldehyde groups. The functional groups are connected to an intricate network of phenylpropanoid units, which are the basic components of lignin [1]. The three primary phenylpropanoids found in lignin are *p*-hydroxyphenyl (H), guaiacyl (G), and syringyl (S). These types are differentiated by the level of methoxylation on their aromatic rings, as shown in Figure 1 [2]. The phenylpropanoid units found in lignin contain aromatic rings that contribute to its antioxidant action [3]. The monolignols undergo random coupling through different connections, resulting in a wide range of C-O-C and C-C linkages. The links consist of α-O-4, β-O-4, 4-O-5 (C-O-C), and β-β, β-1, β-5, 5-5 (C-C) [4,5]. β-O-4 is the main component responsible for the three-dimensional structure of lignin, making up to 50% of all linkages [6,7]. In contrast to cellulose and hemicellulose, which can be easily broken down into sugars [8], lignin, which is highly polymerized, has a stiff structure that is resistant to chemical pretreatment [8]. Breaking the β-O-4 bond has been a key objective in techniques aimed at breaking down lignin. The origin of biomass significantly impacts the arrangement and makeup of lignin. Softwood lignin mostly consists of G units, making up 80-90% of its composition. Hardwood lignin, on the other hand, is a combination of G units (25-50%) and S units (50-70%). Grass lignin is a mixture of G units (25-50%), H units (10-25%), and S units (25-50%) [6,9]. Consistently, lignin with a high content of S/G

(syringyl/guaiacyl) units is favored in biorefining applications to maximize the production of monomers. This is because S/G-rich lignin has the capacity to minimize the formation of unreactive C-C bonds, which can result in the development of condensed lignin that is not desirable during the process of lignin depolymerization. The presence of a high amount of G and a low amount of S in lignin might result in an increase in β-O-4 linkages, which in turn leads to the formation of easily recombining monomers during fractionation [10,11]. Comprehending the structure of lignin and finding its original connections are crucial for effectively converting it into renewable fuels, minerals, or chemicals (Figure 2).

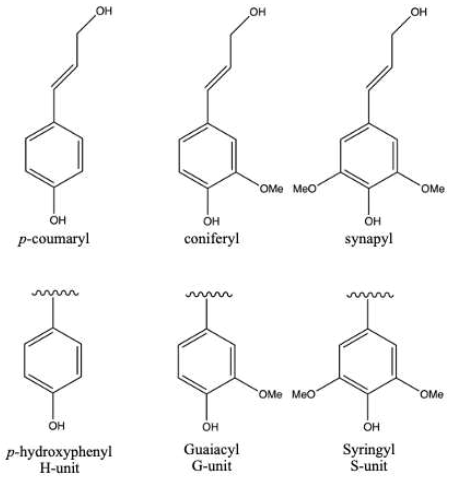


**Fig. 1** Relative structures of group units of lignin.

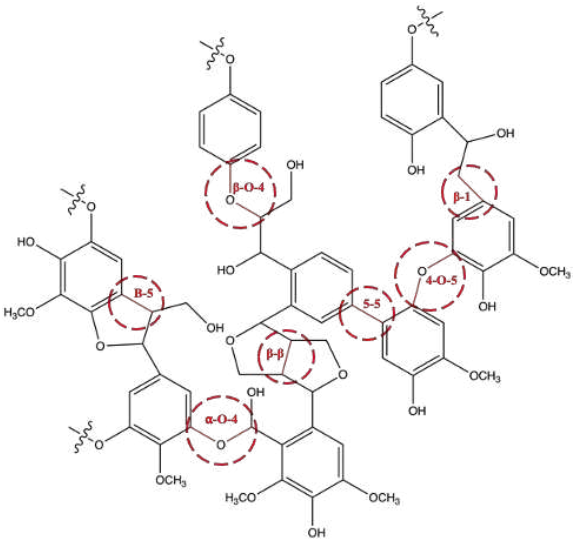


**Fig. 2** Lignin polymer structure and its main linkages.

### 1.2 Valorization of lignin and its derivatives by yeast

Over the past ten years, microorganisms have generated biofuels and valuable substances such as lipids, vanillin, pyrogallol, cis, cis-mucoid acid, lactate, succinate, ferulate, pyridine, and biopolymers (PHAs, monolignols) from lignin and its derivatives [12–17]. The degradation of lignin is the first stage in the production of biofuels and biomaterials. Enzymatic degradation, particularly by microbes, is crucial for acquiring the chemicals necessary for lignin usage. This process has the potential to become a promising and environmentally benign technology in the near future. Microorganisms such as fungi, bacteria, and yeasts have the ability to create many enzymes that can degrade lignin, including laccases, lignin peroxidases, manganese peroxidases, multifunctional peroxidases, and dye-decolorizing peroxidases [18]. There have been reports in recent years about the development of strains and their use as enzymes that can break down lignin [19]. Lignin valorization specific to this study is shown in Fig. 3. In producing lignin derivative alcohols and lipids simultaneously [20].

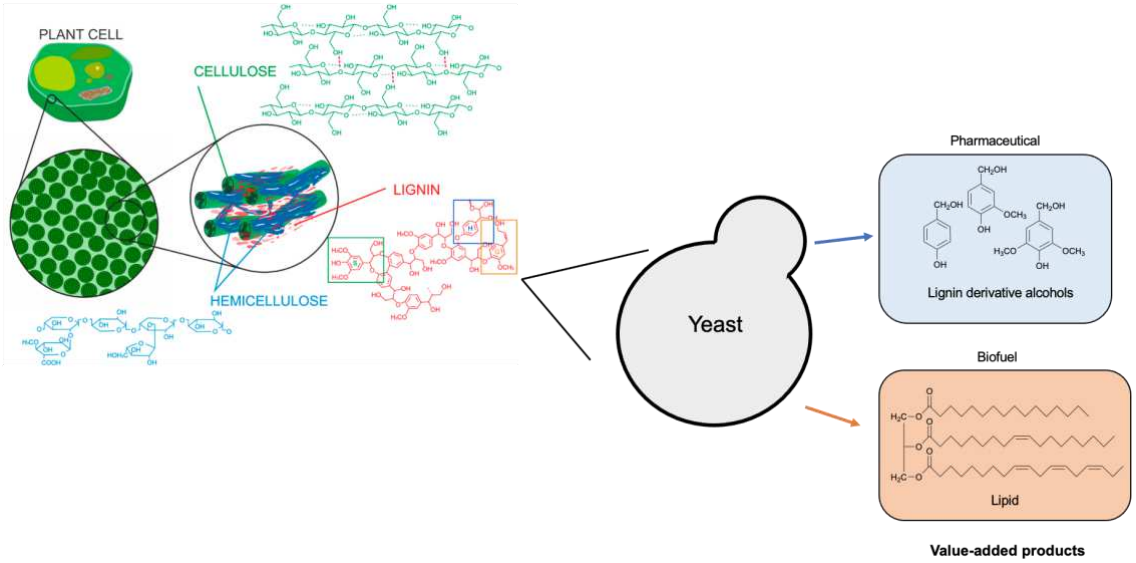


**Fig. 3** Lignin valorization by yeast to produce valuable products.

### 1.2.1 Lipids

A multitude of research have specifically investigated the generation of lipids, known as single-cell oils (SCOs), by microbes [21]. SCOs are classified as the third generation of biofuels. Research has been conducted on many microorganisms, including bacteria, microalgae, fungi, and yeast, that have the ability to metabolize lipids [22]. The majority of model microorganisms known to acquire lipids from lignin and its derivatives are bacteria. The metabolism of lignin by *Rhodococcus opacus* and *R. rhodochrous* has been extensively studied [23,24]. Microbial metabolism, particularly that of yeast, is noteworthy for its capacity to effectively process many aromatic chemicals due to its high cell tolerance [25]. In the future, it may be able to produce biofuels and other chemicals on a large scale by converting aromatic molecules into fatty acids. This process might utilize lignin and its derivatives as raw materials [26]. Trichosporon has attracted considerable interest in

recent years because of its capacity to generate significant amounts of lipids using lignocellulosic substrates and its great resistance to different lignocellulosic inhibitors [27–30]. The capacity of Trichosporon to thrive on lignin derivatives was examined using *T. cutaneum*. The yeast strain *T. cutaneum* ACCC 20271 has been observed to thrive on phenolic aldehydes produced from lignin, including 4-hydroxybenzaldehyde, vanillin, and syringaldehyde. Studies have demonstrated that *T. cutaneum* has superior tolerance to 4-hydroxybenzaldehyde at a concentration of 1.5 g/L, in comparison to vanillin at 0.1 g $L^{-1}$ and syringaldehyde at 0.5 g $L^{-1}$. During the fermentation process, it was discovered that 4-hydroxybenzaldehyde, which is a kind of p-hydroxyphenyl or H lignin, can be effectively used as a substrate for *T. cutaneum* to produce lipids. The lipid production yield was measured to be 16.6% or 0.85 g $L^{-1}$. Simultaneously, the remaining phenolic aldehydes, namely vanillin and syringaldehyde, underwent conversion into alcohols and acids. Next, the aldehyde dehydrogenases of *T. cutaneum* convert 4-hydroxybenzaldehyde into 4-hydroxybenzoate. Subsequently, it is transformed into protocatechuate by dioxygenases using oxygen as the substrate. The conversion of proto-catechuate occurs through the β-ketoadipate pathway, resulting in the production of acetyl-CoA and succinyl-CoA. Acetyl-CoA is either immediately employed for lipid synthesis or first incorporated into the TCA cycle and then utilized as the primary precursor for lipid synthesis [31]. *T. cutaneum* ACCC 20271 and MP11 stains were found to tolerate 4-hydroxybenzaldehyde (0.8 g $L^{-1}$), 4-hydroxy-3-methoxybenzaldehyde (0.8 g $L^{-1}$), and syringaldehyde (0.6 g $L^{-1}$) in wheat straw hydrolysate. These aldehydes were biodegraded by the stains, resulting in sufficient cell growth and a lipid accumulation of 40.87% [32]. *T. oleaginosus*, a species belonging to the

Trichosporon genus, has been documented to amass lipids on various aromatic chemicals, including 4-hydroxybenzoic acid, phenol, and resorcinol. *T. oleaginosus* ATCC 20509 exhibits the ability to withstand and process aromatic substrates through the use of ortho-cleavage aromatic metabolism pathways. Subsequently, the feeding strategy of *T. oleaginosus* in resorcinol using the fed-batch method resulted in a lipid synthesis of 69.5% (1.64 g $L^{-1}$) [33]. Several oily yeast species have shown the capability to break down lignin aromatic molecules. The oily red yeast *Rhodotorula toruloides* has the ability to metabolize *p*-coumaric acid, ferulic acid, vanillic acid, and 4-hydroxybenzoic acid [34]. *Lipomyces starkeyi* has garnered considerable interest as a producer of single cell oils (SCOs) because of its capacity to accumulate lipids in nitrogen-limited mineral medium, reaching amounts as high as 70%. The study also demonstrated the capacity to decrease lignin derivatives, such as syringaldehyde and vanillin [35]. Another species of the Cutaneotrichosporon genus, specifically *C. guehoae*, was shown to use 4-hydroxybenzoic acid as its exclusive source of carbon [36]. Nevertheless, the aforementioned research failed to provide a clear depiction of the relationship between lipid synthesis and the specific yeasts involved.

### 1.2.2 Lignin degrading enzymes

Enzymes play a crucial role in converting lignin into its derivatives or aromatic monomers, which serve as the fundamental components for creating important chemical products. Researchers are now investigating the manufacture of appropriate enzymes [37]. Enzymes that may break down lignin were first found approximately a century ago in a type of fungus called Basidiomycota, specifically in a species

called *Phanerochaete chrysporium*. These enzymes, known as peroxidases and laccases, were discovered in a plant called *Rhus vernicifera* [38]. Subsequently, a number of enzymes capable of breaking down lignin were discovered in fungi and bacteria [39,40]. Lignin-degrading enzymes can be categorized into two classes, namely laccases and peroxidases [41] (Fig. 4). These enzymes are utilized in vitro for the purpose of breaking down lignin and its derivatives. Utilizing in vitro enzymatic conversion offers advantages compared to directed-cell lignin conversion. For instance, it can enhance the interaction between the substrate and enzyme, decrease the time required for cultivation, and improve the imbalance of ATP/NAD(P)H [42]. However, yeast also has a significant function in producing enzymes that can degrade lignin. Various yeasts, including *Saccharomyces cerevisiae*, *Yarrowia lipolytica*, *Pichia pastoris*, *Pichia methalonica*, *Kluyveromyces lactic*, *Kluyveromyces maxianus*, and *Cryptococcus* sp., have been effectively utilized to produce laccases and peroxidases. This is achieved by introducing genes from external sources, not only from fungus-like Ascomycota and Basidiomycota divisions, but also from plants like oomycote and bacteria [43]. Yeast offers several benefits for enzyme synthesis, including as convenient cell handling, cost-effective substrate for cultivation, fast growth, efficient genetic manipulation, and the ability of cells to modify proteins by glycosylation, proteolytic, or disulfide mechanisms [44–46].

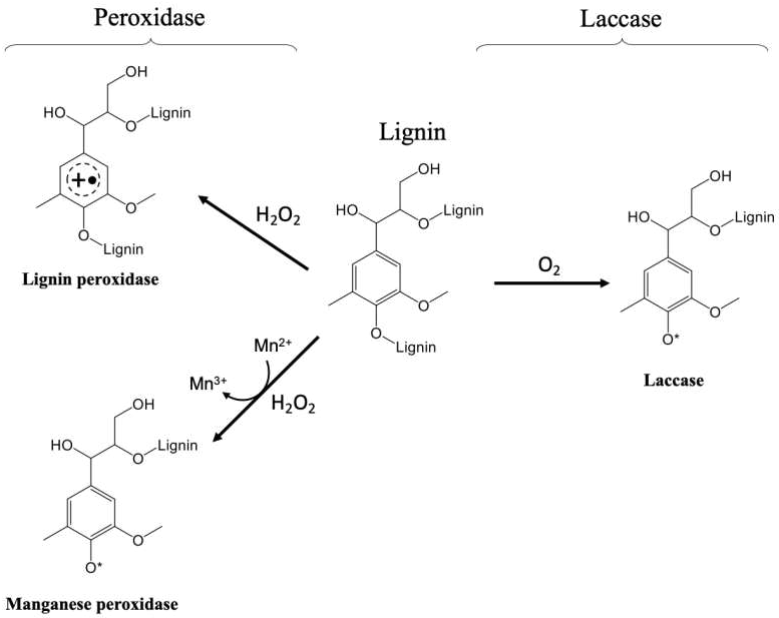


**Fig. 4** Classification of lignin-degrading enzymes.

### 1.2.3 Other value-added products

Having a high tolerance to various chemicals generated from lignin can be advantageous in studies focused on the valorization of lignin [47]. The mechanism of funneling pathways (metha- and ortho-cleavages) has demonstrated the potential of yeasts to transform lignin-derived molecules into other chemicals [48]. According to reports, *Trichosporon guehoae* converts ferulic acid into vanillic acid through fermentation [36]. *T. cutaneum*, a different strain of yeast, demonstrated the capacity to transform lignin aldehyde compounds, specifically syringaldehyde (2 g $L^{-1}$) and vanillin (2 g $L^{-1}$), into their corresponding acids (vanillic acid and syringic acid) and alcohols (syringyl alcohol and vanillyl alcohol) [31]. Several investigations have demonstrated the pharmacological usefulness of vanillic and syringic acid, showcasing their anti-inflammatory, anti-microbial, and anti-cancer properties [49].

Moreover, vanillyl alcohol has potential use in the management of Parkinson's disease [50].

### 1.3 Oxidative depolymerization of lignin

Understanding the mechanisms of lignin oxidation is essential for maximizing its conversion into useful chemical compounds. The oxidation depolymerization of lignin from LB is advantageous for the production of diverse useful aromatic compounds, such as aromatic derivative monomeric aldehydes, aromatic acids, and carboxylic acids. The oxidation process yields useful molecules, specifically *p*-hydroxybenzaldehyde, vanillin, and syringaldehyde, which are lignin derivative aldehydes. The oxidation depolymerization of lignin leads to the breaking of many chemical connections, including the C-C bond, C-O-C bond, aromatic rings, β-O-4 bonds of lignin, and other linkages. This process involves the use of oxidizing agents such as hydrogen peroxide ($H_2O_2$), oxygen (O), nitrobenzene, chlorine oxide, or metal oxides [51–53]. Oxidants such as $H_2O_2$ and $O_2$ trigger several reaction pathways through radical and electrophilic substitution in an alkaline environment. Both pathways produce comparable products, including *p*-hydroxybenzaldehyde, syringaldehyde, and vanillin as individual aldehydes, as well as *p*-hydroxybenzoic acid, vanillic acid, and syringic acid as individual acids. Alkaline conditions promote deprotonation and the formation of phenoxy radicals [54,55]. Oxidative depolymerization often utilizes an alkaline solvent. Phenolic compounds undergo deprotonation in alkaline conditions, resulting in the formation of negatively charged phenolate anions. The process of deprotonation initiates further oxidation, mainly by generating phenoxy radicals. Indirectly, these radicals can also form when peroxy

radicals, which are produced from dioxygen radicals, combine with phenolate anions, resulting in the creation of peroxide anions. The peroxide anions, which are very reactive, react with the carbon atom of the phenolate species through intramolecular nucleophilic assault. This reaction ultimately results in the creation of dioxetane intermediates, which play a crucial role in the following oxidative breakdown of lignin [56]. The nitrobenzene oxidation process initiates with the activation of nitrobenzene through the use of a potent base, commonly sodium hydroxide (NaOH), resulting in the formation of a nitrobenzene radical anion. Subsequently, the nitrobenzene radical anion donates an electron to a lignin phenolate anion, which is an aromatic ring with a negative charge found in the lignin structure. The process involves the oxidation of the phenolate anion to form a phenoxyl radical, while the nitrobenzene radical anion is transformed back to its neutral form, nitrobenzene. The phenoxyl radical experiences a sequence of cleavage and rearrangement processes, which vary based on the particular structure of lignin. Typical routes of degradation involve β-O-4 cleavage (breaking of the Cα-Cβ bond next to the phenolic oxygen, producing fragments with aldehyde groups), α-O-4 cleavage (breaking of the Cβ-Cγ bond, also resulting in fragments with aldehyde groups), and side-chain cleavage, resulting in fragments with aldehyde groups. The aldehyde fragments have the ability to undergo additional chemical reactions, specifically oxidation and decarboxylation, resulting in the formation of the end products: vanillin (derived from guaiacyl units in lignin) and syringaldehyde (derived from syringyl units in lignin). Although aldehyde generation is the preferred reaction pathway in most cases, severe oxidation, also known as overoxidation, can cause the aldehyde chain to break down further, resulting in the creation of the corresponding aromatic acids [57–59]. During the

process of breaking down lignin, certain intermediate hydroxy acids can undergo decarboxylation to produce aromatic acids. Additionally, certain side reactions with these intermediates can also result in the formation of aromatic acids, although they are produced in less quantities. Nitrobenzene shown superior performance in the formation of lignin monomeric aldehydes and acids when compared to oxygen. Nitrobenzene exhibited superior performance in the oxidation of oxygen compared to NaOH at a concentration of 10% [60]. The impact of Cu (metal oxide) on the yield of products in lanthanum cobaltite ($LaCoO_3$) catalysts. Higher copper content leads to the creation of additional reactive sites, resulting in an increase in the formation of *p*-hydroxybenzaldehyde, vanillin, and syringaldehyde [61]. The utilization of polyoxometalate catalysts. Although the presence of $H_3PMo_{12}O_{40}$ in $N_2$ results in limited product formation due to catalyst reduction, the use of methanol as a scavenger enhances conversion by inhibiting re-polymerization. Their research, utilizing a mixture of 80% methanolic water and recycled catalysts, demonstrates a maximum output of 7 wt% for combined vanillin and methyl vanillate [62]. Specific oxidation reactions can be used to produce biopolymers, including adhesives, films, and coatings. To selectively oxidize biopolymers, one can employ different oxidizing agents, such as periodate, hypochlorite, or nitroxyl radicals, in a controlled manner. This allows for the targeting of specific functional groups within the polymer structure, such as -OH groups and C-C cleavages. An illustrative instance is the process of oxidizing polysaccharides, such as starch, to generate biopolymer derivatives that possess favorable characteristics. Insoluble soy flour can be converted into soy flour adhesives through the process of sodium periodate oxidation.

Not only starch, but also other sources such as protein, tannin, and lignin, can be utilized as raw materials for the production of important products [53,63,64].

## 1.4 Adaptive laboratory evolution (ALE) for strain development

Microbial strains are the workhorses of various industries, with applications ranging from biofuel production to bioremediation [65]. However, optimizing these strains for specific tasks can be challenging due to the complex interplay of genes and environment. Adaptive laboratory evolution (ALE) offers a powerful yet convenient tool for addressing this challenge. ALE mimics natural selection in a controlled laboratory environment. By subjecting a microbial population to a specific selective pressure, such as a novel substrate, a stress condition, or a desired product formation, ALE drives the emergence of beneficial mutations [66]. These mutations, often arising randomly, enhance the fitness of the population within the imposed selective pressure. Through repeated cycles of growth, selection, and propagation, ALE allows the population to progressively accumulate these advantageous mutations, leading to the development of strains with improved phenotypes. The key strength of ALE lies in its ability to engineer strains without relying on detailed knowledge of the underlying genetic pathways. This approach proves particularly valuable for complex phenotypes or when the specific genes responsible remain unidentified [67]. Additionally, ALE strains often exhibit broad-spectrum adaptations, making them more robust and adaptable to unforeseen challenges in industrial applications.

## 1.5 Untargeted metabolomics as a tool for further strain development

Following the successful development of strains through adaptive laboratory evolution (ALE), further optimization can be achieved through a powerful analytical technique known as untargeted metabolomics. This approach provides a comprehensive view of the entire metabolite profile within a cell, encompassing a vast array of small molecules involved in cellular processes. Unlike targeted metabolomics, which focuses on specific metabolites of interest, untargeted metabolomics casts a wider net, capturing a rich tapestry of metabolic activity [68]. In the context of strain development, untargeted metabolomics serves as a valuable tool for dissecting the physiological changes underlying the improved phenotypes generated by ALE (Fig. 5) . By comparing the metabolic profiles of the evolved strain with the parental strain, we can identify key metabolic alterations associated with the desired trait [69]. This information provides crucial insights into potential bottlenecks or limitations within the metabolic network, guiding further strain manipulation strategies.

Untargeted metabolomics data, when coupled with bioinformatic tools, allows for the identification of differentially regulated metabolic pathways. This knowledge empowers researchers to target specific enzymes or genes within these pathways for further optimization through genetic engineering or directed evolution approaches [70]. Additionally, untargeted metabolomics can reveal the presence of novel or unexpected metabolites, potentially leading to the discovery of new products or by-products from the engineered strain. Overall, untargeted metabolomics acts as a bridge between the phenotypic improvements achieved through ALE and the underlying metabolic mechanisms. This deeper understanding facilitates the rational

design of subsequent strain development strategies, ultimately leading to strains with even greater efficiency and productivity.

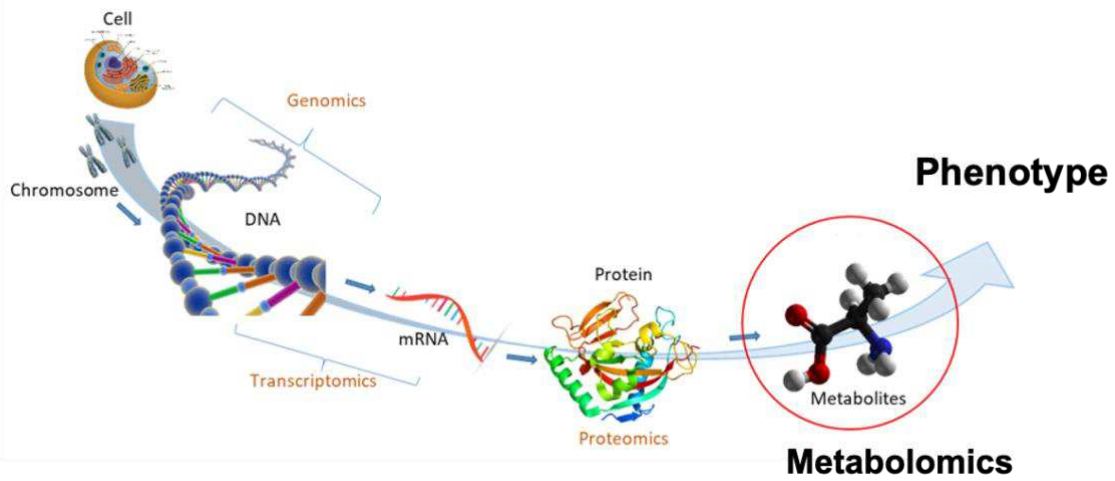


**Fig. 5** Metabolomics position as an extension of the central dogma.

### 1.6 Current challenge

The first major challenge lies in the inherent complexity of lignin itself. Unlike other biopolymers, lignin's structure varies depending on the source, such as the type of wood it comes from. This heterogeneity makes it difficult to develop a single,universally effective method for microbial conversion. Additionally, the complex structure of lignin physically hinders microbes from accessing and breaking down the valuable components they contain. Even after overcoming the initial physical barrier, researchers face a second challenge: the presence of inhibitory compounds. Depolymerization, the process of breaking down lignin into smaller, more manageable units for microbes, can generate compounds that are toxic

to these microorganisms. These inhibitory compounds can significantly reduce the overall efficiency of the conversion process.

Finally, most naturally occurring microbes have a limited capacity to utilize lignin compared to other carbon sources like glucose. This translates to low yields, or titers, of the desired biofuels or bioproducts. While some microbes have evolved the ability to degrade lignin, their natural capabilities often fall short of what's needed for a commercially viable process. Researchers are actively developing strategies to address these challenges and unlock the full potential of microbial lignin valorization. One approach involves engineering microbial strains to improve their tolerance to lignin-derived compounds and enhance their ability to break down and utilize these molecules. Additionally, researchers are working on developing more efficient depolymerization methods that produce a more uniform and microbe-friendly mixture of products. Finally, there's ongoing research focused on identifying and isolating highly effective lignin-degrading microbes from natural environments. By overcoming these hurdles, we can pave the way for a more efficient and cost-effective microbial conversion process, promoting a more sustainable bioeconomy that utilizes this abundant and renewable resource.

# Chapter 2

# The bioconversion of lignin derivative aldehydes into high-value aromatic alcohols and lipids via *Lipomyces starkeyi*

## 2.1 Introduction

Lignocellulosic biomass exhibits vast potential as a renewable resource within the realm of advancements in biorefining technology [71]. As a predominant constituent of biomass and the most prevalent aromatic biopolymer on the planet, lignin, estimated at around 300 billion metric tons, presents promising opportunities for the production of biofuels and various chemical derivatives [72]. Its role in the global economy and its potential to sustain future development are significant [73–75]. Nevertheless, recent research indicates that a considerable portion of lignin is degraded into low-value fuels upon burning, contributing to heat and air pollution [76,77]. Lignin, a natural macromolecule comprising p-hydroxyphenyl (H), guaiacyl (G), and syringyl (S) groups, undergoes depolymerization resulting in major degraded monomer compounds such as 4-hydroxybenzaldehyde, vanillin, and syringaldehyde, corresponding to the H, G, and S lignin groups, respectively [78–80] [81,82]. The conversion of lignin into fuels and valuable chemicals through biological means has emerged as an attractive avenue for its utilization, potentially enhancing the feasibility of biorefineries within the global economy [83,84]. However, the scope of lignin valorization remains constrained due to the scarcity of microorganisms proficient in efficiently utilizing various lignin monomers and

producing value-added products [85]. Leveraging microorganisms, particularly oleaginous yeast, for lignin valorization holds considerable promise in generating a diverse range of valuable biochemical products and biofuels from lignin monomers. Their adeptness in adapting to lignin-derived stressors facilitates the synthesis of bioproducts [71]. Additionally, the single-cell oils or lipids produced by oleaginous yeast represent a potential alternative feedstock for biodiesel industries, given their fatty acid profiles akin to vegetable oils [35].

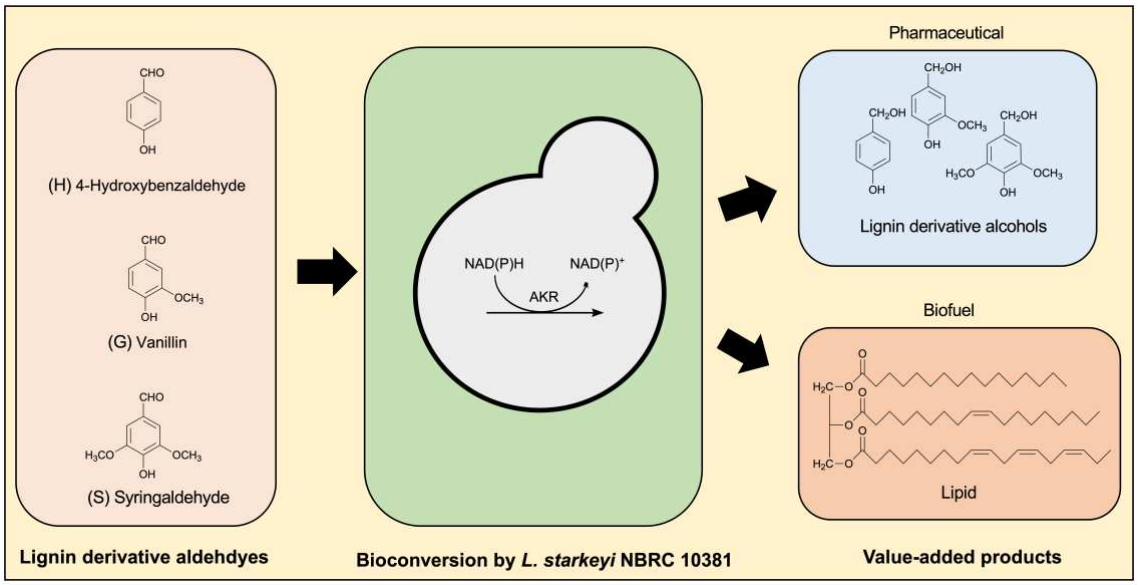


**Fig. 6** Graphical abstract of study chapter 2

Several investigations have highlighted the capability of oleaginous yeast to transform lignin monomers into diverse valuable products. For instance, *Trichosporon oleaginosus* demonstrated lipid accumulation on various lignin compounds, including 4-hydroxybenzoic acid, phenol, and resorcinol, achieving the highest lipid production of 1.64 g L-1 (69.5%) during the fermentation of resorcinol

[33]. *T. cutaneum* ACCC 20271 utilized 4-hydroxybenzaldehyde to produce microbial lipid, yielding approximately 0.85 g L-1 or 16.6% of body weight [86]. Moreover, *T. cutaneum* exhibited the capability to convert vanillin and syringaldehyde into vanillyl alcohol and syringyl alcohol, ultimately yielding vanillic acid and syringic acid, respectively. Furthermore, in the fermentation process of *T. guehoae*, ferulic acid was transformed into vanillic acid [36]. However, to date, no experiment has explored the utilization of lignin derivative aldehyde monomers for the production of lignin alcohols as the primary product using yeast, due to their toxicity to most microorganisms and resistance to bioconversion. Given their potential application in biomedicine, particularly in pharmacology, biocompatibility is crucial [87,88]. Several studies have indicated the pharmacological benefits of lignin derivative alcohols; for instance, 4-hydroxybenzyl alcohol exhibits anti-inflammatory and antiasthmatic properties [89,90], while vanillyl alcohol holds promise in treating Parkinson's disease [91,92]. Additionally, syringyl alcohol, due to its phenolic and benzylic hydroxyl units, serves as a common lignin model for research [93].

Unlike other extensively studied oleaginous yeasts for lignin utilization, the utilization of *Lipomyces starkeyi* as a model organism is relatively novel, despite its potential for high microbial lipid production using lignocellulosic biomass and its derived sugars, along with high tolerance to various lignocellulosic inhibitors [94]. In this investigation, we discovered that *L. starkeyi* could produce lignin alcohols from lignin derivative aldehydes. Consequently, we explored the potential of *L. starkeyi* to utilize three lignin derivative aldehydes, namely 4-hydroxybenzaldehyde, vanillin, and syringaldehyde, to facilitate their conversion into their respective

reduced products (alcohols) and to accumulate lipids (Fig. 6). Subsequently, the three mixed lignin aldehydes were fermented using the strain under different fermentation conditions, and their impact on lipid production was evaluated. This study presents the first instance of bioproducing valuable lignin alcohols from lignin derivative aldehydes using *L. starkeyi* while concurrently achieving high microbial lipid production. Our findings contribute to the advancement of lignin valorization through a bioconversion approach, enhancing the practical prospects of biorefinery technology in the future.

## 2.2 Materials and methods

### 2.2.1 Yeast strain and reagents

In this study, *Lipomyces starkeyi* D35 (NBRC 10381) sourced from the NITE Biological Resource Center (NBRC) at the National Institute of Technology and Evaluation in Japan was utilized. The chemical compounds syringaldehyde, syringic acid, vanillin, vanillic acid, 4-hydroxybenzaldehyde, and 4-hydroxybenzoic acid were procured from Sigma–Aldrich. Additionally, syringyl alcohol was obtained from Thermo Fisher Scientific, while vanillyl alcohol and 4-hydroxybenzyl alcohol were purchased from Tokyo Chemical Industry.

### 2.2.2 Inoculum preparation

The yeast strain was preserved in 30% (w/w) glycerol at -80 °C and revived through streaking on YMPG agar medium consisting of 3 g $L^{-1}$ yeast extract, 3 g $L^{-1}$ malt extract, 5 g $L^{-1}$ peptone, 10 g $L^{-1}$ glucose, and 20 g $L^{-1}$ agar. Following a 2-day incubation at 30 °C, a single colony from the agar plate was transferred into a 100

mL Erlenmeyer flask containing 12 mL of YMPG liquid medium composed of 3 g $L^{-1}$ yeast extract, 3 g $L^{-1}$ malt extract, 5 g $L^{-1}$ peptone, and 50 g $L^{-1}$ glucose as the preculture. The flask was then placed inside an incubator shaker (BioShaker BR-43FH MR, Taitec) and incubated at 30 °C and 190 rpm under aerobic conditions for 24 hours.

### 2.2.3 Medium and fermentation conditions

In this research, we employed two types of growth media: YMPG liquid medium, characterized by a low carbon-to-nitrogen (C:N) ratio, and nitrogen-limited mineral media (NMM), distinguished by a high C:N ratio. The NMM formulation consisted of 50 g $L^{-1}$ glucose as the sole carbon source, supplemented with 1.5 g $L^{-1}$ yeast extract and 0.25 g $L^{-1}$ $(NH_4)_2SO_4$ as nitrogen sources, along with 7 g $L^{-1}$ $KH_2PO_4$ and 5 g $L^{-1}$ $Na_2HPO_4 \cdot 2H_2O$ as phosphate buffer. Additionally, it contained 1.5 g $L^{-1}$ $MgSO_4 \cdot 7H_2O$ and various trace elements (0.1 g $L^{-1}$ $CaCl_2 \cdot 2H_2O$, 0.1 g $L^{-1}$ $MnSO_4 \cdot 4H_2O$, 0.08 g $L^{-1}$ $FeSO_4 \cdot 7H_2O$, 0.002 g $L^{-1}$ $CoCl_2 \cdot 6H_2O$, 0.002 g $L^{-1}$ $CuSO_4 \cdot 5H_2O$), with the pH adjusted to 5. The preculture was transferred to 12 mL of either YMPG or NMM medium supplemented with lignin derivatives at specified concentrations. The inoculum size for the main culture was adjusted to an initial optical density (OD600) of either 1 (low) or 40 (high) in a 100 mL flask. The cultures were then incubated in an orbital shaker incubator at 30 °C and 190 rpm under aerobic conditions.

### 2.2.4 Dry cell weight measurement

The dry cell weight (DCW) was determined gravimetrically using 0.5 mL of the fermentation sample. The cell cultures were centrifuged for 5 minutes at 14,000 × g to separate them, followed by two washes with deionized water. Subsequently, the cells were dried overnight at -80 °C. Lyophilization, performed to eliminate water content, was carried out using a freeze-drying system (FreeZone 4.5 L Freeze Dry System Model 7750020, Labconco).

### 2.2.5 Glucose measurement

Glucose concentration during fermentation was assessed using a high-performance liquid chromatography (HPLC-20AB) system combined with a refractive index detector (RID-10A) from Shimadzu, equipped with an ICSep Coregel-87H column (300 mm length, 7.8 mm inner diameter, provided by Transgenomic). After centrifuging the samples for 5 minutes at 14,000 × g, the supernatant was filtered through a 0.22 µm filter before analysis. A sample injection volume of 20 µL was used, and the column oven temperature was set at 80 °C. The mobile phase consisted of 5 mM H2SO4 with a flow rate of 0.6 mL $min^{-1}$ [95].

### 2.2.6 Quantification of lignin

The quantification of lignin derivatives was conducted using a high-performance liquid chromatography (HPLC-20AB) system paired with a UV–Vis detector (SPD-20A) manufactured by Shimadzu. An Ascentis C18 column (250 mm × 4.6 mm with a 5 µm particle size, supplied by Supelco 50537-U, Sigma–Aldrich) was employed for separation. Supernatant samples were obtained by centrifugation at 14,000 × g

for 5 minutes and filtered through a 0.22 μm filter before analysis. A 10 μL injection volume was utilized, and the column oven temperature was set to 30 °C. The mobile phase comprised methanol and ultrapure water in a 18:82 (v/v) ratio, with 0.2% acetic acid. Analysis was performed at a flow rate of 1 mL $min^{-1}$, with detection at a wavelength of 280 nm [96].

### 2.2.7 Lipid determination via gravimetry analysis

Lipid accumulation was assessed using gravimetric analysis following the Folch extraction method [95]. Freeze-dried cells (20 mg) were transferred into a 2 mL micro vial with an O-ring sealed cap, along with zirconia beads. Lipid extraction was carried out using 1.5 mL of extraction solvent (chloroform:methanol; 2:1 v/v ratio). Cell pulverization was accomplished using a Shake Master Neo M10N21 from BMS at 1500 rpm for 15 minutes. Subsequently, cells were centrifuged for 5 minutes at 14,000 × g, and the resulting pellets were washed twice with 1.5 mL of deionized water. The cells were then dried at 60 °C until reaching a constant weight. The lipid content was determined by the weight difference and expressed as a percentage of the dry cell weight.

### 2.2.8 Lipid observation via BODIPY (493-503)

The lipid bodies were labeled using boron dipyrromethene, also known as BODIPY 493-503. BODIPY is a highly UV-absorbing molecule that emits a relatively narrow peak. As a lipophilic fluorescent dye, it was employed to visualize lipid production within the cells. To prepare the BODIPY solution, 10 mg of the dye stock was dissolved in 1 mL of ethanol. In brief, 100 μL of the sample culture was

centrifuged at 12,000 × g for 1 minute and washed with 0.9% phosphate-buffered saline (PBS). The cells were then resuspended in 45 µL of PBS, to which 5 µL of the BODIPY stock solution was added (resulting in a final concentration of 1 mg $mL^{-1}$). Subsequently, the cells were incubated in the dark for 1 hour before being examined under a digital inverted fluorescence microscope (Biorevo BZ-X800, Keyence) [97].

### 2.2.9 Fatty acid methyl ester analysis via GC–MS

The lipids obtained from the lyophilized cells underwent transesterification to convert them into methyl esters following the procedure outlined in the fatty acid methylation kit (Nacalai Tesque). The resulting fatty acid methyl esters (FAMEs) were dissolved in hexane and subjected to analysis using gas chromatography–mass spectrometry (Shimadzu GC–MS QP-2010). Caprylic acid (C8:0) served as the internal standard. For analysis, a GC capillary column DB-23 (60 m by 0.25 mm inner diameter, with a 0.25 mm film thickness, Agilent) was utilized. Helium gas was employed as the carrier gas. The injection volume was set at 1 µL, and analysis was performed under split injection conditions with the inlet temperature maintained at 250 °C. The oven temperature was initially held at 50 °C for 1 minute, then increased at a rate of 25 °C per minute to 175 °C, followed by a further increase to 230 °C at a rate of 4 °C per minute for 6 minutes. The mass spectrometer detector was set to 250 °C and scanned within the range of 40–500 m z-1 in scan mode. Fatty acids were identified and quantified by comparing their retention time (RT) and fragmentation pattern with a standard mixture of fatty acids (SUPELCOTM 37 component FAME mixture, Sigma–Aldrich) [35,95,98].

### 2.2.10 Gene expression analysis

Gene expression levels were assessed through quantitative PCR (qPCR) analysis. *L. starkey*i NBRC 10381 was cultivated in YPMG medium supplemented with individual lignin derivative aldehydes (4-hydroxybenzaldehyde, vanillin, and syringaldehyde) at 30 °C and 190 rpm. A control group consisting of the strain cultured solely in medium was included. Samples were collected during the early log phase (24 hours). Cells were harvested by centrifugation for 5 minutes at 14,000 × g and 4 °C. Subsequently, the cells were resuspended in RA1 buffer from NeoSpinRNA (Macherey-Nagel) and lysed using a Shake Master Neo M10N21 at 1500 rpm for 15 minutes. RNA extraction followed the protocol outlined in the NucleoSpin RNA kit (Macherey-Nagel). For cDNA synthesis, total RNA was reverse-transcribed using a RaverTra Ace qPCR RT Master Mix kit (Toyobo) and a PCR Thermal Cycler Machine (Takara) under specific incubation conditions: 37 °C for 15 minutes, followed by 50 °C for 5 minutes and then 98 °C for 5 minutes. The concentration of cDNA was measured using a NanoDrop spectrophotometer (NanoDrop One, Thermo Fisher Scientific). Gene expression analysis was conducted in a 20 µL reaction mixture containing KOD SYBR qPCR mix and ROX from Toyobo, along with 50 ng of DNA and 0.4 µL each of forward and reverse primers. The Agilent Mx3005P qPCR system was utilized for analysis. The qPCR protocol involved initial denaturation for 5 minutes at 98 °C, followed by 60 cycles of amplification: 10 s at 98 °C, 11 s at 60 °C, and 30 s of elongation at 68 °C. Alpha-tubulin (Tub1) served as the housekeeping gene. Gene expression levels were quantified using the MxPro software (Agilent) and calculated as fold changes using

the formula 2-(ΔCq), where ΔCq is the difference between the Cq values of the sample and Tub1. Primer sequences utilized in this analysis are provided in Table S1.

## 2.3 Results and discussion

### 2.3.1 Lignin aldehyde tolerance of *L. starkeyi* NBRC 10381

In this investigation, three specific lignin derivative aldehydes namely, 4-hydroxybenzaldehyde, vanillin, and syringaldehyde were chosen to represent typical lignin monomers from hydroxyphenyl (H-lignin), guaiacyl (G-lignin), and syringyl (S-lignin) groups, respectively. Assessing the microbial cells' tolerance towards these three lignin aldehydes was crucial to validate their potential for conversion. Therefore, before investigating the conversion of lignin aldehydes via *L. starkeyi* NBRC 10381, we conducted an evaluation at minimum inhibitory concentrations on a fermentation scale (1 mL) in deep well plates at 30 °C for 72 hours. The aldehyde concentrations ranged from 0 (control) to 32 mM, with increments at 0.5, 1, 2, 4, 8, 16, and 32 mM, within YMPG medium containing 50 g $L^{-1}$ of glucose. NBRC 10381 exhibited markedly different levels of tolerance towards these representative aldehydes. Fermentation in syringaldehyde at concentrations of 8-16 mM showed minimal inhibition of cell growth (refer to Fig. 7). Conversely, 16 mM 4-hydroxybenzaldehyde completely halted cell growth, while vanillin displayed a similar inhibitory effect on NBRC 10381. These results indicated a higher tolerance level compared to previous research on L. starkeyi, where only 0.12 mM vanillin and 0.08 mM syringaldehyde were utilized [35].

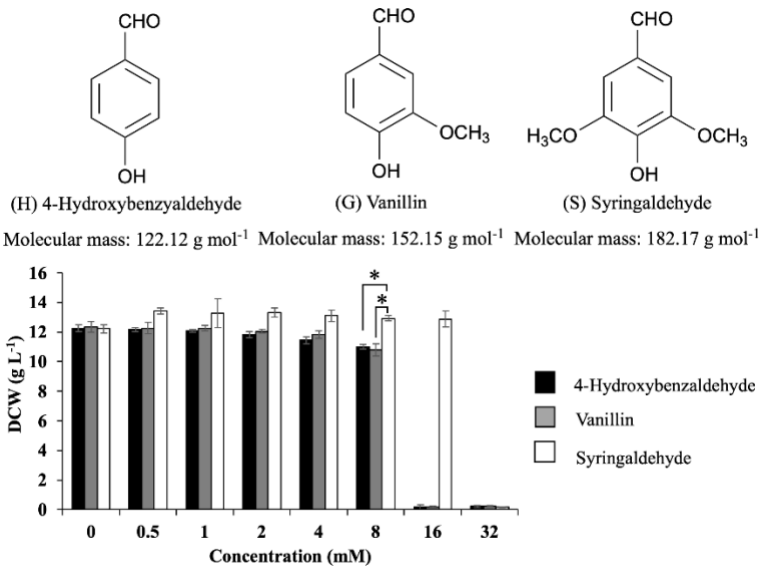


**Fig. 7** Tolerance of *L. starkeyi* NBRC 10381 to lignin derivative aldehydes. Closed bars represent 4-hydroxybenzaldehyde, shaded bars represent vanillin, and open bars represent syringaldehyde. The results showed the average of three replicates of the biological samples with error bars representing the standard deviation from the mean value. *Statistical analysis was performed using Student's t test ($p$ value <0.05).

Based on these findings (refer to Fig. 7), 4-hydroxybenzaldehyde and vanillin exhibited a more pronounced inhibitory impact compared to syringaldehyde, potentially attributed to their lower molecular weights. Specifically, the molecular weights of 4-hydroxybenzaldehyde, vanillin, and syringaldehyde are 122.12, 152.15, and 182.17 g $mol^{-1}$, respectively. The toxicity of phenolic compounds is closely related to their hydrophobicity. Consequently, phenolic aldehydes with lower molecular weights were observed to exert greater toxicity towards the cells compared to those with higher molecular weights, as they could more readily permeate through

cell membranes and consequently lead to more potent inhibition of carbon assimilation [99,100].

### 2.3.2 Different lignin derivative aldehyde conversion and fermentation profiles

Microorganism cells typically exhibit tolerance by converting toxic inhibitors into less harmful compounds through detoxification mechanisms [101,102]. Therefore, representative lignin aldehyde compounds 4-hydroxybenzaldehyde, vanillin, and syringaldehyde were employed at concentrations of 8, 8, and 16 mM, respectively, for individual 12 mL flask-scale fermentations, based on their respective minimum inhibitory concentrations. A starting OD600 nm of 1 (representing low initial inoculum size) was utilized in YMPG medium containing 50 g $L^{-1}$ glucose. The conversions of lignin aldehydes by NBRC 10381 are illustrated in Fig. 8. Glucose consumption and cell growth of the NBRC 10381 strain in the presence of various lignin aldehydes are depicted in Fig. 8a. For 4-hydroxybenzaldehyde, glucose was completely depleted at 72 hours following complete degradation into 4-hydroxybenzyl alcohol, without any accumulation of the corresponding metabolite, 4-hydroxybenzoic acid (Fig. 8b). Vanillin exhibited a similar pattern to 4-hydroxybenzaldehyde, with glucose exhaustion occurring at 72 hours post complete conversion into vanillyl alcohol, without accumulation of the corresponding vanillin acid. In contrast, 16 mM syringaldehyde resulted in a reduced glucose consumption rate (Fig. 8c), prolonging fermentation time. Syringaldehyde was entirely depleted at 72 hours, being converted into syringyl alcohol rather than syringic acid, with complete glucose consumption achieved at 96 hours of fermentation. The high phenolic compound concentration in the fermentation notably

extended the lag phase due to its inhibitory effect on the microorganism [103,104]. To gain deeper insights into NBRC 10381's ability to utilize lignin aldehydes in fermentation, the growth, glucose consumption, and lignin depletion rates were assessed during the logarithmic phase (24-48 hours), as depicted in Fig. 8c. Fermentation in syringaldehyde displayed lower glucose consumption and cell growth rates. Nevertheless, it exhibited a higher lignin depletion rate and relatively greater production of dry cell weight in the final cell production (0.39 mM $h^{-1}$ and 17.01 g $L^{-1}$, respectively) compared to other lignin aldehydes. This observation could be attributed to syringaldehyde's inhibitory effect in prolonging the lag phase without further impacting NBRC 10381's final cell production.

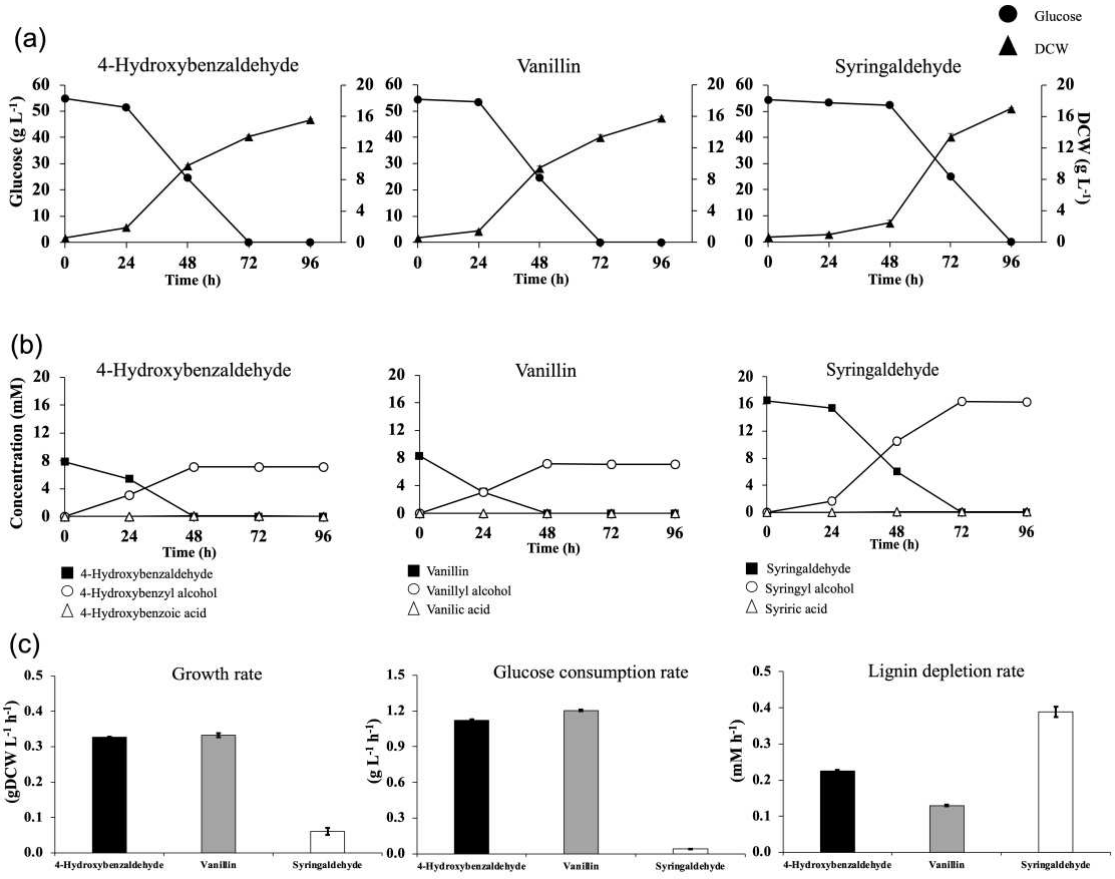

**Fig. 8** Different lignin derivative fermentation profiles of *L. starkeyi* NBRC 10831. (a) Time courses for carbon source consumption (closed circles) and cell growth (closed triangles) in YMPG medium with different lignin aldehydes. (b) Biodegradation of lignin aldehydes (closed squares) into their alcohol (opened circles) and acid derivatives (opened triangles). (c) Growth, glucose consumption, and lignin depletion rates in the fermentation of 4-hydroxybenzaldehyde (closed bars), vanillin (shaded bars), and syringaldehyde (opened bars) at the logarithmic phase. The results show the average of three replicates of the biological samples with error bars representing the standard deviation from the mean value.

**Table 1** The percentage yield of lignin derivative alcohols. [a]

| Type of substrate | Type of product | Time (h) | Percent yield |
|---|---|---|---|
| 4-Hydroxybenzaldehyde | 4-Hydroxobenzyl alcohol | 96 | 90.1 ± 0.30 |
| Vanillin | Vanillyl alcohol | 96 | 97.6 ± 0.30 |
| Syringaldehyde | Syringyl alcohol | 96 | 97.5 ± 0.40 |

[a] Results show the average of three replicates of the biological samples ± standard deviation from the mean value.

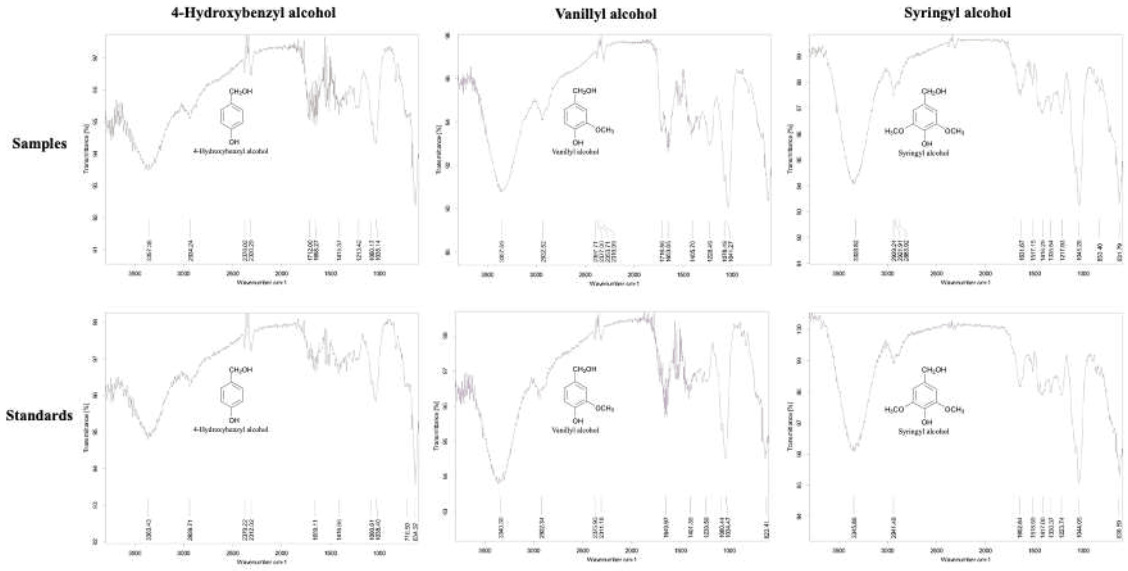


**Fig. 9** ATR-FTIR spectra analysis of lignin derivative alcohols. FTIR spectra were recorded on a Bruker Alpha with ATR (attenuated total reflectance) attachment and reported in wavenumbers ($cm^{-1}$).

In Fig. 8b, NBRC 10381 successfully converted all lignin aldehydes namely, 4-hydroxybenzaldehyde, vanillin, and syringaldehyde into their corresponding lignin derivative alcohols, including 4-hydroxybenzyl alcohol, vanillyl alcohol, and syringyl alcohol, respectively. Notably, there was no accumulation of undesired byproducts throughout the fermentation process, and the alcohols remained predominant until the conclusion of fermentation. The percentage yields of these lignin-derivative alcohols are detailed in Table 1, with 4-hydroxybenzyl alcohol, vanillyl alcohol, and syringyl alcohol achieving high percentage yields of 90.1%, 97.6%, and 97.5%, respectively. In further support of these findings, we conducted fermentations solely on lignin derivative alcohols, yielding similar outcomes (Fig. 10). This scenario holds potential industrial advantages as it ensures consistency in

end-products without alterations to other compounds or reconversion to initial substrates, which could disrupt the production process [105].

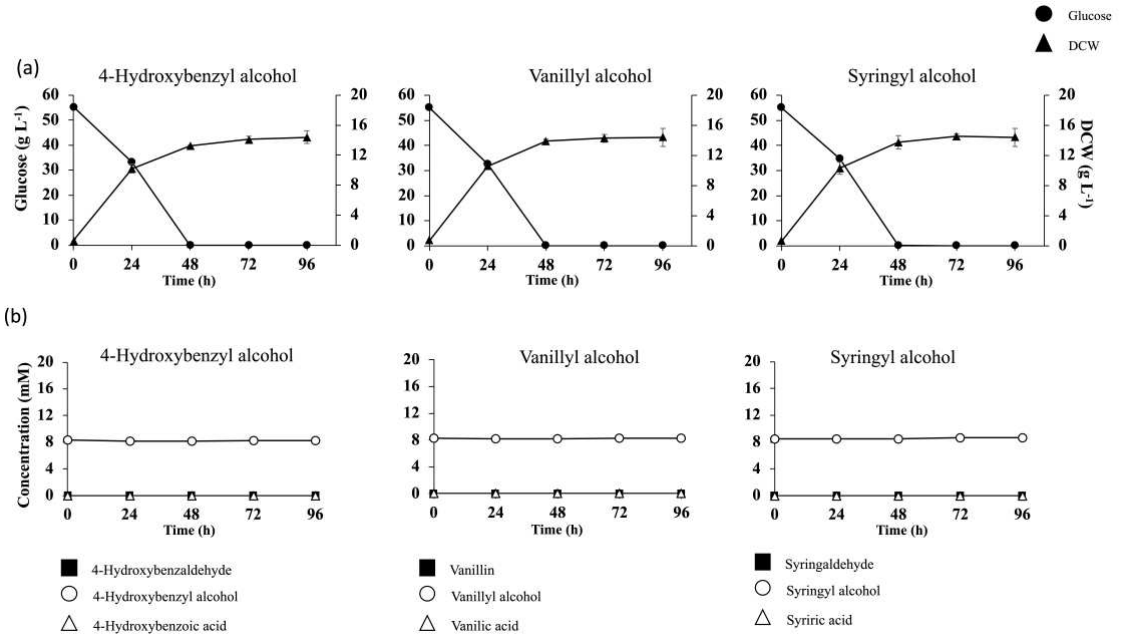


**Fig. 10** Different lignin derivative alcohols fermentation profiles of *L. starkeyi* NBRC 10831. (a) Time courses for carbon source consumption (closed circles) and cell growth (closed triangles) in YMPG medium with different lignin alcohols. (b) Lignin aldehydes (closed squares), lignin alcohol (opened circles), and acid derivatives (opened triangles). The results show the average of three replicates of the biological samples with error bars representing the standard deviation from the mean value.

The presumed pathway for lignin alcohol accumulation by NBRC 10381 from its derivative aldehydes was inferred based on the relative quantification of gene expression using qPCR (as depicted in Fig. 11a). Three key genes associated with

lignin aldehyde conversion were chosen for analysis: alcohol dehydrogenase (ADH), aldehyde-ketone reductase (AKR), and aldehyde dehydrogenase (ALDH). Since lignin conversion, cell growth, and glucose consumption were most active during the logarithmic phase, gene expression analysis was conducted at the onset of this phase (24 hours). The findings are illustrated in Fig. 11b. Notably, the AKR gene exhibited high expression levels across all fermentations. AKR is recognized for its role in reducing lignin aldehydes to alcohols [106]. However, the fermentation of syringaldehyde demonstrated a comparatively lower expression level of AKR compared to 4-hydroxybenzaldehyde and vanillin. This observation may be attributed to the inhibitory effects of high syringaldehyde concentrations during the early logarithmic phase. The ALDH gene, responsible for oxidizing lignin aldehydes into acids [107], showed no expression in any of the fermentations. Interestingly, all fermentations exhibited a consistent pattern for the ADH gene. The ADH gene demonstrated its capacity to oxidize lignin alcohols back into their corresponding aldehydes [108]. These findings align with the understanding that NBRC 10381 predominantly converts lignin aldehydes into alcohols rather than acids. Subsequently, once produced, the lignin alcohols remained unchanged in the medium.

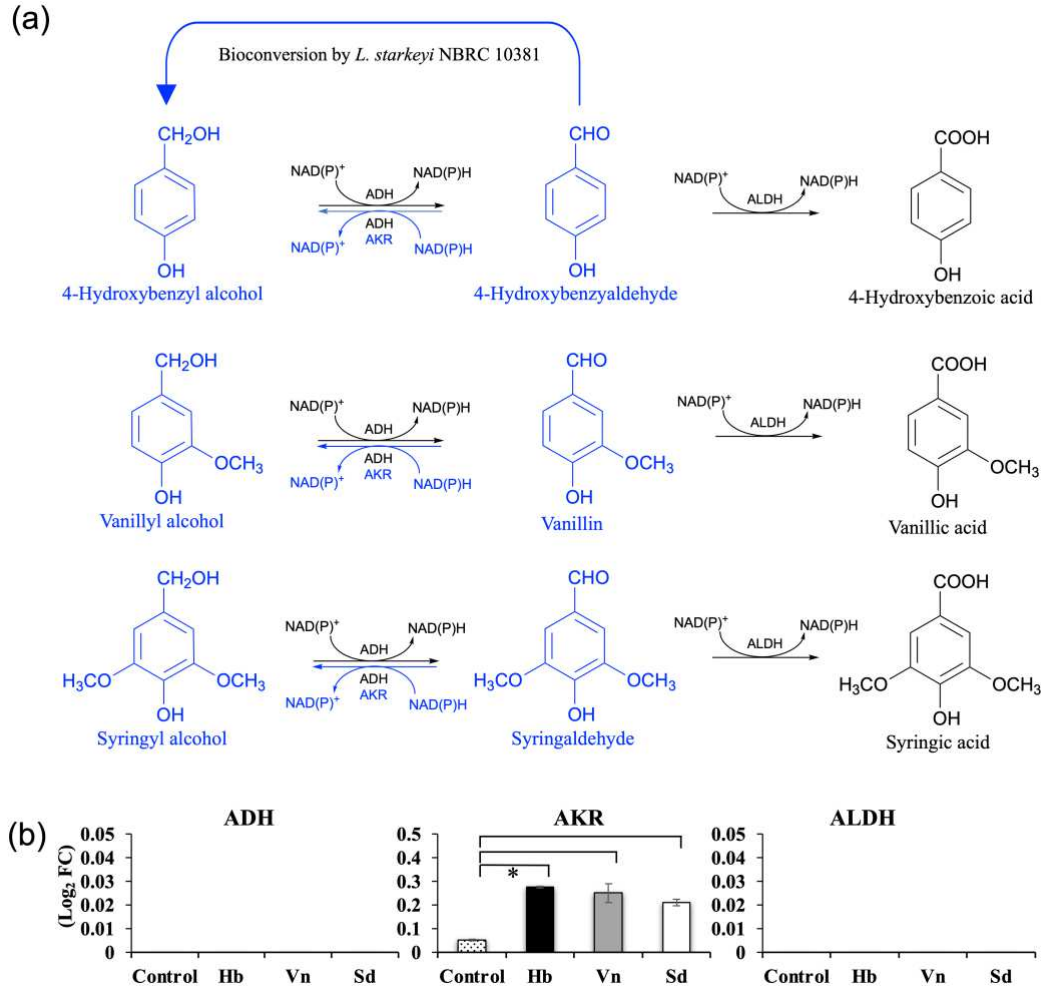


**Fig. 11** Metabolic pathway for lignin monomers and their gene expression. (a) Metabolic pathway for lignin derivative aldehydes into derivative alcohols via *L. starkeyi* NBRC 10381. (b) Quantitative gene expression of *L. starkeyi* NBRC 10381 in the cultivation in lignin derivative aldehydes, namely, 4-hydroxybenzaldehyde (closed bars), vanillin (shaded bars), and syringaldehyde (opened bars). ADH, alcohol dehydrogenase; AKR, aldehyde-ketone reductase; ALDH, aldehyde dehydrogenase. $Log_2$ FC (fold change) represents transcriptional genes compared to

the expression level of the TUB1 gene as a housekeeping gene. The results show the average of three replicates of the biological samples with error bars representing the standard deviation from the mean value. *Statistical analysis was performed using Student's t test (*p* value <0.05).

### 2.3.3 Lipid accumulation and fatty acid profile during fermentation of the different lignin aldehydes

The lipid production of NBRC 10281 during fermentation with various aldehydes is outlined in Table 2. Following 96 hours of culture in 4-hydroxybenzaldehyde, the dry cell weight and lipid content reached 15.58 g $L^{-1}$and 27.79% (w/w), respectively. Comparable lipid accumulation was observed in the fermentation of vanillin as with 4-hydroxybenzaldehyde. The highest cell mass and lipid accumulation were achieved with NBRC 10831 in syringaldehyde, reaching 17.01 g $L^{-1}$and 30.72%, respectively (Student's t-test, $p < 0.05$). Syringaldehyde was converted into syringyl alcohol by aldehyde-ketone reductase, generating one $NAD(P)^+$ (as illustrated in Fig. 11a). Given that the concentration of syringaldehyde exceeded that of other aldehydes, the additional $NAD(P)^+$ supplied through syringyl alcohol production could potentially be utilized for the conversion of malate to pyruvate via NAD(P)H release in the cytosol [109]. Subsequently, pyruvate could be directed to the TCA cycle, with NAD(P)H then utilized by fatty acid synthase, essential for fatty acid biosynthesis [110,111].

**Table 2** Biomass and lipid production of *L. starkeyi* NBRC 10381 for different lignin aldehydes.[a]

| Type of lignin | Time (h) | Initial DCW ($g\ L^{-1}$) | Final DCW ($g\ L^{-1}$) | Initial lipid content (%, $w\ w^{-1}$) | Final lipid content (%, $w\ w^{-1}$) | Lipid titer ($g\ L^{-1}$) |
|---|---|---|---|---|---|---|
| Control | 96 | 0.61 ± 0.04 | 14.36 ± 0.11 | 9.04 ± 1.30 | 24.07 ± 0.43 | 3.46 ± 0.00 |
| 4-Hydroxybenzaldehyde | 96 | 0.58 ± 0.05 | 15.58 ± 0.14 | 9.04 ± 1.30 | 27.79 ± 1.60 | 4.33 ± 0.00 |
| Vanillin | 96 | 0.55 ± 0.06 | 15.79 ± 0.21 | 9.04 ± 1.30 | 26.95 ± 2.26 | 4.26 ± 0.00 |
| Syringaldehyde | 96 | 0.65 ± 0.05 | 17.01 ± 0.11 | 9.04 ± 1.30 | 30.72 ± 1.52 | 5.23 ± 0.00 |

[a] Results show the average of three replicates of the biological samples ± standard deviation from the mean value.

**(a)**

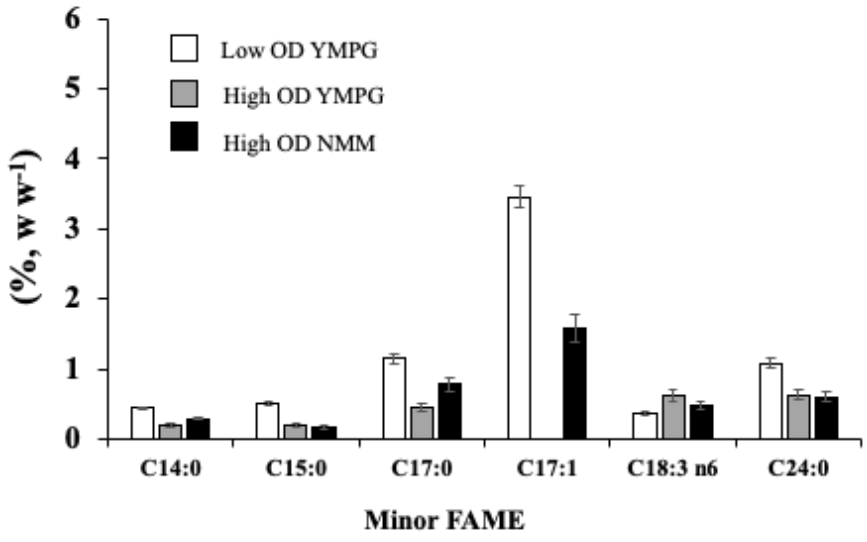

**(b)**

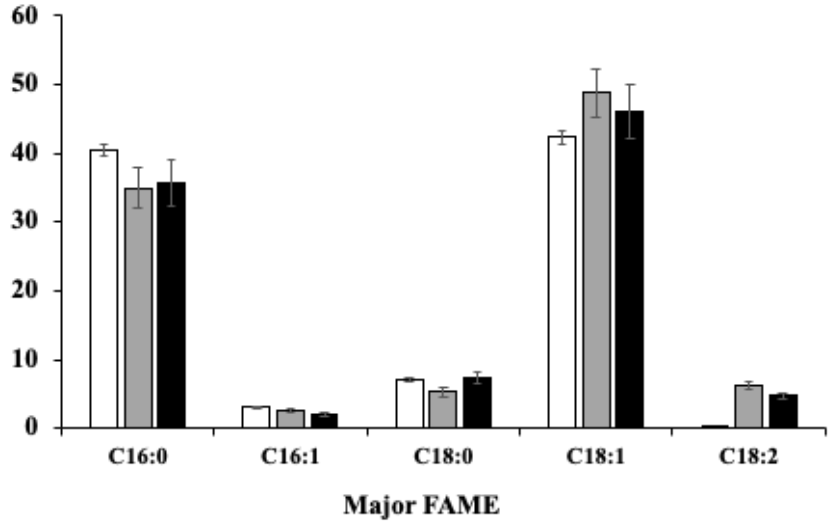


**Fig. 12** Profiles of fatty acids produced during fermentation of different lignin derivative aldehydes. 4-hydroxybenzaldehyde (closed bars), vanillin (shaded bars), syringaldehyde (opened bars), and control (dotted bars). The results show the average of three replicates of the biological samples with error bars representing the standard deviation from the mean value.

The fatty acid composition of lipids produced in each fermentation using different aldehydes is depicted in Fig. 12. Predominantly, the lipids consisted of fatty acids containing 16 and 18 carbon atoms, notably palmitic acid (C16:0), palmitoleic acid (C16:1), stearic acid (C18:0), oleic acid (C18:1), and linoleic acid (C18:2). These fatty acid profiles closely resembled those found in most vegetable oils [45]. Across all aldehyde fermentations, C18:1 emerged as the primary fatty acid, constituting over 45% of the total fatty acids, followed by C16:0, which accounted for more than 30%. The substantial proportion of C18:1 suggests that NBRC 10381

could potentially be classified as a biodiesel producer in industrial applications [112]. Notably, *Lipomyces starkeyi* NBRC 10831 exhibited the highest production of C18:1 among other strains of oleaginous yeast groups [95]. Moreover, the fatty acid composition remained consistent across all lignin aldehydes, indicating that specific aldehydes did not influence certain fatty acid productions. This observation aligns with previous studies of *Lipomyces starkeyi*, even in the absence of lignin aldehydes [113,114].

### 2.3.4 Effect of the mixed lignin aldehyde on lipid production under different fermentation conditions

After assessing the ability of NBRC 10381 to efficiently convert various lignin aldehydes while producing lipids under conditions of low carbon-to-nitrogen (C:N) ratio and low initial inoculum size, a fermentation experiment involving mixed lignin aldehydes under three different conditions was conducted to evaluate its impact on lipid production. The mixture of lignin aldehydes comprised 4 mM 4-hydroxybenzaldehyde, 4 mM vanillin, and 8 mM syringaldehyde (half the concentration utilized in the fermentation of individual lignin aldehydes). Subsequently, the mixed lignin aldehyde was cultivated under three scenarios: low initial inoculum size on a low C:N ratio medium (low OD600 YMPG), high initial inoculum size on a low C:N ratio medium (high OD600 YMPG), and high initial inoculum size on a high C:N ratio medium (high OD600 NMM). As showed in Fig. 13a, the mixed lignin aldehyde significantly impeded cell growth when the initial inoculum size was low. The lag phase of NBRC 10381 was extended until 72 hours before growth resumed. The combined presence of phenolic compounds exerted a

synergistic inhibitory effect on cell metabolism, causing a considerable delay in cell growth and a reduction in the final dry cell weight [115].

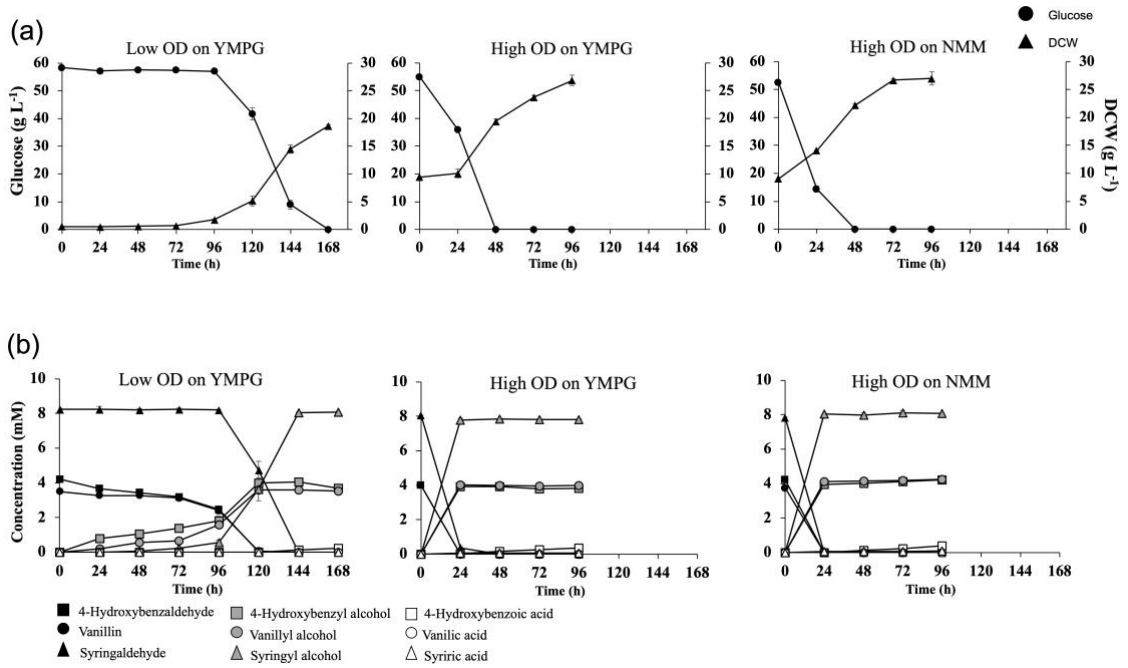


**Fig. 13** Mixed lignin derivative aldehyde fermentation profile of *L. starkeyi* NBRC 10831. (a) Time courses for carbon source consumption (closed circles) and cell growth (closed triangles) under different fermentation conditions. (b) Biodegradation of mixed lignin aldehydes (4-hydroxybenzaldehyde (closed squares), vanillin (closed circles), syringaldehyde (closed triangles)) into their alcohol (4-hydroxybenzyl alcohol (shaded squares), vanillyl alcohol (shaded circles), syringyl alcohol (shaded triangles)), and acid derivative ((4-hydroxybenzoic acid (opened squares), vanillic acid (opened circles), syringic acid (opened triangles)). The results show the average of three replicates of the biological samples with error bars representing the standard deviation from the mean value.

On the contrary, NBRC 10381 cells exhibited accelerated growth in both high-OD YMPG and NMM fermentations, leading to a significant reduction in fermentation duration compared to low-OD YMPG conditions (up to 120 hours). The conversion of aldehydes to lignin alcohols corresponded directly with sugar consumption and lignin degradation (Fig. 13), with a higher initial inoculum size enhancing NBRC 10381's performance in the fermentation process. Augmenting the initial inoculum size intensified the active cell fraction, increasing the likelihood of more cells adapting and thriving in the stressed environment [116]. Consequently, this facilitated efficient lignin alcohol production. All mixed lignin aldehyde fermentations displayed a consistent trend with individual lignin aldehydes, wherein all aldehydes were transformed into alcohols, and these produced alcohols persisted until the culmination of fermentation without any formation of undesirable byproducts (Fig. 13b). NBRC 10831 facilitated the concurrent assimilation of all lignin aldehydes and glucose rather than sequential assimilation across all fermentation conditions. This simultaneous utilization of lignin and glucose holds significance in utilizing lignocellulosic biomass to mitigate costs associated with lignin alcohol and lipid production. In the bioprocess industry, simultaneous utilization offers cost-effectiveness advantages [117,118]. The potential applications extend beyond pharmaceutical industries for lignin alcohol usage; the lipids produced also hold promise for biodiesel industries due to their biochemical and physicochemical properties [89–94].

**Table 3** Biomass and lipid production of *L. starkeyi* NBRC 10381 for mixed lignin aldehydes.[a]

| Type of lignin | Time (h) | Initial DCW ($g\ L^{-1}$) | Final DCW ($g\ L^{-1}$) | Initial lipid content (%, w $w^{-1}$) | Final lipid content (%, w $w^{-1}$) | Lipid titer ($g\ L^{-1}$) |
|---|---|---|---|---|---|---|
| Low OD YMPG | 168 | 0.55 ± 0.08 | 18.68 ± 0.22 | 8.47 ± 1.64 | 30.02 ± 0.56 | 5.61 ± 0.00 |
| High OD YMPG | 96 | 9.42 ± 0.09 | 26.85 ± 0.89 | 10.22 ± 0.72 | 33.09 ± 3.29 | 8.88 ± 0.03 |
| High OD NMM | 96 | 9.05 ± 0.21 | 26.97 ± 1.18 | 9.26 ± 1.48 | 54.72 ± 1.95 | 14.76 ± 0.02 |

[a] Results show the average of three replicates of the biological samples ± standard deviation from the mean value.

**(a)**

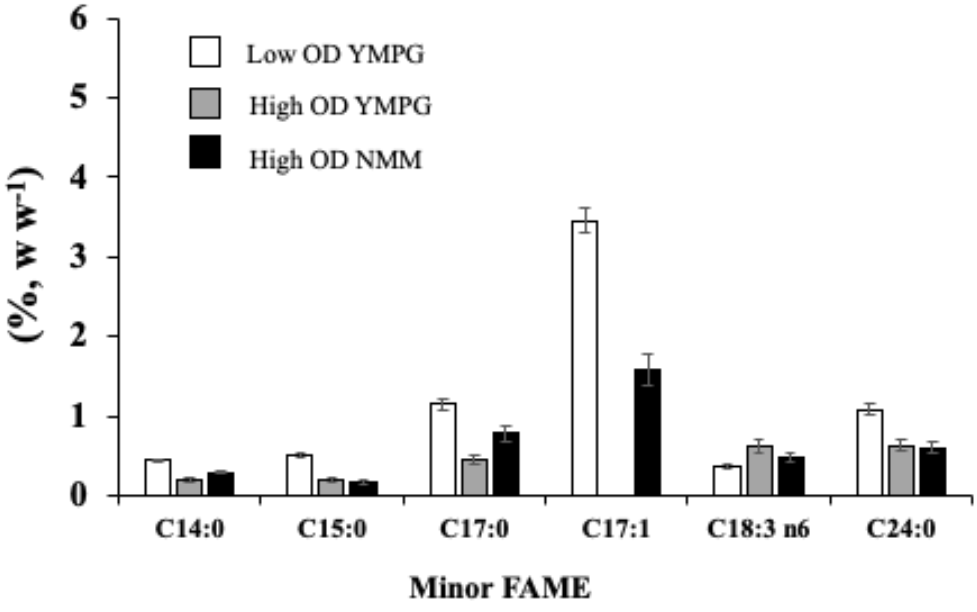

**(b)**

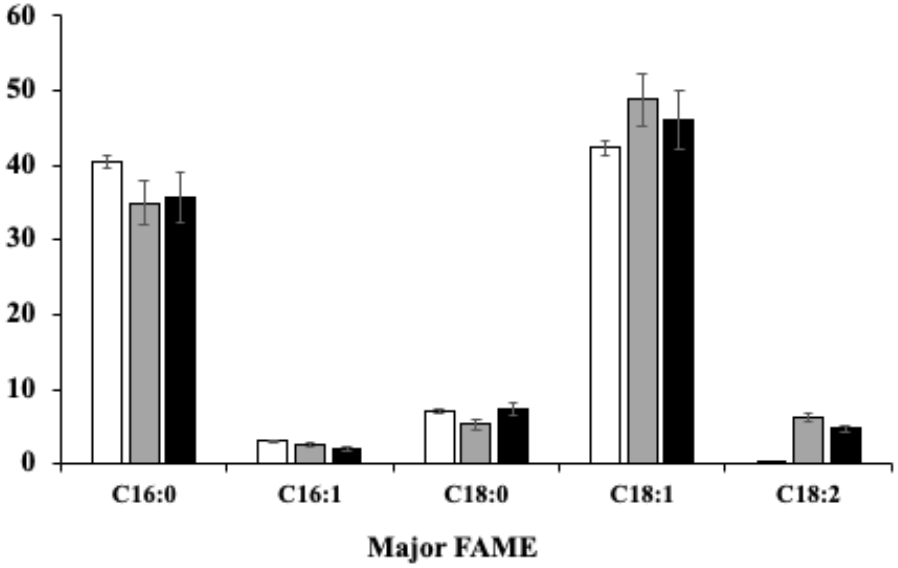
60
50
40
30
20
10
0
C16:0
C16:1
C18:0
C18:1
C18:2
Major FAME

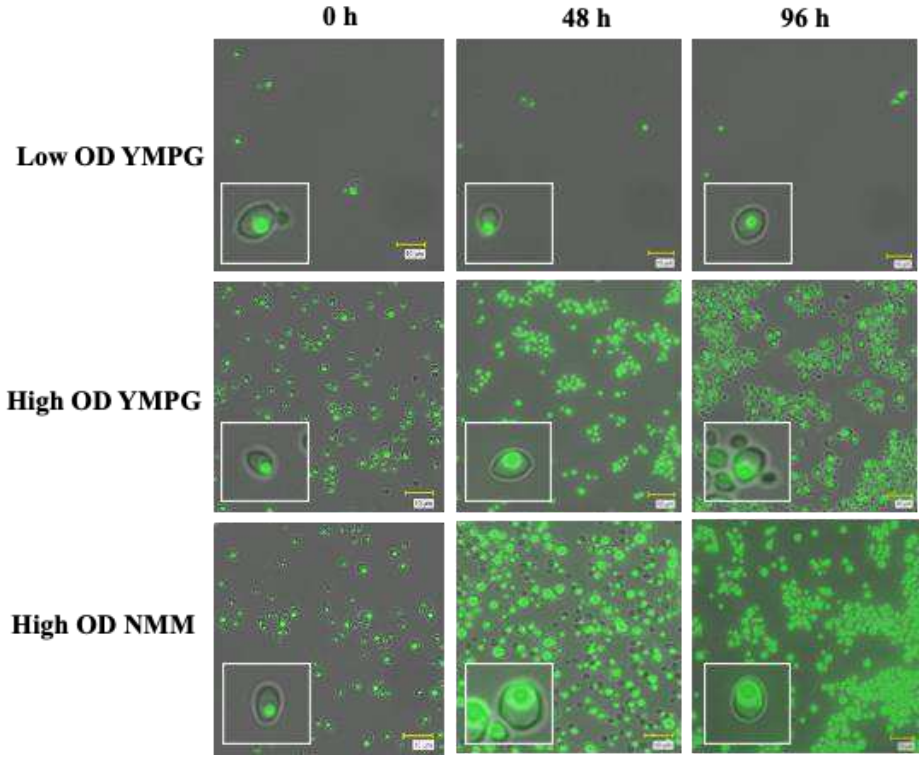
0 h
48 h
96 h
Low OD YMPG
High OD YMPG
High OD NMM

**Fig. 14** Profiles of fatty acids produced on mixed lignin derivative aldehydes and single-cell oil visualization. (a) Fatty acid profiles under different fermentation conditions. Low $OD_{600}$ YMPG (opened bars), high $OD_{600}$ YMPG (shaded bars), and high $OD_{600}$ NMM (closed bars). The results show the average of three replicates of the biological samples with error bars representing the standard deviation from the mean value. (b) Bodipy lipid visualization of *L. starkeyi* NBRC 10381.

The lipid accumulation resulting from the fermentation of mixed lignin aldehydes is detailed in Table 3. In low OD600 YMPG and high OD600 YMPG conditions, the lipid content measured 30.02% and 33.09% (w/w), respectively. However, the lipid production titer was notably higher in the high OD600 YMPG condition (8.88 g $L^{-1}$) compared to the low OD600 YMPG condition (5.61 g $L^{-1}$) due to the greater amount of DCW generated by the end of fermentation ($p < 0.05$). Mixed lignin aldehydes impacted both cell growth and lipid content in the low OD600 YMPG condition. The combined inhibition from phenolic compounds decreased the lipid content production in NBRC 10381 [119]. Additionally, the highest lipid content was attained in the high OD600 NMM condition at 54.72% (w/w), with lipid production reaching up to 14.76 g $L^{-1}$. A medium with a high C:N ratio substantially enhanced lipid accumulation in NBRC 10381 compared to a low C:N ratio medium (up to 2.6-fold). Restricted nitrogen availability within cells resulted in heightened adenosine monophosphate (AMP) deaminase activity to produce ammonium ions ($NH4^+$) (essential nitrogen supply for cell growth) by cleaving AMP into inosine monophosphate (IMP) while inhibiting the formation of isocitrate dehydrogenase

(IDH). This process facilitated the transfer of citrate into the cytosol for lipid production [120,121]. All lipids produced from mixed lignin aldehyde fermentations predominantly consisted of C18:1 and C16:0 fatty acids (Fig. 14a), indicating that different fermentation conditions did not induce major changes in the fatty acid composition of this strain. The primary fatty acids, particularly C18:1 and C16:0, were also identified in previous studies [122–124]. BODIPY 493-503 was employed in this study to visualize the accumulation of triacylglycerides within lipid bodies inside NBRC 10381 cells grown under various fermentation conditions and time intervals (Fig. 14b). The results indicated an increase in lipid bodies from 0 h to 48 h of fermentation in high OD600 YMPG and high OD600 NMM conditions. Conversely, fermentation under low OD600 YMPG conditions exhibited different outcomes due to the prolonged lag phase induced by mixed lignin aldehydes in NBRC 10381. The stained results confirmed that lipid production in NBRC 10381 on NMM was superior to that on YMPG.

## 2.4 Conclusions

This study introduces a novel biorefinery approach for converting lignin derivative aldehydes into both lignin alcohols and high-value lipids. The findings suggest that the oleaginous yeast *L. starkeyi* NBRC 10381 can efficiently generate lignin alcohols specifically, 4-hydroxybenzyl alcohol, vanillyl alcohol, and syringyl alcohol from corresponding lignin derivative aldehydes: 4-hydroxybenzaldehyde, vanillin, and syringaldehyde, respectively. The conversion of these aldehydes into alcohols via NBRC 10381 not only stimulated cell growth but also facilitated lipid accumulation. However, the combined inhibitory effect of mixed lignin aldehydes

significantly impeded cell growth. Therefore, employing strategies such as a high inoculum size and a medium with a high C:N ratio enhanced the fermentation process. This resulted in a reduction of bioconversion time by 5 days and a 2.6-fold increase in lipid production. Overall, *L. starkeyi* NBRC 10381 exhibited promising performance in producing lignin alcohols from lignin derivative aldehydes while simultaneously generating high-value single-cell oil with potential applications in biorefinery settings.

# Chapter 3

# Production of lignin monomeric alcohols and lipids from oil palm empty fruit bunch by a combination of alkaline nitrobenzene depolymerization and *Lipomyces starkeyi* bioconversion

## 3.1 Introduction

As widely acknowledged, the expansion of palm oil production is fueled by increasing demand for its versatile applications, directly correlating with rapid growth in the oil palm industry. This growth carries potential negative environmental impacts [125,126]. Indonesia, being the largest producer of crude palm oil, contributes approximately 59% of global production, yielding over 46 million tons annually and generating more than two oil palm empty fruit bunches (OPEFB) [127,128]. Consequently, it's crucial to incorporate biorefinery practices into the production process of this commodity to ensure its sustainability. To achieve environmental friendliness and optimize profits, OPEFB should be maximally utilized to produce valuable chemical feedstock from each biomass component (lignin, hemicellulose, and cellulose) for various applications [129,130]. Lignin, being one of the primary lignocellulosic constituents in biomass, is the most abundant aromatic substance of biopolymers globally, estimated at over 300 billion tons [71]. This abundance presents promising opportunities for the production of various value-added biochemicals and biofuels, making a significant contribution to sustainable development and the global economy in the foreseeable future [131,132]. However,

recent research highlights a challenge: much lignin is considered worthless fuel upon decomposition, leading to environmental pollution [19,133]. Lignin, an organic macromolecule, comprises three phenylpropanoid types: syringyl (S-lignin), guaiacyl (G-lignin), and *p*-hydroxyphenyl (H-lignin), with common degraded monomer compounds such as syringaldehyde, vanillin, and 4-hydroxybenzaldehyde representing these respective lignin groups [134,135].

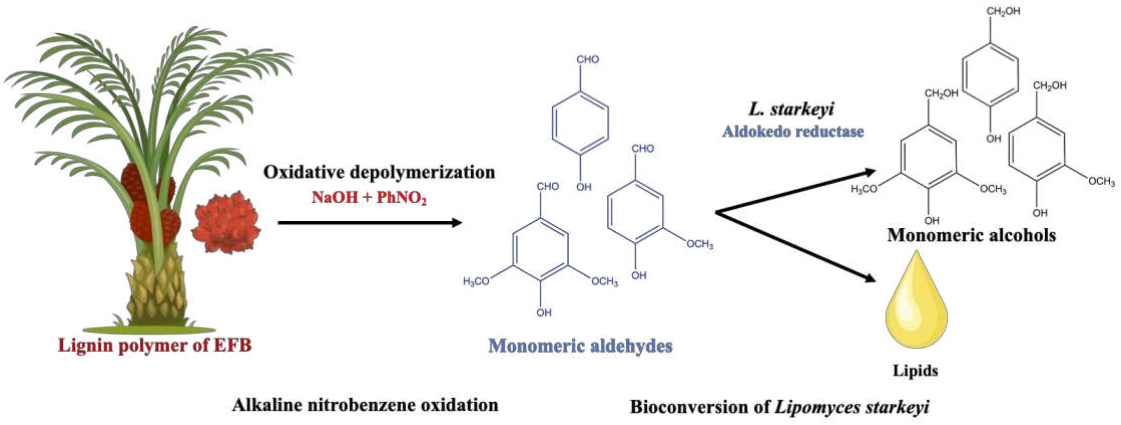


**Fig. 15** Graphical abstract of study chapter 3.

Pretreatment technology plays a vital role in lignocellulosic biorefineries. Chemical oxidative depolymerization during pretreatment has been demonstrated to effectively break down complex lignin polymers into low molecular weight aromatics, such as monomers, surpassing alternative methods [81,136]. Nitrobenzene oxidation has shown promise as a depolymerization method for producing lignin monomers when compared to other techniques like direct oxygen oxidation, cutinase hydrolysis enzyme, and manganese peroxidase (MnP) enzyme oxidation [60]. Thus,

there is a need to develop efficient depolymerization methods under mild conditions. Additionally, the possibility of biologically converting lignin monomeric aldehydes into fuels and valuable chemicals has emerged as an attractive strategy for enhancing the economic viability of biorefineries globally [83,137]. However, the potential for lignin valorization is hindered by the limited availability of microorganisms capable of efficiently metabolizing various lignin monomers and producing high-value products [138]. Previous studies have highlighted the ability of certain microorganisms, such as Trichosporon yeasts, to transform lignin monomeric aldehydes into diverse biochemicals. For instance, *T. guehoae* has demonstrated its capability to convert ferulic acid into vanillic acid [36], while *T. cutaneum* successfully converted syringaldehyde and vanillin into syringyl and vanillyl alcohol, respectively, yielding vanillic acid and syringic acid as final products [86]. However, to date, only *Lipomyces starkeyi* has been reported to efficiently convert lignin monomeric aldehydes into valuable monomeric alcohols while also producing lipids as a by-product [139]. Several studies have highlighted the pharmacological benefits of lignin monomeric alcohols. For example, 4-hydroxybenzyl alcohol has emerged as an antiasthmatic and anti-inflammatory agent [89,90], while vanillyl shows promise in Parkinson's disease research, and syringyl is commonly used as a lignin model in research due to its benzylic hydroxyl and phenolic structures [91,93]. Nonetheless, no study has been conducted utilizing palm industry waste like OPEFB to simultaneously produce valuable lignin monomeric alcohols and lipids via alkaline oxidative depolymerization and yeast bioconversion.

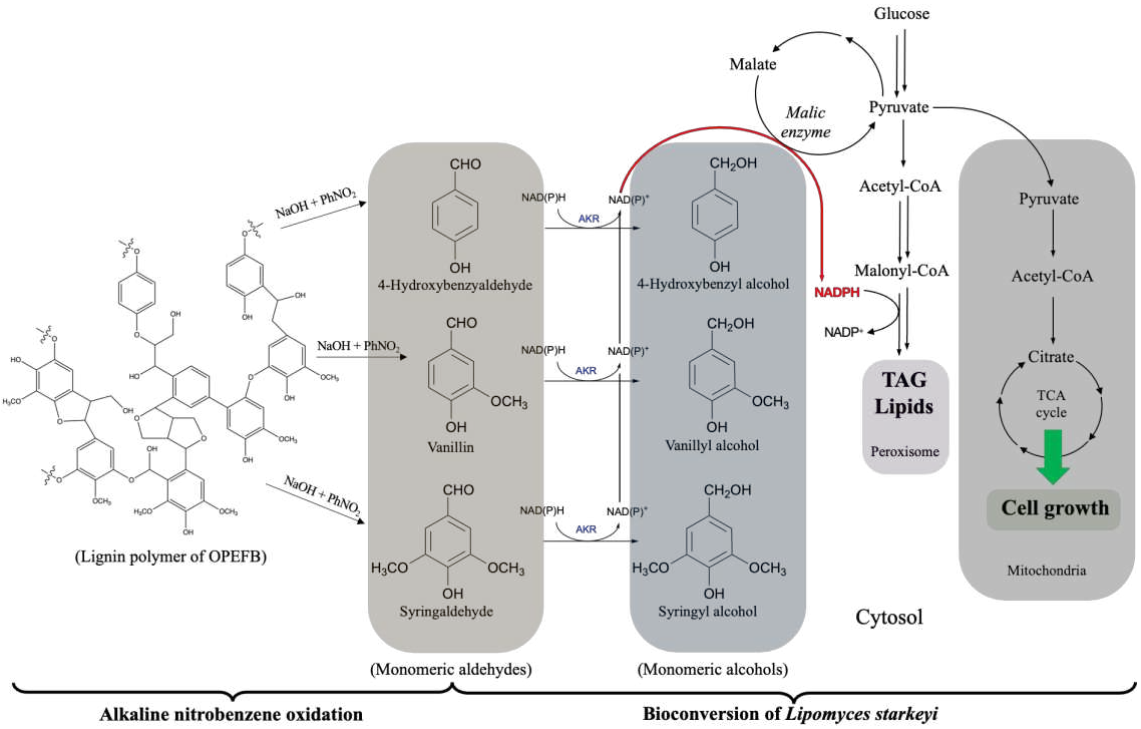


**Fig. 16** Pathway of combinatory strategy for lignin monomeric alcohols and lipid production from OPEFB using alkaline nitrobenzene oxidation and bioconversion of *Lipomyces starkeyi.*

In this study, we integrate both chemical and biological methods to efficiently generate lignin monomeric alcohols (syringyl, vanillyl, and 4-hydroxybenzyl alcohol) and lipids from OPEFB (Fig. 16). Initially, we extract lignin monomeric aldehydes from OPEFB through NaOH nitrobenzene depolymerization. Subsequently, these aldehydes are transformed into lignin monomeric alcohols and lipids using L. starkeyi. We also explore the potential of enhancing lipid production

in *L. starkeyi* through bioconversion. To enhance the conversion process, we investigate the impacts of NaOH concentration, nitrobenzene addition, and reaction time on the yield of monomeric compounds from the chemical oxidation of OPEFB lignin. This study provides a fresh perspective on the production of valuable lignin alcohols and lipids from OPEFB by combining alkaline nitrobenzene depolymerization with *L. starkeyi* bioconversion. Additionally, it presents a crucial methodology for maximizing lignin utilization through chemical biology approaches, contributing to a better understanding of future biorefinery technologies essential for industrial advancement.

## 3.2 Material and methods

### 3.2.1 Strain preparation

In this study, *Lipomyces starkeyi* D35 (NBRC10381), obtained from the National Institute of Technology and Evaluation Biological Resource Center, Japan, was used as the model organism. To maintain the yeast strain, it was stored in a 30% (w/w) glycerol solution at -80 °C. The *L. starkeyi* culture was initially grown on Potato Dextrose Agar (PDA) medium. Subsequently, for further experimentation, the yeast was transferred to a Yeast Malt Peptone Glucose (YMPG) agar medium containing 20 g L–1 agar, 10 g L–1 glucose, 5 g L–1 peptone, 3 g L–1 malt extract, and yeast extract. Incubation was carried out for 2 days at 30 °C.

### 3.2.2 Raw material, reagents, medium, and fermentation conditions

The original Oil Palm Empty Fruit Bunch (OPEFB) was sourced from Indonesia, provided by an oil palm plantation in Sukabumi, Indonesia. The OPEFB underwent crushing into small flakes (0.7 mm mesh) and was subsequently dried in a plastic beaker covered with aluminum foil at 80 °C overnight (for at least 20 hours), followed by a cooling period of 30 – 45 minutes. Before analysis and pretreatment, the biomass was stored in a sealed bag at room temperature. Commercial lignin monomers, such as syringaldehyde, vanillin, 4-hydroxybenzaldehyde, syringic acid, vanillic acid, 4-hydroxybenzoic acid, and hydroxycinnamic acids like ferulic acid and *p*-coumaric acid, were obtained from Sigma Aldrich Co. LLC. 4-hydroxybenzyl and vanillyl alcohol were acquired from Tokyo Chemical Industry Co. Ltd (Japan), while syringyl monomer alcohol was sourced from Thermo Fisher Scientific Inc. (USA). Sodium hydroxide, nitrobenzene, sulfuric acid, ethyl acetate, and methanol were procured from Nacalai Tesque (Japan). For fermentation, a single colony was transferred into YMPG-50 (12 mL) liquid medium (with 50 g $L^{-1}$ glucose, 5 g $L^{-1}$ peptone, 3 g $L^{-1}$ malt extract, and yeast extract) within a 100 mL Erlenmeyer flask for pre-culture overnight. The pre-culture was then transferred to a new 12 mL YMPG-50 medium supplemented with three different groups of lignin monomers as the main culture. These groups included aldehydes medium (consisting of 4.81 nM syringaldehyde, 0.64 nM vanillin, and 0.05 mM 4-hydroxybenzaldehyde), aldehydes-acids medium (with 4.81 nM syringaldehyde, 0.64 nM vanillin, 0.05 mM 4-hydroxybenzaldehyde, 0.54 mM syringic acid, 0.12 mM vanillic acid, and 2.25 mM 4-hydroxybenzoic acid), and OPEFB, which was dried lignin monomeric powder obtained from NaOH nitrobenzene oxidative depolymerization. Inoculation

was done using a specific optical density ($OD_{600}$) value of 1 in a 100 mL flask and subjected to incubation in a BioShaker BR-43FH MR orbital incubator shaker (Taitec Corp., Japan) at 190 rpm and 30 °C under aerobic conditions.

### 3.2.3 Alkaline nitrobenzene oxidative pretreatments

The pretreatment procedure, involving alkaline nitrobenzene oxidation, was applied to 0.2 g of dried treated OPEFB mixed with 0.5 mL of nitrobenzene (PhNO2) in solutions containing 1, 5, and 10% wt. of sodium hydroxide (NaOH) in 10 mL volumes. A control group, lacking nitrobenzene, was included for comparison. The oxidation reaction was carried out using a laboratory-scale thermostirrer (LT) HHE-19G-UP (Koike Precision Instruments, Kawasaki, Japan), which combines a heater and magnetic stirrer. The LT was programmed to gradually increase the temperature to the desired level at a rate of around 4 °C per minute. The samples were treated at 180 °C for varying durations of 30, 60, 120, and 180 minutes. Following treatment, 30 mL of chloroform was added to the mixture to eliminate excess nitrobenzene and its reduced byproducts, which were then separated through centrifugation at 3000 rpm for 5 minutes, yielding a bottom layer. Concentrated sulfuric acid was utilized to adjust the pH to 1-2 for the extraction of oxidation products. Subsequently, three rounds of extraction were performed using 10 mL of ethyl acetate (EtOAc), and the solvent was evaporated using a rotary evaporator. This pretreatment process is illustrated in Figure 17. Finally, the dried oxidation products were dissolved in 1 mL of methanol for further analysis using HPLC-UV/Vis [60].

### 3.2.4 Determination of cell growth

A gravimetric method was utilized to ascertain the Dry Cell Weight (DCW) by employing 0.5 mL of the cultivation samples. The cells were separated via centrifugation at 14,000 × g for 5 minutes. Subsequently, the cells were washed with sterilized water and then subjected to overnight lyophilization at a freezing temperature of -80 °C using a freeze dryer (Freeze Dry, FreeZone from Labconco, USA) to eliminate any residual moisture. The DCW was then determined based on the weight of the dried cells. The growth rate of the cells within the initial 24 hours was calculated using Equation 1.

*L. starkeyi* growth rate (g DCW $L^{-1}$ $h^{-1}$)

$$= \frac{\text{Total increment of cell number } (\text{g DCW L}^{-1})}{\text{Total time of increment (h)}} \quad (1)$$

### 3.2.5 Glucose quantification by HPLC-RID

Throughout the fermentation process, glucose concentration was determined using an HPLC (high-performance liquid chromatography) system (Shimadzu, Japan) coupled with a RI (refractive index) detector. This setup featured an ICSep Coregel-87H column (7.8 mm i.d. and 300 mm length, supplied by Transgenomic). Prior to analysis, the samples underwent centrifugation at 14,000 × g for 5 minutes, followed by filtration using a 0.22 μm filter to prepare the supernatant. The analysis involved injecting a 20 μL sample volume, with the column oven maintained at 80 °C. A mobile phase comprising 5 mM $H_2SO_4$ was used, with a flow rate of 0.6 mL

min–1 [140]. The glucose consumption rate during fermentation within the initial 24 hours was calculated using Equation 2.

Glucose consumption rate (g $L^{-1}$ $h^{-1}$)

$$= \frac{\text{Total glucose consumed by } L.starkeyi \text{ (g L}^{-1}\text{)}}{\text{Total time of glucose consumed by } L.starkeyi \text{ (h)}} \quad (2)$$

### 3.2.6 Lignin monomers quantification by HPLC-UV/Vis

The quantification of lignin derivatives was conducted using an HPLC-20AB system (Shimadzu, Japan), outfitted with an ultraviolet-visible spectroscopy (UV/Vis) detector SPD-20A. Analysis was performed employing a C18 column (250 mm length x 4.6 mm, 5µm particle size) obtained from Supelco Ascentis (Merck KGaA, Darmstadt, Germany). Supernatant samples were prepared for analysis by centrifugation at 14,000 × g for 5 minutes followed by filtration using a 0.22 µm filter. Each measurement involved injecting 10 µL of sample, and the column temperature was maintained at 30 °C for 45 minutes. The mobile phase consisted of a mixture of methanol and ultra-pure water in a ratio of 18:82 v/v with the addition of 0.2% (v/v) acetic acid, flowing through the column at a rate of 1 mL min–1. Analyte measurements were conducted at a wavelength of 280 nm [139]. The product yield of lignin monomers produced from OPEFB was calculated based on Equation 3.

Lignin monomeric product yield (%)

$$= \frac{\text{lignin monomer produced (g L}^{-1}\text{)}}{\text{Initial OPEFB (g L}^{-1}\text{) used in pretreatment}} \times 100 \quad (3)$$

### 3.2.7 Single-cell oil measurement

The quantification of single-cell oil (lipid) production was conducted using a gravimetric method, following the procedure outlined by Floch [95]. Freeze-dried samples weighing 20 mg were placed into 2 mL O-ring cap-sealed micro vials (Watson, Japan). Zirconia balls were added to aid in extraction. An extraction solvent comprising a chloroform:methanol mixture in a 2:1 v/v ratio, totaling 1.5 mL in volume, was used for lipid extraction. The cells were then pulverized at 1500 rpm for 15 minutes using a Master Neo pulverizer (Bio Medical Science, Japan). Subsequently, the cells underwent centrifugation at 14,000 × g for 5 minutes. The resulting cell pellets were washed with sterilized water and dried at 60 °C until reaching a constant weight. The lipid content was determined by the difference in weight before and after drying and expressed as a percentage of the Dry Cell Weight (DCW).

### 3.2.8 Fatty acid methyl esters quantification by GC/MS

The fatty acid methyl esters (FAMEs) derived from the lipids of the lyophilized samples were obtained via a transesterification process outlined in the FAMEs kit mix (Nacalai Tesque, Japan). The resulting FAMEs were dissolved in hexane and analyzed using GC/MS (gas chromatography-mass spectrometry) QP-2010 (Shimadzu, Japan). To provide a reference, an internal standard, C8:0 (caprylic acid), was added to the sample. Analysis was conducted using a capillary GC column DB-

23 (0.25 mm i.d. 60 m length, 0.25 mm thickness) (Agilent), with helium serving as the carrier gas. A sample injection volume of 1 μL was utilized, and the analysis employed split injection with an inlet temperature of 250 °C. The oven temperature program began at 50 °C for 1 minute, followed by a gradient increase at 25 °C min–1 until reaching 175 °C, then further elevated to 230 °C at a rate of 4 °C min–1, and held for 6 minutes. The MS detector operated at 250 °C and scanned the 40 to 500 m/z range. Identification and quantification of fatty acids were accomplished by comparing retention times (rt) and m/z patterns with a fatty acid standard, SUPELCO 37 FAME mix (Sigma–Aldrich) [95].

## 3.3 Results and discussion

### 3.3.1 Monomeric aldehydes production via alkaline nitrobenzene oxidation

In this study, we derived lignin monomeric aldehydes from OPEFB lignin using a combination of sodium hydroxide and nitrobenzene oxidative depolymerization (Fig. 17). Subsequently, these aldehydes were utilized in the synthesis of valuable lignin alcohols employing *L. starkeyi*. The quantity of monomeric compounds generated from lignin nitrobenzene oxidation was affected by the concentration of sodium hydroxide and the duration of the reaction, as depicted in Fig. 18. The production encompassed three primary lignin aldehydes: syringaldehyde, vanillin, and 4-hydroxybenzaldehyde. However, given the source was raw biomass, it was anticipated that not only lignin aldehydes but also monomeric acids (such as vanillic, syringic, and 4-hydroxybenzoic acid) and related hydroxycinnamic acids (HCAs) like p-coumaric acid and ferulic acid would be formed during the reactions (Fig. 18c).

The occurrence of HCAs from lignin polymer took place at relatively low temperatures during the initial reaction in the alkaline nitrobenzene oxidation process, involving the breakdown of ester bonds and specific ether linkages [141,142]. These characteristic monomeric compounds had also been identified in prior research employing alkaline nitrobenzene oxidation [60,143]. The outcomes (Fig. 18) revealed a consistent trend in the production levels of all monomeric compounds, indicating that the presence of nitrobenzene in the oxidation process resulted in higher yields compared to those obtained without it. Nitrobenzene acted as a potent oxidizing agent in the sodium hydroxide solution, generating a nitrobenzene radical anion that facilitated the cleavage of major lignin linkages, including α-O-4 and β-O-4 [144]. Additionally, increasing the concentration of NaOH in the reaction contributed to significant enhancements in the production of monomeric compounds. The findings indicated that the optimal titer of all monomeric lignin productions was achieved when using a 10% NaOH concentration in the reaction. It has been demonstrated that alkalinity plays a crucial role in the nitrobenzene oxidation of lignin, as it facilitates the cleavage of ether and ester linkages, accelerates oxidation reactions leading to retro-aldol cleavage of C$\alpha$-C$\beta$ bonds in the phenylpropane units (β-O-4), promotes hydrolysis, and stabilizes intermediates, ultimately creating conditions conducive to efficient depolymerization and yielding the desired monomeric compounds [144].

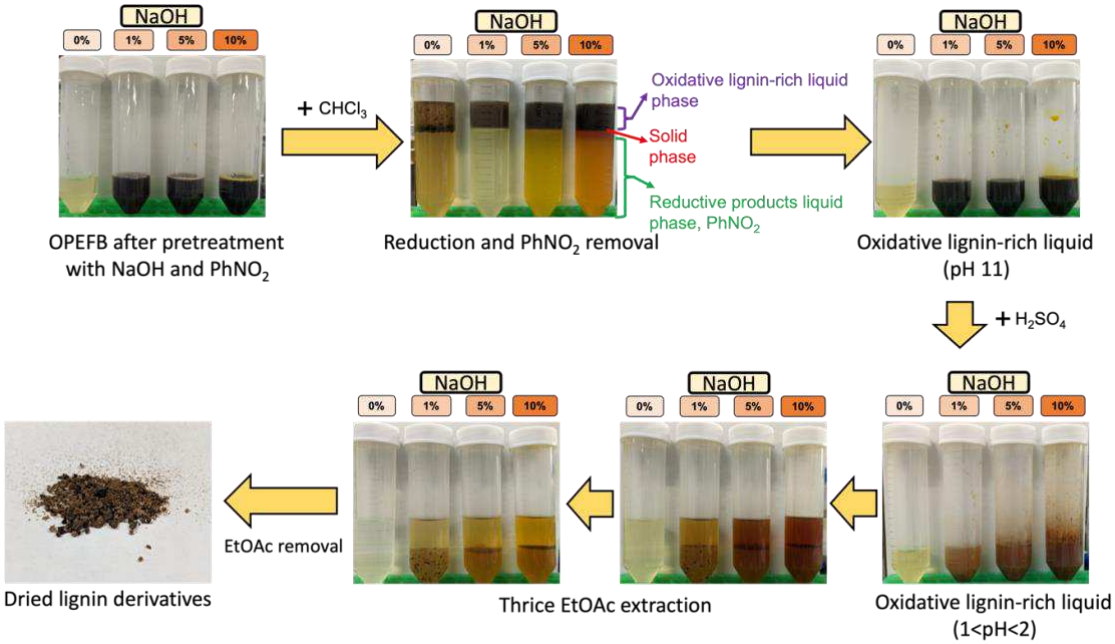


**Fig. 17** The workflow of lignin monomeric productions via alkaline nitrobenzene oxidative depolymerization from oil palm empty fruit bunch.

The highest produced aldehyde was syringaldehyde (3.49 mM at 60 min) that overpassed 4-hydroxybenzaldehyde (1.11 mM at 60 min), while vanillin is achieved to 4.81 mM at 60 min. The holding time of the reaction is another considerable parameter of enhancing titer yield. Increasing the reaction time after the reaching optimal time, 60 min, led to a decrement of syringaldehyde (3.66 mM at 180 min) and vanillin (0.43 mM at 180 MM) titer. The longer reaction time may make primary aldehydes to be over-oxidized to further convert to acid form, syringic acid [145]. Different molecular structures have various susceptibilities to oxidative degradation, which induce producing different aromatic products during the nitrobenzene oxidation [144]. The different optimum time of the highest titer of all the oxidation

products (aldehydes, acids, and HCAs) directly show the impact of the duration of oxidation on the final monomeric products formed during the nitrobenzene oxidation.

a)

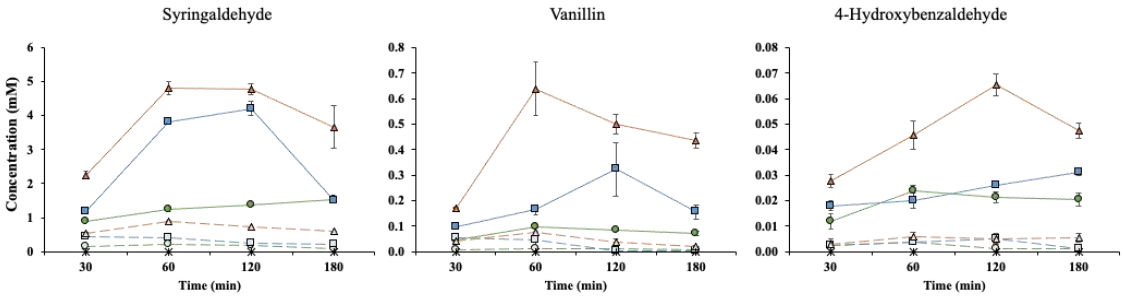


b)

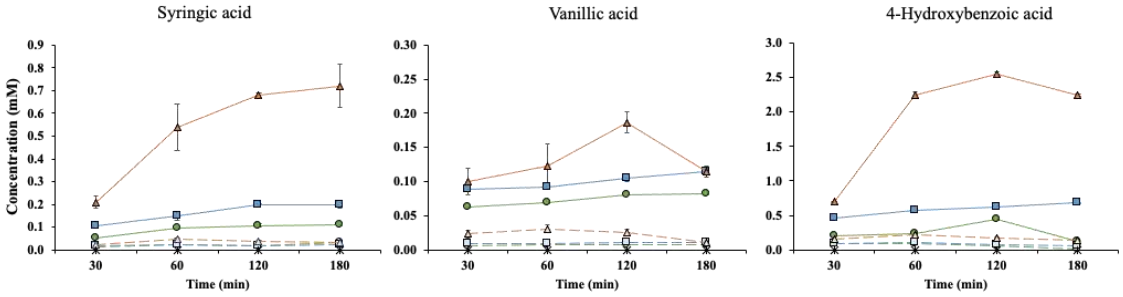


c)

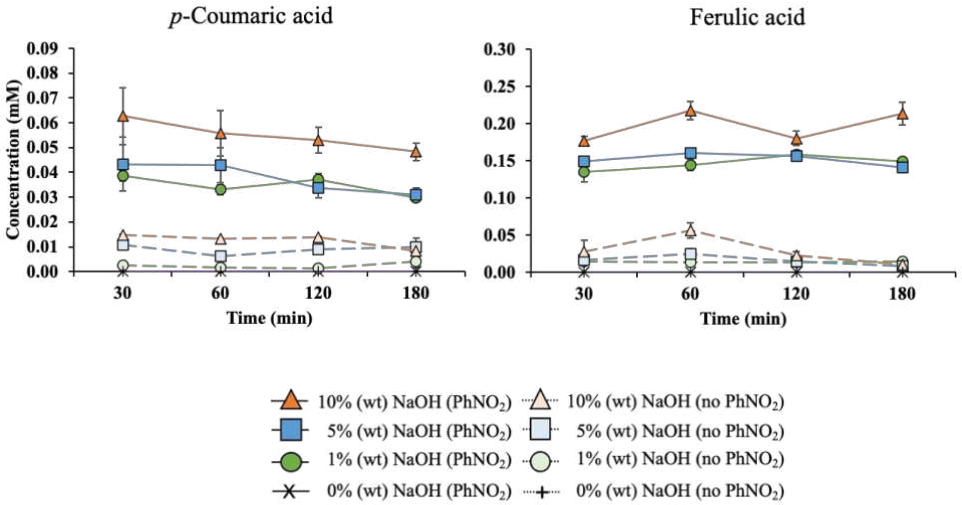

**Fig. 18** Effect of sodium hydroxide concentration and reaction time on the titer of (a) lignin monomeric aldehydes, (b) lignin monomeric acids, and (c) hydroxycinnamic acids productions. The results presented the mean of three biological replicate samples with error bars illustrating the standard deviation from the mean value in the dataset.

The alkaline nitrobenzene oxidation of biomass often yields lignin monomeric aldehydes, with vanillin and syringaldehyde being the most frequent ones. The presence of these aldehydes is indicated by the amount of the guaiacyl and syringyl unit groups in the lignin [146]. On the contrary, our investigation yielded two primary lignin monomers: syringaldehyde and 4-hydroxybenzoic acid. According to the previous study, the lignin in OPEFB fiber was shown to have the largest proportion of syringyl groups [147]. The highest concentration of syringaldehyde was mostly derived from the oxidation of syringyl units in OPEFB. Under alkaline conditions, the ester bonds that connect phenolic acids can be easily broken at low temperatures. However, the cleavage of phenolic β-aryl ethers requires high temperatures and oxidizing agents. Therefore, when nitrobenzene is used as an oxidant, the amount of syringaldehyde produced from the breakdown of syringyl units increases dramatically, especially in highly alkaline conditions. In the context of a significant increase in the formation of 4-hydroxybenzoic acid, Sun et al. [148] conducted a study that revealed a significant amount of esterified p-hydroxybenzoic acid present in the OPEFB lignin. The conversion of p-coumaric acid to 4-hydroxybenzaldehyde was then transformed into hydroxybenzoic acid. This conversion was facilitated by the high alkalinity environment and the presence of nitrobenzene, which acted as a

powerful oxidant. These factors contributed to the high concentration of 4-hydroxybenzoic acid [141,149]. As a result, the concentration of *p*-coumaric acid decreases significantly with longer reaction time, as shown in Figure 18c.

### 3.3.2 Fermentation profile of *L. starkeyi* under various lignin derivatives

The lignin monomeric aldehydes, such as syringaldehyde, vanillin, and 4-hydroxybenzaldehyde, were obtained from OPEFB through alkaline nitrobenzene oxidative depolymerization. These monomeric derivatives were then utilized as a substrate to produce valuable lignin alcohols through bioconversion using *L. starkeyi* NBRC 10381, as shown in Fig. 16. The fermentation process utilized the most concentrated amount of lignin aldehydes created through the oxidation of alkaline nitrobenzene, specifically using a 10% NaOH solution with nitrobenzene for a reaction duration of 60 minutes (Table 4). In order to assess the ability of *L. starkeyi* to convert monomeric aldehydes derived from OPEFB into monomeric alcohols, a simulated fermentation medium was created using commercially available chemicals that had a comparable composition as shown in Table 4. The study included three distinct medium profiles: OPEFB (comprising lignin monomeric derivatives from OPEFB in YMPG-50), aldehydes (consisting solely of monomeric aldehydes from commercial chemicals in YMPG-50), and aldehydes-acids (comprising monomeric aldehydes and acids without HCAs from commercial chemicals in YMPG-50). The control group consisted of YMPG-50 without any lignin.

**Table 4** Lignin monomeric compounds produced in 10 % of NaOH with nitrobenzene for 60 min.[a]

| Monomer lignin | Concentration (mM) | Production yield (%) |
|---|---|---|
| Aldehydes | | |
| 4-Hydroxybenzaldehyde | 0.05 ± 0.01 | 0.03 ± 0.01 |
| Vanillin | 0.64 ± 0.10 | 0.49 ± 0.08 |
| Syringaldehyde | 4.81 ± 0.21 | 4.39 ± 0.19 |
| Acids | | |
| 4-Hydroxybenzoic acid | 2.25 ± 0.04 | 1.55 ± 0.03 |
| Vanilllic acid | 0.12 ± 0.03 | 0.10 ± 0.03 |
| Syringic acid | 0.54 ± 0.10 | 0.53 ± 0.10 |
| HCAs | | |
| *p*-Coumaric acid | 0.06 ± 0.01 | 0.05 ± 0.01 |
| Ferulic acid | 0.22 ± 0.01 | 0.21 ± 0.01 |

[a] The reported results provide the mean of three biological replicate samples with error bars illustrating the standard deviation from the mean value in the dataset.

a)

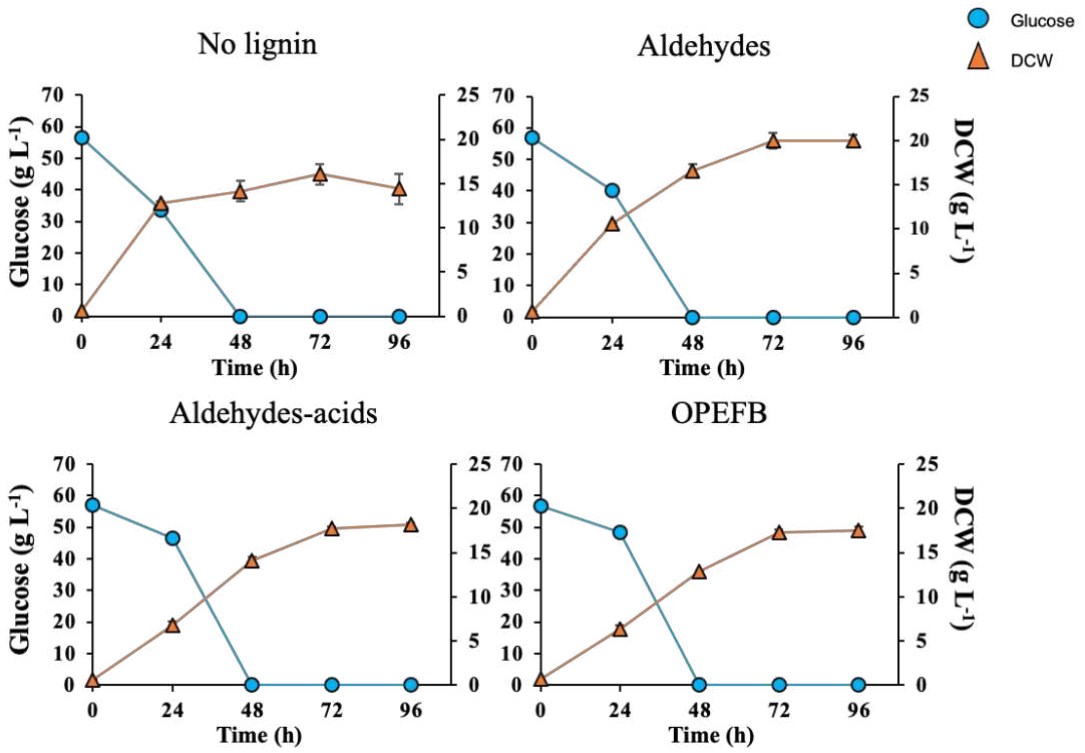


b)

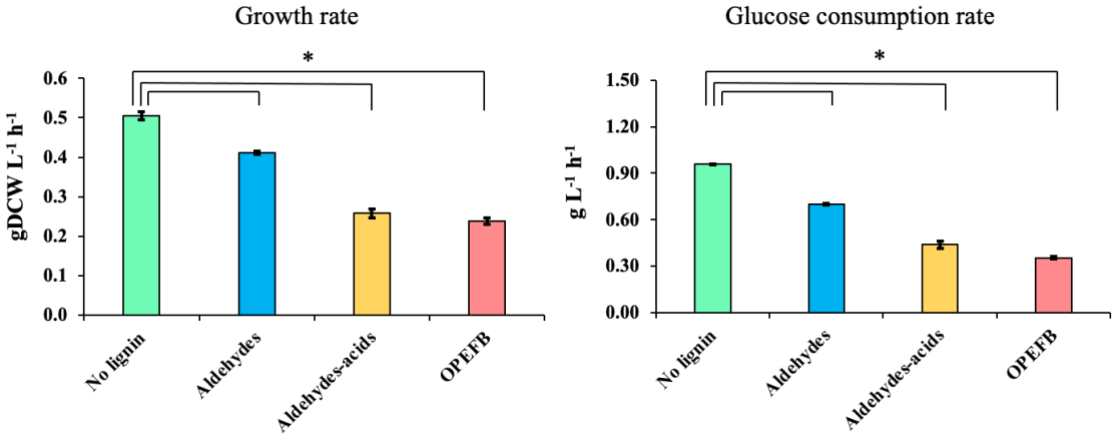


**Fig. 19** Fermentation profiles of *L. starkeyi* under different mediums. (a) Time courses for cell growth and glucose consumption in different mediums. (b) Growth and glucose consumption rates in different medium fermentation. The results

presented the mean of three biological replicate samples with error bars illustrating the standard deviation from the mean value in the dataset. *The statistical analysis employed Student's t-test, with significance set at a p-value < 0.05.

Based on the fermentation profile data, the growth of *L. starkeyi* on the aldehydes, aldehydes-acids, and OPEFB medium outperformed no lignin medium (Fig. 19a). The highest DCW produced was on the aldehydes fermentation that reached up to 19.94 g $L^{-1}$, followed by aldehydes-acids at 18.17 g $L^{-1}$ and OPEFB at 17.54 g L−1. On the other hand, growth on no lignin media only acquired up to 14.38 g $L^{-1}$. Growth on no lignin likewise reaches a stationary phase and plateau after 48 h of fermentation. Meanwhile, the rest of the fermentation profiles grew until 72 h before entering the stationary phase, even though the presence of the lignin derivatives in the fermentation could impede the cells from developing. *L. starkeyi* was discovered to have the ability not only to tolerate diverse phenolic aromatic compounds but also to utilize them and create additional molecules [139,150,151]. In the previous work, the *L. starkeyi* NBRC 10381 was found to be able to convert all types of monomeric aldehydes and create useful lignin monomeric alcohols by using the AKR (aldehyde-ketone reductase) enzyme intracellularly. The conversion of a lignin monomeric aldehyde to alcohol by AKR releases one $NAD(P)^+$ generation that is potentially employed for the conversion from malate towards pyruvate by releasing cytosolic NAD(P)H. This pyruvate is possibly connected to the Krebs cycle for cell development [139,152] and also for triacylglyceride (TAG) lipid synthesis (Fig. 16). This explains why the fermentation on no lignin shows a higher growth rate and glucose consumption rate compared to others. *The L. starkeyi* grows quicker

during the log phase at first 24 h (Fig. 19b) because the cell could be only concentrated on generating cells by utilizing glucose instead of converting the lignin derivatives.

### 3.3.3 Conversion of lignin monomeric aldehydes to valuable alcohols

The measured products included monomeric alcohols (syringyl, vanillyl, 4-hydroxybenzyl alcohol) derived from monomeric aldehydes, as well as all other monomeric aldehydes and acids. Figure 20 shows the conversion of lignin monomeric aldehydes by *L. starkeyi*. Syringaldehyde underwent conversion to syringyl alcohol within a fermentation period of 24 hours in the aldehydes-only medium. Vanillin underwent a conversion to vanillyl alcohol, along with a minor quantity of 4-hydroxybenzaldehyde, which was also turned into its alcohol counterpart (4-hydroxybenzyl alcohol) without the occurrence of any undesired lignin monomeric acids. A comparable trend was also seen in the fermentation process of aldehydes-acids and OPEFB. All aldehydes derived from lignin monomers present in the culture, such as syringaldehyde, vanillin, and 4-hydroxybenzaldehyde, were transformed into their corresponding alcohols, namely syringyl alcohol, vanillyl alcohol, and 4-hydroxybenzyl alcohol. At the start of the medium, there are many types of lignin monomeric acid, such as syringic acid, vanillic acid, and 4-hydroxybenzoic acid. There is no apparent evidence of any significant impact on the cells of *L. starkeyi*. However, all the individual units of lignin acid were still present on the medium.

a)

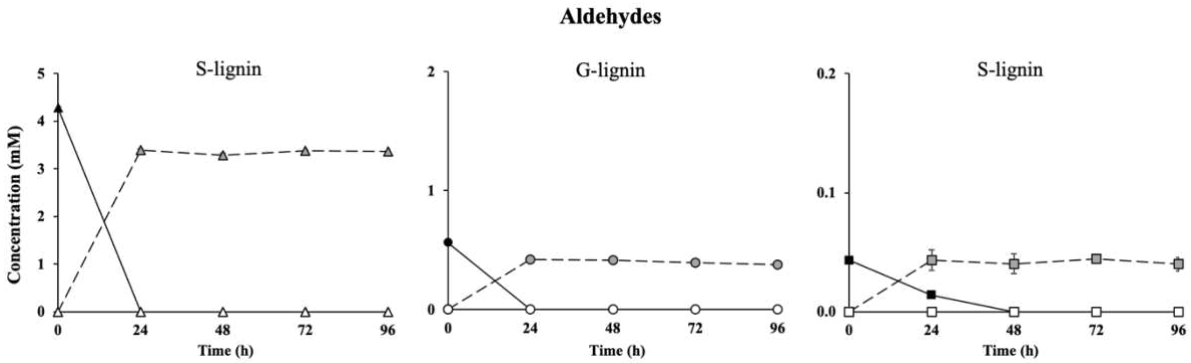
Aldehydes
S-lignin
G-lignin
S-lignin
Concentration (mM)
Time (h)

b)

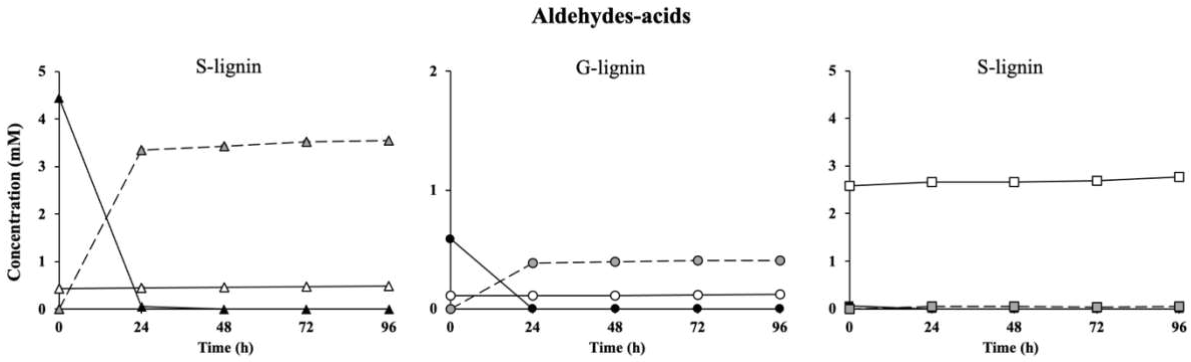
Aldehydes-acids
S-lignin
G-lignin
S-lignin
Concentration (mM)
Time (h)

c)

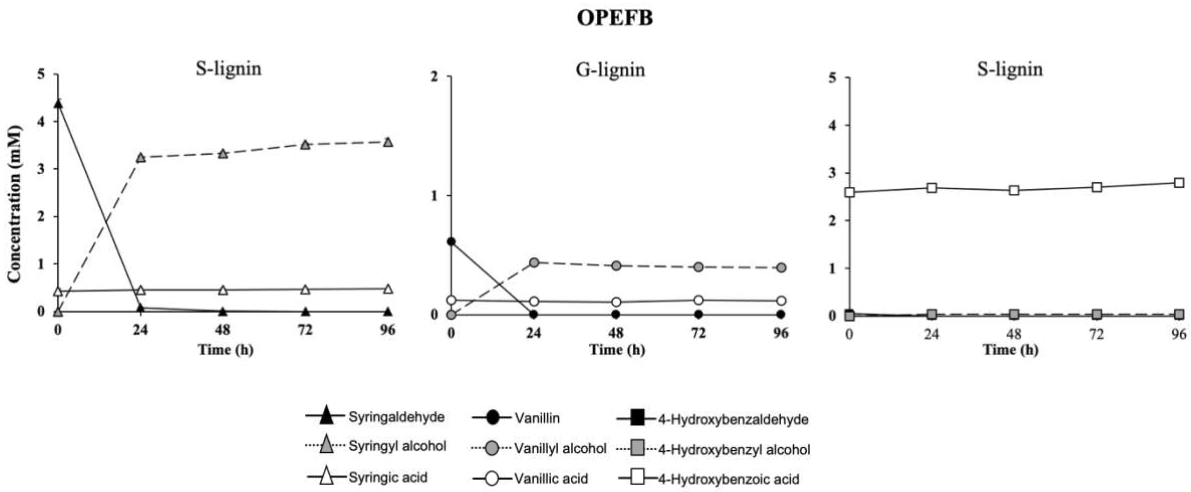
OPEFB
S-lignin
G-lignin
S-lignin
Concentration (mM)
Time (h)
Syringaldehyde
Vanillin
4-Hydroxybenzaldehyde
Syringyl alcohol
Vanillyl alcohol
4-Hydroxybenzyl alcohol
Syringic acid
Vanillic acid
4-Hydroxybenzoic acid

**Fig. 20** Biodegradation of lignin monomeric aldehydes into monomeric alcohols during fermentation. (a) Aldehydes (monomeric aldehydes-only). (b) Aldehydes-acids (monomeric aldehydes and monomeric acids). (c) OPEFB (all lignin monomeric derivatives from OPEFB). The results presented the mean of three biological replicate samples with error bars illustrating the standard deviation from the mean value in the dataset.

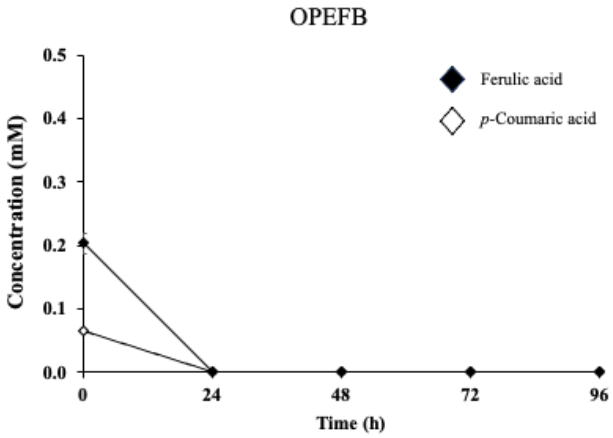


**Fig. 21** Depletion of hydroxycinnamic acids in OPEFB during fermentation. The results presented the mean of three biological replicate samples with error bars illustrating the standard deviation from the mean value in the dataset.

Three essential genes are involved in the bioconversion of lignin monomeric aldehydes. The genes AKR, ADH (alcohol dehydrogenase), and ALDH (aldehyde dehydrogenase) are included in this list [86]. In the previous work, the expression of the AKR gene was significantly upregulated in the presence of the phenolic chemical during fermentation. AKR is renowned for its ability to convert monomeric aldehydes into alcohols by means of reduction [106]. In contrast, the ALDH gene,

which is responsible for the conversion of aldehydes into acids, and the ADH gene, which is responsible for the conversion of alcohols into aldehydes, were found to be inactive [107]. The evidence reveals that *L. starkeyi* exhibits a predilection for converting monomeric aldehydes into monomeric alcohols rather than monomeric acids. After the production of all the individual alcohol molecules, they remained unchanged in the external environment without undergoing any more chemical reactions. The acids present in the aldehydes-acids and OPEFB mediums persist throughout the fermentation process.

Regarding the presence of HCAs in the OPEFB, *L. starkeyi* was capable of metabolizing both p-coumaric acid and ferulic acid without any detrimental effect on its cells (Fig. 21). Hydroxycinnamic acids, such as *p*-coumaric acid and ferulic acid, are known to be toxic to various microorganisms. This toxicity arises from their ability to disrupt the integrity of microbial membranes, interfere with cellular metabolism, and induce oxidative stress by generating reactive oxygen species (ROS). These effects ultimately hinder the growth and survival of the microorganisms [153]. Figures 19a and 20 indicate that *L. starkeyi* is capable of simultaneously absorbing monomeric aldehydes and glucose, in contrast to the sequential assimilation found in other situations. The simultaneous usage of lignin monomers and glucose has great potential for improving the efficiency of converting lignocellulosic biomass, which could lead to reduced costs associated with lignin alcohol and lipid synthesis. This technique is well-suited to the cost-effective goals of the bioprocess industry, offering a valuable opportunity to improve efficiency and economic sustainability [117].

### 3.3.4 Intracellular lipid accumulation and fatty acid profiling

Monomeric alcohol has numerous advantages for pharmaceuticals, and the intracellular lipids collected by L. starkeyi also show potential for biofuel production because of their physicochemical and metabolic features. *L. starkeyi* is known for its ability to accumulate a significant amount of lipids (up to 70%) within its cell bodies [111]. In Table 5, the lipid production of L. starkeyi was determined at 96 hours during the fermentation of several lignin monomeric media. The fermentation of OPEFB resulted in a lipid content of 33.40% (w $w^{-1}$) and a dry cell weight of 17.54 g $L^{-1}$. The lipid content reached 35.78% (w $w^{-1}$) and the dry cell weight was 18.17 g $L^{-1}$ when grown on aldehydes-acids medium. The lipids attained their maximum production, with a cell mass of 39.38% (w $w^{-1}$) and 19.94 g $L^{-1}$, when the aldehydes-only medium was used. The findings obtained from the no-lignin fermentation were significantly lower than these results, as shown by a student's t-test ($p < 0.05$). The AKR enzyme catalyzes the conversion of monomeric aldehydes into alcohols, resulting in the production of extra $NAD(P)^+$. The surplus of $NAD(P)^+$ could potentially be used for converting malate to pyruvate by releasing cytosolic NAD(P)H [152]. Pyruvate may be connected to the Krebs cycle, and subsequently, NAD(P)H is utilized for FAS (fatty acid synthase), which is crucial for the manufacture of fatty acids [110,111]. The medium containing only aldehydes resulted in the maximum lipid accumulation and dry cell weight, followed by the medium containing both aldehydes and acids, and the fermentation of OPEFB. It is possible that the presence of lignin monomeric acids and hydroxycinnamic acids during fermentation could hinder cell productivity. The antibacterial capabilities of lignin monomeric acids can potentially disrupt cellular processes within microbes,

leading to harm to the cell [48]. HCAs, similar to lignin monomeric acids, have been recognized for their cytotoxicity due to their ability to induce oxidative stress. They achieve this by generating reactive oxygen species (ROS) that disrupt cellular metabolism [153].

**Table 5** Dry cell weight and lipid production of *L. starkeyi* in.[a]

| Conditions | Time (h) | Initial DCW ($g\ L^{-1}$) | Final DCW ($g\ L^{-1}$) | Initial lipid content (%, w $w^{-1}$) | Final lipid content (%, w $w^{-1}$) | Lipid titer ($g\ L^{-1}$) |
|---|---|---|---|---|---|---|
| No lignin | 96 | 0.60 ± 0.07 | 14.38 ± 1.76 | 10.06 ± 0.67 | 31.55 ± 2.17 | 4.54 ± 0.04 |
| Aldehydes | 96 | 0.65 ± 0.07 | 19.94 ± 0.65 | 10.06 ± 0.67 | 39.38 ± 2.67 | 7.85 ± 0.02 |
| Aldehydes-acids | 96 | 0.65 ± 0.11 | 18.17 ± 0.26 | 10.06 ± 0.67 | 35.78 ± 0.56 | 6.50 ± 0.00 |
| OPEFB | 96 | 0.67 ± 0.20 | 17.54 ± 0.41 | 10.06 ± 0.67 | 33.40 ± 1.68 | 5.86 ± 0.01 |

[a] The reported results provide the mean of three biological replicate samples with error bars illustrating the standard deviation from the mean value in the dataset.

a)

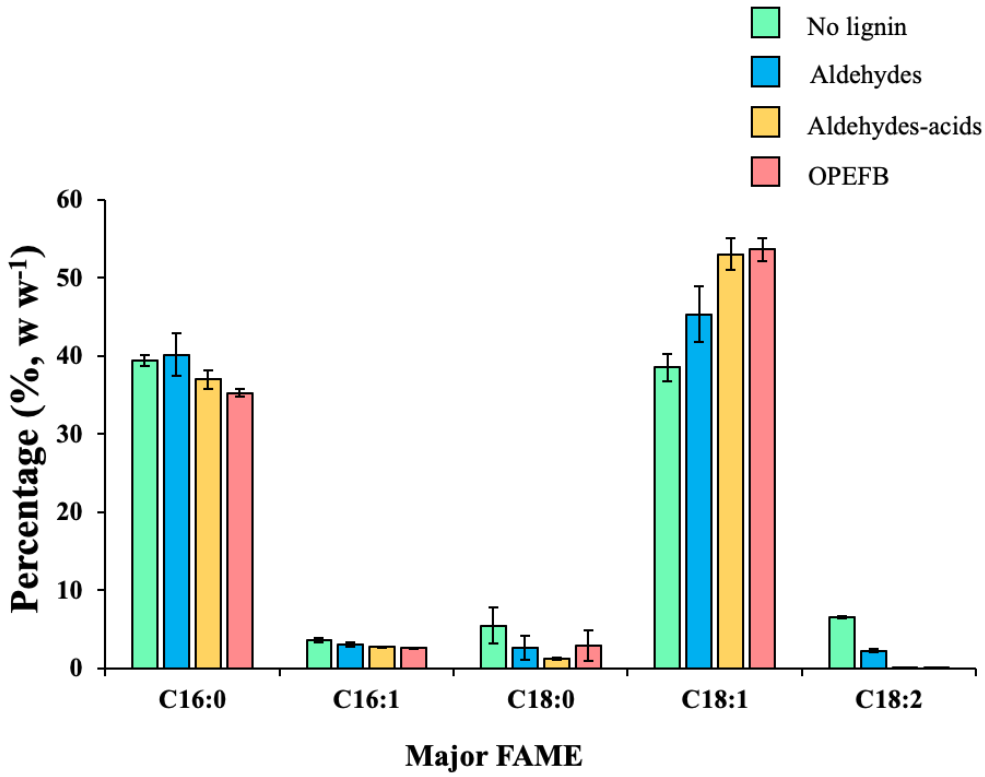
No lignin
Aldehydes
Aldehydes-acids
OPEFB
Percentage (%, w w-1)
60
50
40
30
20
10
0
C16:0
C16:1
C18:0
C18:1
C18:2
Major FAME

b)

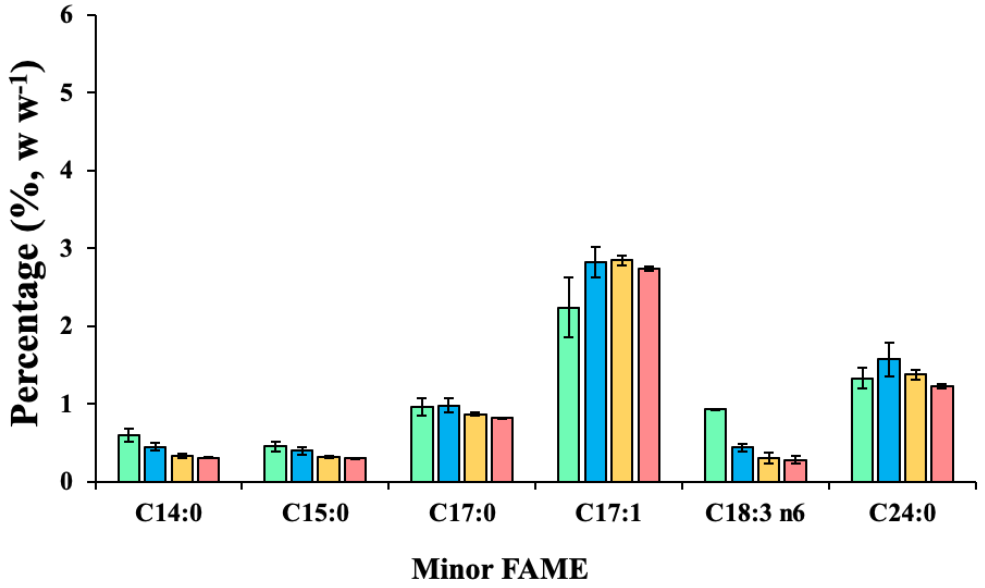
Percentage (%, w w-1)
6
5
4
3
2
1
0
C14:0
C15:0
C17:0
C17:1
C18:3 n6
C24:0
Minor FAME

**Fig. 22** Fatty acids profiles produced during the fermentation of different mediums. (a) Percentage of major FAME in the lipids. (b) Percentage of minor FAME in the lipids. The results presented the mean of three biological replicate samples with error bars illustrating the standard deviation from the mean value in the dataset.

Figure 22 displays the lipid content obtained from several fermentations. The lipids were primarily composed of long-chain fatty acids (LCFAs), specifically C16:0 (palmitic acid) and C18:1 (oleic acid), which are commonly found in various vegetable oils [154]. Significantly, oleic acid was found to be the main fatty acid in all fermentations, making up more than 40% of the total fatty acids. This was followed by palmitic acid, which accounted for approximately 30%. The substantial amount of oleic acid found in *L. starkeyi* indicates that it has the potential to be a major contributor to large-scale biodiesel production. Out of all the different types of oily yeast groups, *L. starkeyi* showed the greatest amount of oleic acid production [95]. Some fatty acids, including myristic acid (C14:0), pentadecanoic acid (C15:0), and gamma-linolenic acid (C18:3), exhibit a decrease in fermentation when lignin monomers are present. This decrease is also observed in palmitic acid and linolelaidic acid, which are significant fatty acids (Fig. 22a). In contrast, there is a large increase in oleic acid. Inhibitors, such as phenolic chemicals, may hinder the increase of long-chain fatty acids (LCFAs) in microorganisms by disrupting the process of fatty acid production. The inhibition of specific enzymes, such as β-ketoacyl carrier protein (ACP) synthases (KSs) or acetyl-CoA carboxylase, can disrupt the elongation and initiation steps of fatty acid synthesis. This disruption leads to a reduction in the systematic production of long-chain fatty acids (LCFAs) and an imbalanced profile

of fatty acids [155,156]. However, this phenomenon can serve as a beneficial means of regulating the synthesis of lipids, particularly those rich in specific long-chain fatty acids (LCFAs) such as oleic acid, for diverse biotechnological purposes.

## 3.4 Conclusion

This study presents a new and innovative method for converting OPEFB lignin into useful monomeric alcohols using an integrated biorefinery approach and specific techniques. The initial application of OPEFB was the exploitation of alkaline nitrobenzene oxidative depolymerization. This process successfully yielded all lignin monomeric aldehydes, such as syringaldehyde, vanillin, and 4-hydroxybenzaldehyde. The maximum concentration of vanillin and syringaldehyde was obtained by reacting a 10% NaOH solution with nitrobenzene at a temperature of 180 °C for a duration of 60 minutes. In the second application, lignin monomeric aldehydes were converted into monomeric alcohols using *L. starkeyi*. This process successfully produced syringyl, vanillyl, and 4-hydroxybenzyl alcohol in all fermentation variations. The conversion of monomeric increased lipid production as a by-product is compared to the control fermentation. Therefore, the existence of lignin monomeric acids in the fermentation process involving aldehydes and acids, as well as the presence of lignin monomeric acids and HCAs in OPEFB, may hinder cell productivity when compared to fermentation involving only aldehydes. In summary, *L. starkeyi* has shown great promise as a means of exploiting lignin biomass, such as OPEFB, through the process of alkaline nitrobenzene oxidation. This process yields valuable lignin monomeric alcohols with a high single-cell oil content, which holds significant potential for use in biorefinery applications.

# Chapter 4

# Adaptive laboratory evolution of *Lipomyces starkeyi* for high production of lignin derivative alcohols and lipids with comparative untargeted metabolomics-based analysis

## 4.1 Introduction

Lignocellulosic biomass represents a promising renewable resource for the sustainable production of biofuels and biochemicals, offering a potential solution to the world's growing energy and environmental challenges [131,157,158]. Among its constituents, lignin, a complex and abundant polymer, is particularly intriguing due to its potential as a feedstock for biofuel production. However, the valorization of lignin remains a considerable challenge, primarily due to its recalcitrant nature and the complex chemistry involved in its breakdown [71]. In recent years, significant efforts have been directed toward harnessing lignin-derived monomeric aldehydes as material substrates for the production of valuable bioproducts, including valuable alcohols and lipids. *Lipomyces starkeyi*, a non-conventional oleaginous yeast species, has emerged as a promising candidate for this purpose, owing to its remarkable ability to metabolize a wide range of carbon sources, including lignin-derived compounds in specific aldehydes [139]. However, achieving high yields of target products from lignin monomers using *L. starkeyi* necessitates overcoming various metabolic and regulatory hurdles inherent in its natural physiology. Adaptive Laboratory Evolution (ALE) presents a powerful approach for developing

microorganisms to adapt to specific environmental conditions or substrates through iterative cycles of growth and selection [66]. By subjecting *L. starkeyi* (WT) to gradually increasing selective lignin derivative aldehydes, like syringaldehyde, ALE allows for the emergence of desired traits, such as enhanced substrate utilization, metabolic efficiency, and product synthesis. In the context of lignin valorization, ALE holds great promise for optimizing microbial strains towards improved conversion of lignin-derived aldehydes into target bioproducts, including alcohols and lipids.

This study aims to explore the potential of ALE as a strategy to enhance the production of lignin-derivative alcohols and lipids from syringaldehyde by *L. starkeyi*. Through systematic evolution experiments coupled with comprehensive phenotypic and metabolic characterization, we seek to elucidate the adaptive mechanisms underlying enhanced substrate utilization and product synthesis in *L. starkeyi*. Additionally, untargeted metabolomics analysis was employed to identify important metabolites that may play a pivotal role in the metabolic rewiring of the evolved strain. Furthermore, we aim to evaluate the performance of evolved strains in terms of productivity, yield, and substrate specificity, with the ultimate goal of developing robust microbial platforms for cost-effective and sustainable biorefining of lignocellulosic biomass. By leveraging the inherent adaptability of microbial systems through ALE, coupled with advanced metabolomics techniques, this research endeavors to contribute to the ongoing efforts towards unlocking the full potential of lignin as a renewable feedstock for the production of advanced biofuels and biochemicals, thereby advancing the transition towards a bio-based economy.

## 4.2 Materials and methods

### 4.2.1 Mutants development by serial flask cultivation

Commercial syringaldehyde was acquired from Sigma Aldrich Co. LLC. Syringyl alcohol was from Thermo Fisher Scientific Inc. (USA). Methanol and chloroform were purchased from Nacalai Tesque (Japan). *Lipomyces starkeyi* D35 (NBRC10381) was employed as a model organism in this study, obtained from the National Institute of Technology and Evaluation Biological Resource Center, Japan. Yeast was maintained in a 30 % (w $w^{-1}$) of glycerol solution at -80 °C. The yeast was then prepared by inoculating it onto a PDA (Potato Dextrose Agar) medium. Afterward, one colony was transferred to a YMPG (Yeast Malt Peptone Glucose) agar medium containing 20 g $L^{-1}$ agar, 10 g $L^{-1}$ glucose, 5 g $L^{-1}$ peptone, 3 g $L^{-1}$ malt extract, and yeast extract. Incubation was conducted for 2 days at 30 °C. For fermentation, a single colony was transferred into YMPG-50 (12 mL) liquid medium (50 g $L^{-1}$ glucose, 5 g $L^{-1}$ peptone, 3 g $L^{-1}$ malt extract, and yeast extract) within a 100 mL Erlenmeyer flask as a pre-culture overnight. Subsequently, the pre-culture was transferred to a new 12 mL YMPG-50 supplemented with 8 mM syringaldehyde as the main culture in the 100 mL flask. The inoculation used for the fermentation in the main culture was set at 1 unit ($OD_{600}$). The flask was then subjected to incubation in a BioShaker BR-43FH MR orbital incubator shaker (Taitec Corp., Japan) and maintained the condition at 190 rpm at 30 °C in aerobic conditions. The strain was evolved through serial transfer in shake flasks containing YMPG-50 medium with controlled increment syringaldehyde. Starting with 1 unit ($OD_{600}$) of wild-type *L. starkeyi* D35 as a parental strain, cultured in 12 mL YMPG-50 medium supplemented with 8 mM syringaldehyde. The growth OD was measured frequently and when the

cell growth reaches more than 30 units, the cells are then transferred to a new medium with a similar concentration of syringaldehyde. Cells were only transferred to a higher concentration of syringaldehyde when the growth rate reached 0.62 units ($OD_{600}$) $h^{-1}$.

### 4.2.2 Measurement of cell growth

To determine the DCW (Dry Cell Weight), a gravimetric method was employed using 0.5 mL of fermentation samples. The cell was separated by centrifugation for 5 min at 14,000 × g. Right after, the cells were washed with sterilized water and lyophilized overnight to completely expel all of the water content. The lyophilization was using a freeze dryer (Freeze Dry, FreeZone from Labconco, USA). Afterward, DCW was determined based on the weight of the dried cells.

### 4.2.3 Glucose consumption measurement by HPLC-RID

During the fermentation, glucose concentration was determined by employing an HPLC (high-performance liquid chromatography) (Shimadzu, Japan) connected to a RI (refractive index) detector. This system was equipped with a column of ICSep Coregel-87H (7.8 mm i.d. and 300 mm length, supplied by Transgenomic). Prior to analysis, the samples were prepared by 14,000 × g centrifugation for 5 min, followed by a filtration filter (0.22 mm) to prepare the supernatant. The analysis involved the injection of a 20 μL sample volume, with the column oven maintaining a temperature of 80 °C. The analysis was carried out using a mobile phase consisting of 5 mM $H_2SO_4$, with a mobile phase flow rate of 0.6 mL $min^{-1}$ [140].

### 4.2.4 Lignin monomers measurement by HPLC-UV/Vis

Quantification of lignin derivatives was carried out using an HPLC-20AB system (Shimadzu, Japan), equipped with an ultraviolet-visible spectroscopy (UV/Vis) detector SPD-20A. The analysis utilized a C18 column (250 mm length x 4.6 mm, 5µm particle size) sourced from Supelco Ascentis (Merck KGaA, Darmstadt, Germany). Supernatant samples were prepared for analysis by centrifuging for 5 min of 14,000 × g, followed by a filtration filter (0.22 mm). For each measurement, 10 µL of sample was injected, and the column oven was maintained at a temperature of 30 °C for 45 min. The mobile phase used was a mixture of methanol and ultra-pure water in a ratio of 18:82 v $v^{-1}$ with an addition of 0.2 % (v $v^{-1}$) acetic acid, which was propelled through the column at 1 mL $min^{-1}$ flow rate with measurement of analytes was achieved at a wavelength of 280 nm [139].

### 4.2.5 Lipid measurement

The quantification of single-cell oil (lipid) production was carried out using a gravimetric approach, adhering to the method from Floch [95]. The freeze-dried samples were weighed 20 mg into a 2 mL O-ring cap-sealed micro vial (Watson, Japan). To facilitate the extraction, zirconia balls were introduced into the micro vial. The extraction solvent of 1.5 mL volume, consisting of chloroform:methanol mixture in a 2:1 v v–1 ratio, was used to extract the lipids. The cells were then subjected to pulverization at 1500 rpm for 15 min employing a Master Neo pulverizer (Bio Medical Science, Japan). Following this, the cells underwent centrifugation at 14,000 × g for 5 min. Subsequently, the cell pellets were rinsed with sterilized water. Drying

of the cells was performed at 60 °C until a plateau weight was achieved. The content of lipids was determined based on the difference in weight before and after drying and expressed as a percentage of the DCW.

### 4.2.6 Fatty acid methyl esters profiling by GC/MS

The fatty acid methyl esters or FAMEs of the lipids from the lyophilized samples were obtained through a transesterification process following the outlined in the FAMEs kit mix (Nacalai Tesque, Japan). Resulting FAMEs were then resurrected in hexane and subjected to analysis employing GC/MS (gas chromatography-mass spectrometry) QP-2010 (Shimadzu, Japan). An internal standard, a C8:0 (caprylic acid), was added to the sample for reference. The analysis was carried out using a capillary GC column DB-23 (0.25 mm i.d. 60 m length, 0.25 mm thickness) (Agilent), with a carrier gas of helium. The sample injection volume of 1 µL was applied, and the analysis was conducted in the split injection with a temperature of inlet at 250 °C. The temperature of the oven program was initiated for 1 min at 50 °C, followed by a gradient at 25 °C $min^{-1}$ until it reached 175 °C, and a subsequent increase to 230 °C (4 °C $min^{-1}$), lasting for 6 min. The MS detector operated at 250 °C and operated the 40 to 500 m $z^{-1}$ range with the scan mode. The identification and measurement of fatty acids were achieved by comparing the retention times (rt) and the m $z^{-1}$ pattern with a fatty acid standard, SUPELCO 37 FAME mix (Sigma–Aldrich) [95].

### 4.2.7 Fast filtration, extraction, and derivatization of intracellular metabolites

Sampling for intracellular metabolome analysis by fast filtration method was performed. The cells were collected at the logarithmic phase (24 h) (5 units of $OD_{600}$) with a 0.45 μm pore size, 25 mm diameter nylon membrane filter (Millipore, USA). The cells were quenched in liquid nitrogen with the aim of stopping the metabolism rapidly and stored at −80 °C prior to extraction. Extraction of the metabolites was performed using 3 mL of extraction solvent (methanol:ultra-pure water:chloroform; 5:2:2 v $v^{-1}$ of ratio) containing 10 μg/L of ribitol as an internal standard in thawing incubation condition. Thawing was conducted at −80 °C for 1 h and then −30 °C for 30 min (three times). Afterward, 1 mL of supernatant was transferred to a new microtube and mixed with 200 μL of ultra-pure water. The sample was then centrifuged at 10,000 × g for 10 min at 4°C, and 950 μL of the upper polar phase was collected. The sample was concentrated by using a spin dryer for 2 h and lyophilized in the freeze-drier overnight. Derivatization prior to GC/MS analysis was conducted through oximation and trimethylsilylation. The first derivatization was performed by adding methoxiamine hydrochloride (100 μL, 20 mg/ml in pyridine) for 90 min at 30 °C. MSTFA (N-methyl-N-(trimethylsilyl)trifluoroacetamide) was added to the mixture as the second derivatization agent (50 μL) and incubated for 30 min for 37 °C.

### 4.2.8 Analysis of intracellular untargeted metabolites by GC/MS

Untargeted analysis of intracellular metabolites was carried out using gas chromatography mass spectrometry (GC/MS). GC/MS QP2010 and AOC-20i autosampler (Shimadzu, Kyoto, Japan) equipped with a 0.25 mm x 30 m x 0.25 μm

inert Cap 5 MS/NP column (GL Science Inc., Tokyo, Japan). The derivatized sample (1 μL) was subjected to GC/MS in split mode with an injection temperature of 230 °C. Helium was used as the carrier gas at 1.12 mL $min^{-1}$ with a linear velocity of 39 cm/s. The temperature of the column was held at 80 °C for 2 min and increased by 15 °C/min to 330 °C, then held for 6 min. The transfer line and ion source in the MS part were 250 and 200 °C, respectively. The EI (electron ionization) generated ions at 0.93 kV. The spectra were recorded at 10,000 u/s over the mass range *m/z* (mass to charge ratio) 85-500. The terminal alkane standard mixture ($C_8$–$C_{40}$), as a retention index calibration, was injected for tentative identification.

### 4.2.9 Metabolome data and multivariate analysis

The data produced from GC/MS were exported into ANDI files (cdf) using Shimadzu GCMS Solution software (Kyoto, Japan). Then, it was converted into ABF format using Reifycs Analysis Base File software. Subsequently, MS-DIAL v. 3.9.22 (Riken, Kanagawa, Japan) was employed to correct the baseline, detect the peaks, and align the peak retention times. Detected peaks were then annotated based on the retention time and mass spectrometry information to the public metabolite library, GL-Science database shared by RIKEN. The patterns of data were searched based on differences and similarities by multivariate analysis using MetaboAnalyst 6.0 (https://www.metaboanalyst.ca) for PCA (Principal Component Analysis) without data transformation. The relative intensity of each metabolite was normalized by comparison with the internal standard (ribitol) as an explanatory variable. The data was auto-scaled to reduce the masking effect of total metabolites.

## 4.3 Results and discussion

### 4.3.1 Evolved phenotypic changes

We employed adaptive laboratory evolution (ALE) to increase the bioconversion capacity of *Lipomyces starkeyi* to convert lignin aldehyde into valuable lignin alcohol and lipids by constantly alternating the medium substrates. The parental strain of wild-type *L. starkeyi* D35 (NBRC10381) was used. The evolution of the strain within shake flasks in YMPG-50 medium, punctuated by incremental additions of syringaldehyde. The initial inoculum size used in the fermentation was 1 ($OD_{600}$). The growth OD was measured routinely and when the cells reached 30 units, the cells transferred to a new medium with a similar concentration of syringaldehyde. The higher concentration of syringaldehyde was only added in the medium when the growth rate reached 0.62 ($OD_{600}$) $h^{-1}$. The highest syringaldehyde concentration used was 24 mM after 26 transfers. However, effective bioconversion of *L. starkeyi* to convert syringaldehyde to produce syringyl alcohol and lipids simultaneously was in a 22 mM concentration of syringaldehyde at 20 transfers. The culture evolved for 81 days and at the endpoint of the adaptive evolution, the evolved *L. starkeyi* that was able to convert 22 mM of syringaldehyde, called DALE 22.

Fermentation of DALE 22 and WT (D35) in the presence of 22 mM syringaldehyde, DALE 22 outperformed WT in every way. Fig. 23 shows that DALE 22 successfully produced 18.74 mM of syringyl alcohol from 22.28 mM syringaldehyde after 96 h with 41.87 % of lipid content (5.41 g $L^{-1}$) (Table 6). In contrast, the parental strain could not grow and lost its ability to convert syringaldehyde into syringyl alcohol. A high concentration of syringaldehyde present in the medium may be resulting severe cell damage to the WT even at the beginning

of the fermentation, so the cells not only lose the conversion ability but also cannot grow. Lignin monomeric compounds such as syringaldehyde are considered inhibitors for some living organisms [159]. Harnessing the adaptive evolution (merit of ALE to enhance the native capability).

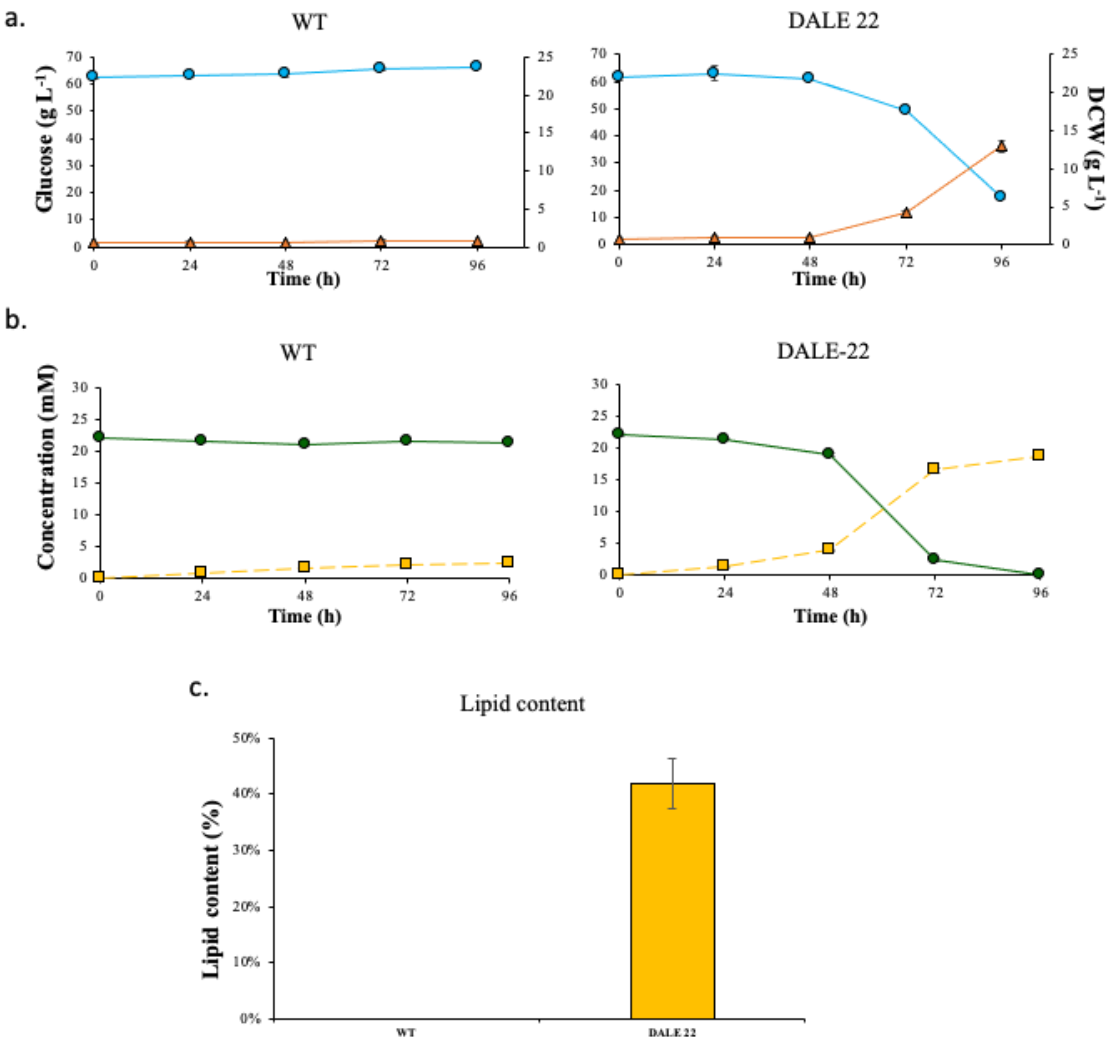


**Fig. 23** Fermentation profile of DALE-22 and WT in the 22 mM concentration of syringaldehyde. (a) Growth curve and glucose consumption. (b) Syringaldehyde conversion and syringyl alcohol production. (c) Lipid content. The results presented

the mean of three biological replicate samples with error bars illustrating the standard deviation from the mean value in the dataset.

**Table 6** Dry cell weight and lipid production of *L. starkeyi* in 22 mM syringaldehyde.[a]

| Type of lignin | Time (h) | Initial DCW (g $L^{-1}$) | Final DCW (g $L^{-1}$) | Final lipid content (w $w^{-1}$ %) | Lipid titer (g $L^{-1}$) |
|---|---|---|---|---|---|
| WT | 96 | 0.55 ± 0.07 | 0.77 ± 0.02 | 0.00 ± 0.00 | 0.00 ± 0.00 |
| DALE 22 | 96 | 0.79 ± 0.17 | 12.93 ± 0.72 | 41.87 ± 4.57 | 5.41 ± 0.03 |

[a] The reported results provide the mean of three biological replicate samples with error bars illustrating the standard deviation from the mean value in the dataset.

### 4.3.2 Fermentation profile of evolved strain in mild syringaldehyde

To investigate important metabolites that may play an important role in the evolved strain compared to the parental strain, we fermented the lower concentration of syringaldehyde (4 mM), which is suitable for the parental strain to grow. We then later examined the intracellular metabolite employing untargeted metabolomics analysis by using a GC/MS system. Cells are incredibly complex, with many regulations happening at once in a short period of time, especially metabolites. By keeping the fermentation at the same condition, the specific role of the regulation in the cells can be obtained [160].

Based on the results of fermentation profiling (Fig. 24), the growth patterns of evolved and wild-type strains seem comparable. However, the higher cells produced were found from evolved strains (18.21 g $L^{-1}$) compared to parental stains (17.10 g $L^{-1}$) with a growth rate of 0.40 DCW $h^{-1}$ $L^{-1}$ and 0.31 DCW $h^{-1}$ $L^{-1}$ at the logarithmic

state, respectively (Table 7). These results showed that DALE-22 has a better tolerance than wild-type even in the similar condition of fermentation. The syringaldehyde was depleted after 24 h of fermentation and successfully produced 3.19 mM and 3.18 mM syringyl alcohol for evolved strains and parental strains, respectively. The syringyl alcohol was found to be a valuable lignin monomeric compound and commonly used in lignin model research. The latest report, syringyl alcohol, shows the impressive catalytic performance in carbon nanotubes as a probe [161]. The lipid content of DALE-22 was found to be higher compared to the parental strain (Fig. 24c). These results indicated that a higher adaptive level of DALE-22 affected the better production of by-products, like lipids.

The fatty acid profiles resulting from fermentation activities in 4 mM syringaldehyde are shown in Figure 25. The main fatty acid composition of the lipids (Fig. 25a) was made up of long-chain fatty acids (LCFAs), such as C16:0 (palmitic acid) and C18:1 (oleic acid), which are comparable to the prevalent compositions of many vegetable oils [154]. Remarkably, in both fermentations, oleic acid constituted over 40% of the total fatty acids and was the main fatty acid. Approximately 30% of the total fatty acids in WT were composed of palmitic acid. Conversely, DALE-22 is notably lower. Owing to its high oleic acid content, DALE-22 could eventually be a key component in the commercial production of biodiesel. Among the oleaginous yeast strains, L. starkeyi species exhibited the highest oleic acid synthesis [95,162], although DALE-22 was even able to produce at a greater level than its wild-type strain. It was discovered that the DALE-22 had higher levels of the main fatty acids C18:2 (linolelaidic acid), C18:1 (oleic acid), and C18:0 (stearic acid). However, C16:1 and C16:0 fatty acids (oleic acid). A rise in WT is seen in minor fatty acids, such as C14:0

(myristic acid) and C15:0 (pentadecanoic acid) (Fig. 25b). Inhibitors such phenolic compounds may affect the rise in LCFAs in the bacteria by blocking the synthesis of fatty acids. By targeting important enzymes such as acetyl-CoA carboxylase or β-ketoacyl carrier protein (ACP) synthases (KSs), it may inhibit the elongation and initiation steps of fatty acid synthesis, respectively. This would lessen the systematic production of LCFAs and the ensuing imbalance profile of fatty acids [155,156]. This suggests that DALE-22 produces more C18 LCFAs than WT because it exhibits a greater tolerance to syringaldehyde.

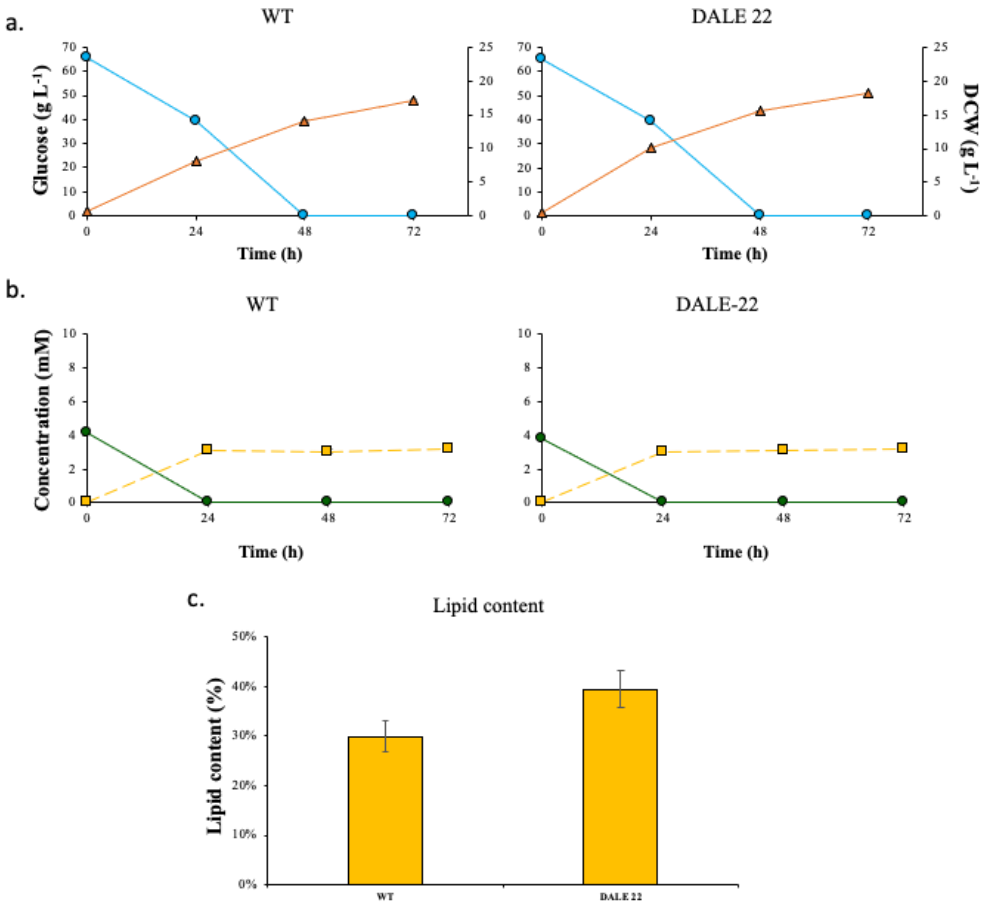


**Fig. 24** Fermentation profile of DALE-22 and WT in the 4 mM concentration of syringaldehyde. (a) Growth curve and glucose consumption. (b) Syringaldehyde conversion and syringyl alcohol production. (c) Lipid content. The results presented the mean of three biological replicate samples with error bars illustrating the standard deviation from the mean value in the dataset.

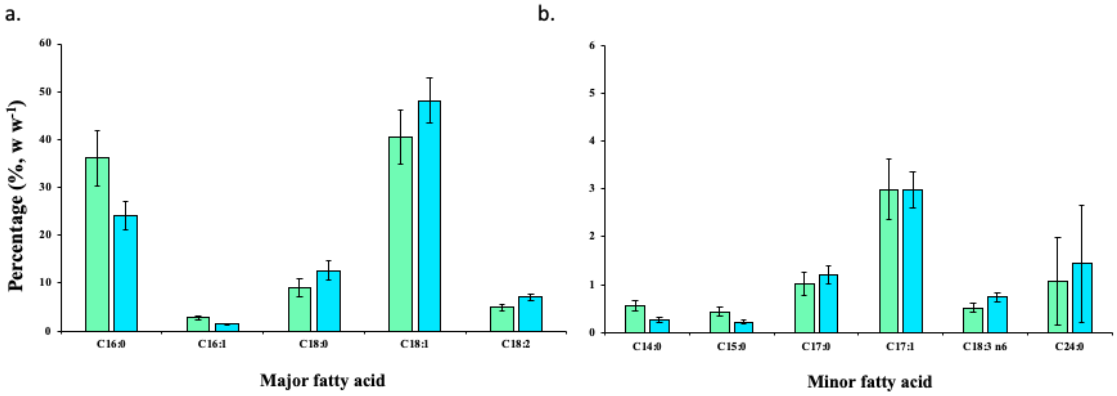


**Fig. 25** Profiles of fatty acids produced during the fermentation of DALE-22 and WT in 4 mM concentration of syringaldehyde. (a) Major fatty acid percentage in lipids. (b) Minor fatty acid percentage in lipids. The data displayed represents the average of three biological replicate samples, with error bars showing the standard deviation from the mean.

**Table 7** Dry cell weight and lipid production of *L. starkeyi* in 4 mM syringaldehyde.[a]

| Type of lignin | Time (h) | Initial DCW ($g\ L^{-1}$) | Final DCW ($g\ L^{-1}$) | Final lipid content ($w\ w^{-1}$ %) | Lipid titer ($g\ L^{-1}$) |
|---|---|---|---|---|---|
| WT | 72 | 0.54 ± 0.10 | 17.10 ± 0.14 | 29.87 ± 3.18 | 5.11 ± 0.00 |
| DALE 22 | 72 | 0.39 ± 0.02 | 18.21 ± 0.10 | 39.38 ± 3.66 | 7.17 ± 0.00 |

[a] The reported results provide the mean of three biological replicate samples with error bars illustrating the standard deviation from the mean value in the dataset.

### 4.3.3 Untargeted metabolomics analysis of evolved strain

Intracellular metabolites during the logarithmic phase of both DALE-22 (evolved strain) and WT (parental strain) were carried out with untargeted GC/MS.

After identification was conducted, 73 metabolites belonging to amino acids, organic acids, nucleoside phosphate, nucleoside, sugars, sugar phosphate, and other compounds were successfully annotated in DALE-22 and WT (Fig. 26). The relative intensity of each metabolite was obtained by normalization with ribitol as an internal standard. Ribitol was used as an internal standard for the analysis as it is not present in any biological samples, especially in the *L. starkeyi* cells and is reported to be a stable chemical in the extraction solvent until analysis occurred [163]. The multivariate analysis was used for 73 metabolites. PCA (Principle component analysis) of the GC/MS dataset showed that two principal components (PC) described 79.8 % of the total variance (Fig. 26).

Considering that glucose consumption, growth, lipid production as well as bioconversion of lignin monomeric are most active during the logarithmic phase, analysis and monitoring of the metabolite during this phase may best reflect the phenotype state of the cells during bioconversion. As such, a detailed PCA was conducted for the logarithmic phase. The results showed that DALE-22 and WT were separated along PC 1, accounting for 61.9 % of the total variance (Fig. 26). These results might indicate the relation between the conversion capacity and tolerance phenotype from the two strains. DALE-22 is notably different in growth, bioconversion capacity, and lipid production.

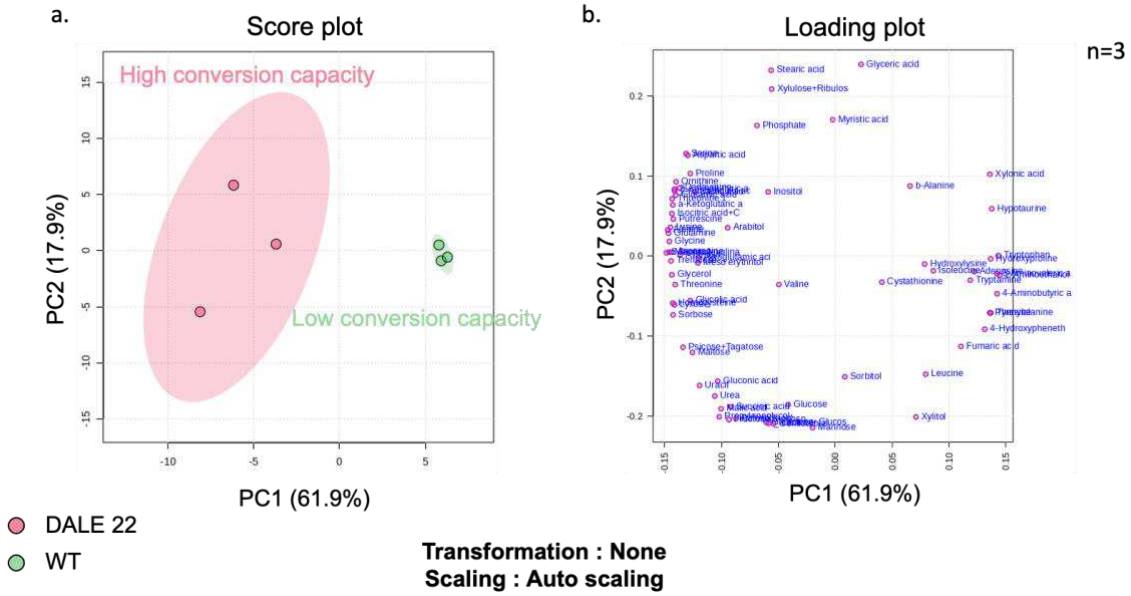


c.

**Amino acid**
Alanine
Leucine
2-Aminobutyric acid
Valine
Threonine
Isoleucine
Proline
Glycine
Serine
b-Alanine
Hydroxyproline
4-Aminobutyric acid
Aspartic acid
Pyroglutamic acid
Homocysteine
Asparagine
2-Aminoadipic acid
Phenylalanine
Glutamic acid
5-Aminovaleric acid
Lysine
Tryptophan
Cystathionine
Tryptamine

**Organic acid**
Lactic acid
Glycolic acid
Succinic acid
Glyceric acid
Fumaric acid
Malic acid
a-Ketoglutaric acid
Gluconic acid
Iso/Citric acid
Myristic acid
Palmitic acid
Stearic acid

**Sugar**
Lyxose
Xylulose/Ribulose
Psicose/Tagatose
Glucose
Galactose/Glucose
Mannose
Sorbose
Maltose
Lactose
Trehalose
Mannitol
Sorbitol

**Others**
Propyleneglycol
Urea
2-Aminoethanol
Glycerol
Phosphate
Uracil
Meso erythritol
4-Hydroxyphenethyl alcohol
Allantoin
Inositol
Gentiobiose
Putrescine
Ornithine
5-Amino levulinate
Xylitol
Arabitol
Gluconic acid
Hydroxylysine

**Sugar phosphate**
Fructose 6-phosphate

**Nucleoside**
Uracil

**Nucleoside phosphate**
Adenosine

**Fig. 26** Principal component analysis (PCA) of the DALE-22 and WT. (a) Score plot. (b) Loading plot. (c) Total metabolites detected. The results presented the mean of

three biological replicate samples with error bars illustrating the standard deviation from the mean value in the dataset.

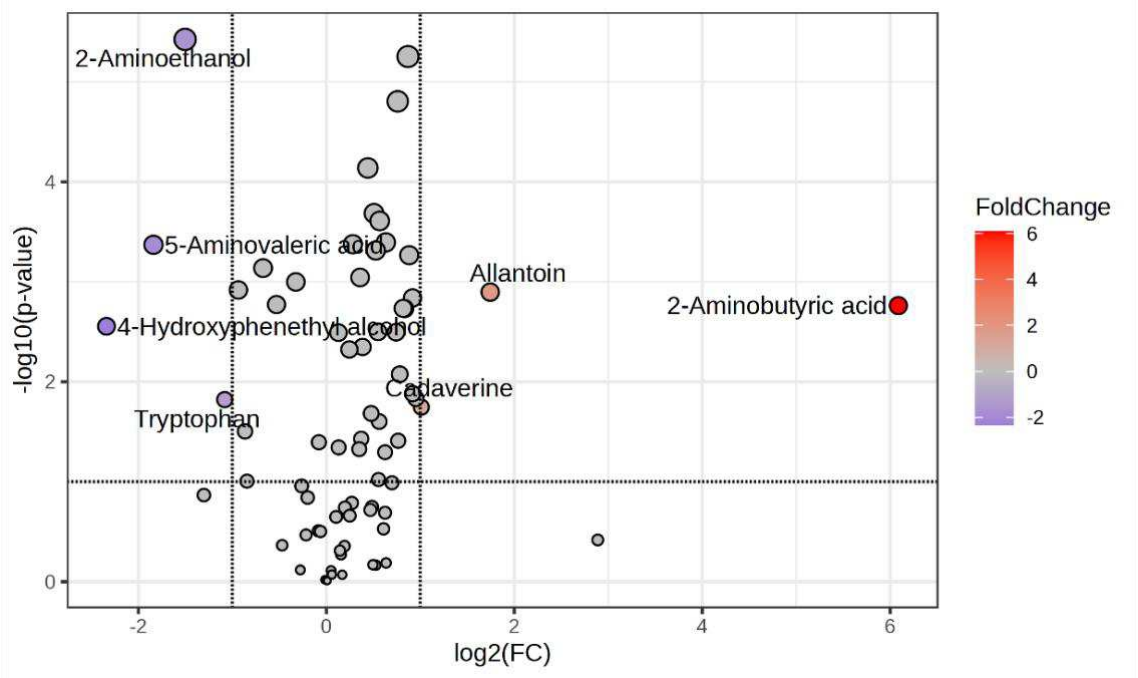


**Fig. 27** The volcano plots illustrate the distinct metabolites in DALE-22 in comparison to WT. The x-axis represents the binary logarithm of fold changes, while the y-axis represents the negative common logarithm of the p-value derived from pairwise student t-tests.

a)

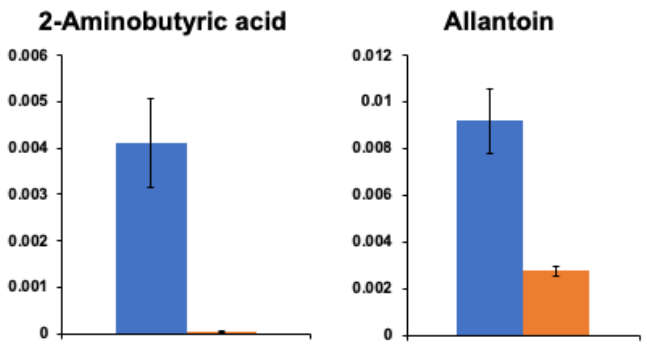


b)

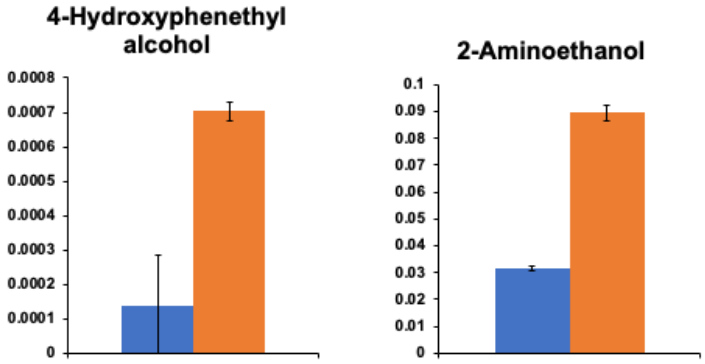


c)

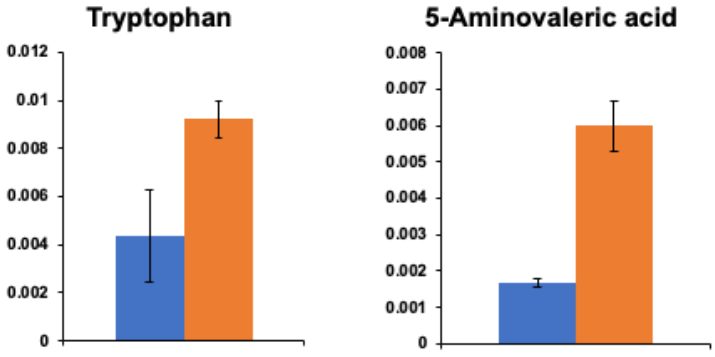


**Fig. 28** Relative quantification of significantly correlated metabolites performed by GC/MS of DALE-22 (blue) and WT (orange). (a) Stress response and protective molecules. (b) Osmolytes and cellular water balance. (c) Amino acid breakdown and by-products. The results presented the mean of three biological replicate samples

with error bars illustrating the standard deviation from the mean value in the dataset. To be more detailed, differential analysis was used to further observe the differences in the metabolites. The volcano plot illustrated the metabolites that were significantly upregulated (Fig. 27). When comparing DALE-22 and WT, metabolites that were significant with p-values lower than 0.05 were shown with points above the line. The dots were located above the value of minus log10 t-test p-values of 1.746. To describe how much of the quantity changes in metabolites, the log2 fold change values were used. A log2 fold change of 1 means the metabolite on the right side with a red dot increased twice in DALE-22 compared to the subsequent measurement, whereas a log2 fold change of 2 means a metabolite on the right side with the red dot is 4 times larger. On the other hand, negative values of log2 fold change correspond to a decrease of metabolites in DALE-22 compared to a subsequent measurement. It was represented with purple dots. Compared to the parental strain, 2-aminobutyric acid was the most abundant compound found in DALE-22 (Fig. 28). This metabolite, known as GABA, can act as a protective molecule during stress conditions in microorganisms. A cell with the ability to produce more GABA during stress (as a response product of the cells) might have improved tolerance [164]. Additionally, allantoin was known as an oxidative stress protectant abundantly found in the DALE-22. Allantoin is a by-product of purine catabolism (breakdown of purine nucleotides). While not directly involved in stress response, this metabolite is a potent antioxidant. Cells with higher levels of allantoin might show better tolerance to oxidative stress [165]. On the other hand, 2-amino ethanol (ethanolamine) and 4-hydrophenethyl alcohol were found higher in the parental strain compared to DALE-22. These metabolites can contribute to osmotic balance or act as a signaling molecule. Cells

that have a better ability to utilize these compounds might have improved to specific environment stresses [166–168]. Along with it, tryptophan and 5-amino valeric acid were lower in the DALE-22. Tryptophan is an essential amino acid used for protein synthesis. It can be broken down through different pathways depending on the cell's needs and the enzymes present. An incomplete breakdown of tryptophan can generate byproducts that might be toxic at high concentrations. A cell with a more efficient pathway to utilize or eliminate these byproducts might have better tolerance [169]. In the case of 5-amino valeric acid, these are produced during the breakdown of other amino acids, including lysine and glutamate. Similar to tryptophan by-products, their accumulation can be toxic. Cells with better tolerance, such as DALE-22, might have better activity of enzymes that metabolize or export these intermediates [170].

## 4.4 Conclusion

In this study, flask-scale adaptive laboratory evolution (ALE) was applied to obtain novel evolved *Lipomyces starkeyi* strained named DALE-22 after 81 days of consecutive fermentation. The results indicated that the oleaginous yeast *L. starkeyi* DALE-22 shows significantly better performance in terms of bioconversion capacity up to 22 mM of syringaldehyde, cell growth, and by-products such as syringyl alcohol and lipid production compared to WT, known as the parental strain. Since DALE-22 shows a better phenotype than WT. Untargeted-based metabolomics analysis was performed to see the compound regulation and find key metabolites that may be important in the cells during bioconversion of lignin monomeric aldehydes, syringaldehyde. Six important metabolites that might play an important role in the

DALE-22 corresponding to the cell tolerance were identified. This finding might give some perspective in the future for further cell development with even higher bioconversion capability. Overall, this study demonstrated the promising potential of ALE in the improvement of *L. starkeyi* DALE-22 with better tolerance and bioconversion capacity. This study also provides important information regarding the important metabolites that can be beneficial for further cell development and carry promising prospects for biorefinery applications in the future.

# Chapter 5

## General conclusion and future direction

Overall, this study investigated the potential of *Lipomyces starkeyi* as a microbial platform for lignin valorization and the production of valuable biochemicals. The research successfully demonstrated that *L. starkeyi* can be a promising biological platform to utilize lignin to become various valuable biochemicals including syringyl alcohol, vanillyl alcohols, 4-hydroxybenzyl alcohol, and lipids. This finding suggests that *L. starkeyi* is a promising candidate for the sustainable conversion of lignin waste into valuable products. Key findings from our study include:

- Feasibility of Lignin Valorization. Novel biorefinery platform for bioconversion of lignin derivative aldehydes, such as syringaldehyde, vanillin, and 4-hydroxybenzaldehyde to produce valuable lignin monomeric alcohols, including syringyl alcohol, vanillyl alcohol, and syringyl alcohol, respectively.
- Conversion of lignin aldehydes into alcohols promotes not only cell growth but also lipid content in the *L. starkeyi.*
- Major fatty acids found in the lipids product were C18:1 (oleic acid) and C16:0 (palmitic acid).
- Aldehyde-ketone reductase enzyme was found to be an important enzyme to convert the aldehydes to alcohols and by releasing $NAD(P)^+$ that potentially be used for malate to pyruvate conversion via NAD(P)H release in the cytosol. Pyruvate could be channeled to the TCA cycle, and NAD(P)H could then be used for fatty acid synthase, which is needed in fatty acid biosynthesis.

- Implementing fermentation strategies of high initial inoculum size could be beneficial to reducing the inhibition effect toward the presence of lignin monomeric mixtures. While high C:N ratio was approved to boost the lipid content in the cells.
- A novel integrated biorefinery strategy approach was demonstrated in converting OPEFB (lignocellulosic biomass) lignin into monomeric alcohols and lipids.
- A mixture of 10 % NaOH with nitrobenzene at 180 °C for 60 min successfully produced the highest titer of syringaldehyde and vanillin.
- *L. starkeyi* has successfully converted the lignin aldehydes from OPEFB to lignin alcohols and enhanced lipid production.
- A novel strain of *L. starkeyi* named DALE-22 was obtained from parental strain D35 by harnessing the adaptive laboratory evolution (ALE) and showed better performance at converting higher levels of lignin aldehyde (22 mM) to alcohol.
- Six compounds that might play an important role in the better phenotypic conversion of DALE-22 that corresponds to cell tolerance were identified, including 2-amino butyric acid, allantoin, 4-hydroxyphenethyl alcohol, 2-amino ethanol, tryptophane, and 5-amino valeric acid.

Future direction of the next work is required to push the potential of "greener" biochemical products (syringyl alcohol, vanillyl alcohol, 4-hydroxybenzyl alcohol, and lipids) from lignocellulosic waste for commercialization of renewable chemicals, fuels, and polymer products. To address the hope, integrated and innovative approaches are surely necessary. A key area of the future work includes:

- Optimization of lignin conversion: Future research could focus on optimizing the efficiency of lignin degradation and conversion by Lipomyces starkeyi. This could involve genetic engineering of the yeast strain to enhance its lignin-degrading capabilities or improve fermentation conditions for higher product yields.
- Diversification of product portfolio: Exploring the potential of *L. starkeyi* to produce a broader range of value-added biochemicals from lignin could be a promising direction. This could involve screening for additional metabolic pathways or engineering the yeast for the synthesis of specific target compounds.
- Scale-up and Industrial Application: Transitioning from lab-scale (flask) experiments to industrial-scale (bioreactor) production will be crucial for realizing the commercial potential of lignin valorization by *L. starkeyi*. Future research may focus on scaling up the fermentation process, optimizing downstream purification techniques, and assessing the feasibility of large-scale production.
- Environmental Impact Assessment: Conducting a comprehensive environmental impact assessment of lignin valorization using Lipomyces starkeyi will be essential for evaluating the sustainability of this approach. Future studies could investigate factors such as energy consumption, greenhouse gas emissions, and potential ecological implications to ensure that the process aligns with broader sustainable development goals (SDGs).

By addressing these future directions, this study can contribute significantly to the development of sustainable and efficient methods for lignin valorization and the production of valuable biochemicals from this abundant renewable resource. Overall, the dissertation lays the groundwork for utilizing *Lipomyces starkeyi* as a microbial platform for lignin valorization, with future research directions focusing on optimization, diversification, scale-up, and sustainability considerations.

## References

[1] J.K. Kenny, J.W. Medlin, G.T. Beckham, Quantification of Phenolic Hydroxyl Groups in Lignin via 19 F NMR Spectroscopy, ACS Sustain Chem Eng 11 (2023) 5644–5655. https://doi.org/10.1021/acssuschemeng.3c00115.

[2] U. Shakeel, X. Li, B. Wang, F. Geng, M.S.U. Rehman, K. Zhang, J. Xu, Structural characterizations of lignins extracted under same severity using different acids, Int J Biol Macromol 194 (2022) 204–212. https://doi.org/10.1016/j.ijbiomac.2021.11.171.

[3] J. Ponomarenko, M. Lauberts, T. Dizhbite, L. Lauberte, V. Jurkjane, G. Telysheva, Antioxidant activity of various lignins and lignin-related phenylpropanoid units with high and low molecular weight, Holzforschung 69 (2015) 795–805. https://doi.org/10.1515/hf-2014-0280.

[4] Z. Sun, B. Fridrich, A. de Santi, S. Elangovan, K. Barta, Bright Side of Lignin Depolymerization: Toward New Platform Chemicals, Chem Rev 118 (2018) 614–678. https://doi.org/10.1021/acs.chemrev.7b00588.

[5] B.M. Upton, A.M. Kasko, Strategies for the Conversion of Lignin to High-Value Polymeric Materials: Review and Perspective, Chem Rev 116 (2016) 2275–2306. https://doi.org/10.1021/acs.chemrev.5b00345.

[6] C. Li, X. Zhao, A. Wang, G.W. Huber, T. Zhang, Catalytic Transformation of Lignin for the Production of Chemicals and Fuels, Chem Rev 115 (2015) 11559–11624. https://doi.org/10.1021/acs.chemrev.5b00155.

[7] Y. Pu, S. Cao, A.J. Ragauskas, Application of quantitative 31P NMR in biomass lignin and biofuel precursors characterization, Energy Environ Sci 4 (2011) 3154. https://doi.org/10.1039/c1ee01201k.

[8] A.A. Houfani, N. Anders, A.C. Spiess, P. Baldrian, S. Benallaoua, Insights from enzymatic degradation of cellulose and hemicellulose to fermentable sugars– a review, Biomass Bioenergy 134 (2020) 105481. https://doi.org/10.1016/j.biombioe.2020.105481.

[9] A. Lourenço, H. Pereira, Compositional Variability of Lignin in Biomass, in: Lignin - Trends and Applications, InTech, 2018. https://doi.org/10.5772/intechopen.71208.

[10] E.M. Anderson, M.L. Stone, R. Katahira, M. Reed, W. Muchero, K.J. Ramirez, G.T. Beckham, Y. Román-Leshkov, Differences in S/G ratio in natural poplar variants do not predict catalytic depolymerization monomer yields, Nat Commun 10 (2019) 2033. https://doi.org/10.1038/s41467-019-09986-1.

[11] C.G. Yoo, A. Dumitrache, W. Muchero, J. Natzke, H. Akinosho, M. Li, R.W. Sykes, S.D. Brown, B. Davison, G.A. Tuskan, Y. Pu, A.J. Ragauskas, Significance of Lignin S/G Ratio in Biomass Recalcitrance of Populus trichocarpa Variants for

Bioethanol Production, ACS Sustain Chem Eng 6 (2018) 2162–2168. https://doi.org/10.1021/acssuschemeng.7b03586.

[12] C. Weng, X. Peng, Y. Han, Depolymerization and conversion of lignin to value-added bioproducts by microbial and enzymatic catalysis, Biotechnol Biofuels 14 (2021) 84. https://doi.org/10.1186/s13068-021-01934-w.

[13] M. Kosa, A.J. Ragauskas, Bioconversion of lignin model compounds with oleaginous Rhodococci, Appl Microbiol Biotechnol 93 (2012) 891–900. https://doi.org/10.1007/s00253-011-3743-z.

[14] P.D. Sainsbury, E.M. Hardiman, M. Ahmad, H. Otani, N. Seghezzi, L.D. Eltis, T.D.H. Bugg, Breaking Down Lignin to High-Value Chemicals: The Conversion of Lignocellulose to Vanillin in a Gene Deletion Mutant of *Rhodococcus jostii* RHA1, ACS Chem Biol 8 (2013) 2151–2156. https://doi.org/10.1021/cb400505a.

[15] J. Becker, M. Kuhl, M. Kohlstedt, S. Starck, C. Wittmann, Metabolic engineering of *Corynebacterium glutamicum* for the production of cis, cis-muconic acid from lignin, Microb Cell Fact 17 (2018) 115. https://doi.org/10.1186/s12934-018-0963-2.

[16] J. Yu, H. Stahl, Microbial utilization and biopolyester synthesis of bagasse hydrolysates, Bioresour Technol 99 (2008) 8042–8048. https://doi.org/10.1016/j.biortech.2008.03.071.

[17] W. Wu, T. Dutta, A.M. Varman, A. Eudes, B. Manalansan, D. Loqué, S. Singh, Lignin Valorization: Two Hybrid Biochemical Routes for the Conversion of Polymeric Lignin into Value-added Chemicals, Sci Rep 7 (2017) 8420. https://doi.org/10.1038/s41598-017-07895-1.

[18] L. Pollegioni, F. Tonin, E. Rosini, Lignin-degrading enzymes, FEBS Journal 282 (2015) 1190–1213. https://doi.org/10.1111/febs.13224.

[19] R. Reshmy, P. Athiyaman Balakumaran, K. Divakar, E. Philip, A. Madhavan, A. Pugazhendhi, R. Sirohi, P. Binod, M. Kumar Awasthi, R. Sindhu, Microbial valorization of lignin: Prospects and challenges, Bioresour Technol 344 (2022) 126240. https://doi.org/10.1016/j.biortech.2021.126240.

[20] I. Hasanov, M. Raud, T. Kikas, The Role of Ionic Liquids in the Lignin Separation from Lignocellulosic Biomass, Energies (Basel) 13 (2020) 4864. https://doi.org/10.3390/en13184864.

[21] B. Bharathiraja, S. Sridharan, V. Sowmya, D. Yuvaraj, R. Praveenkumar, Microbial oil – A plausible alternate resource for food and fuel application, Bioresour Technol 233 (2017) 423–432. https://doi.org/10.1016/j.biortech.2017.03.006.

[22] Y. Li-Beisson, G. Peltier, Third-generation biofuels: current and future research on microalgal lipid biotechnology, OCL 20 (2013) D606. https://doi.org/10.1051/ocl/2013031.

[23] W.E. Anthony, R.R. Carr, D.M. DeLorenzo, T.P. Campbell, Z. Shang, M. Foston, T.S. Moon, G. Dantas, Development of *Rhodococcus opacus* as a chassis for lignin valorization and bioproduction of high-value compounds, Biotechnol Biofuels 12 (2019) 192. https://doi.org/10.1186/s13068-019-1535-3.

[24] S.A. Shields-Menard, M. AmirSadeghi, M. Green, E. Womack, D.L. Sparks, J. Blake, M. Edelmann, X. Ding, B. Sukhbaatar, R. Hernandez, J.R. Donaldson, T. French, The effects of model aromatic lignin compounds on growth and lipid accumulation of

*Rhodococcus rhodochrous*, Int Biodeterior Biodegradation 121 (2017) 79–90. https://doi.org/10.1016/j.ibiod.2017.03.023.

[25] D. Botstein, S.A. Chervitz, M. Cherry, Yeast as a Model Organism, Science (1979) 277 (1997) 1259–1260. https://doi.org/10.1126/science.277.5330.1259.

[26] D. Huccetogullari, Z.W. Luo, S.Y. Lee, Metabolic engineering of microorganisms for production of aromatic compounds, Microb Cell Fact 18 (2019) 41. https://doi.org/10.1186/s12934-019-1090-4.

[27] J. Wang, Q. Gao, H. Zhang, J. Bao, Inhibitor degradation and lipid accumulation potentials of oleaginous yeast *Trichosporon cutaneum* using lignocellulose feedstock, Bioresour Technol 218 (2016) 892–901. https://doi.org/10.1016/j.biortech.2016.06.130.

[28] M.I. Šantek, J. Lisičar, L. Mušak, I.V. Špoljarić, S. Beluhan, B. Šantek, Lipid Production by Yeast *Trichosporon oleaginosus* on the Enzymatic Hydrolysate of Alkaline Pretreated Corn Cobs for Biodiesel Production, Energy & Fuels 32 (2018) 12501–12513. https://doi.org/10.1021/acs.energyfuels.8b02231.

[29] L.Y. Zhu, M.H. Zong, H. Wu, Efficient lipid production with *Trichosporon fermentans* and its use for biodiesel preparation, Bioresour Technol 99 (2008) 7881–7885. https://doi.org/10.1016/j.biortech.2008.02.033.

[30] X. Chen, Z. Li, X. Zhang, F. Hu, D.D.Y. Ryu, J. Bao, Screening of Oleaginous Yeast Strains Tolerant to Lignocellulose Degradation Compounds, Appl Biochem Biotechnol 159 (2009) 591–604. https://doi.org/10.1007/s12010-008-8491-x.

[31] M. Hu, J. Wang, Q. Gao, J. Bao, Converting lignin derived phenolic aldehydes into microbial lipid by *Trichosporon cutaneum*, J Biotechnol 281 (2018) 81–86. https://doi.org/10.1016/j.jbiotec.2018.06.341.

[32] Y. Zhang, J. Bao, Tolerance of *Trichosporon cutaneum* to lignin derived phenolic aldehydes facilitate the cell growth and cellulosic lipid accumulation, J Biotechnol 343 (2022) 32–37. https://doi.org/10.1016/j.jbiotec.2021.09.009.

[33] A. Yaguchi, A. Robinson, E. Mihealsick, M. Blenner, Metabolism of aromatics by *Trichosporon oleaginosus* while remaining oleaginous, Microb Cell Fact 16 (2017) 206. https://doi.org/10.1186/s12934-017-0820-8.

[34] J. Yaegashi, J. Kirby, M. Ito, J. Sun, T. Dutta, M. Mirsiaghi, E.R. Sundstrom, A. Rodriguez, E. Baidoo, D. Tanjore, T. Pray, K. Sale, S. Singh, J.D. Keasling, B.A. Simmons, S.W. Singer, J.K. Magnuson, A.P. Arkin, J.M. Skerker, J.M. Gladden, *Rhodosporidium toruloides*: a new platform organism for conversion of lignocellulose into terpene biofuels and bioproducts, Biotechnol Biofuels 10 (2017) 241. https://doi.org/10.1186/s13068-017-0927-5.

[35] A.B. Juanssilfero, P. Kahar, R.L. Amza, N. Miyamoto, H. Otsuka, H. Matsumoto, C. Kihira, A. Thontowi, Yopi, C. Ogino, B. Prasetya, A. Kondo, Selection of oleaginous yeasts capable of high lipid accumulation during challenges from inhibitory chemical compounds, Biochem Eng J 137 (2018) 182–191. https://doi.org/10.1016/j.bej.2018.05.024.

[36] V. Sànchez i Nogué, B.A. Black, J.S. Kruger, C.A. Singer, K.J. Ramirez, M.L. Reed, N.S. Cleveland, E.R. Singer, X. Yi, R.Y. Yeap, J.G. Linger, G.T. Beckham,

Integrated diesel production from lignocellulosic sugars via oleaginous yeast, Green Chemistry 20 (2018) 4349–4365. https://doi.org/10.1039/C8GC01905C.

[37] R.R. Singhania, A.K. Patel, T. Raj, C.-W. Chen, V.K. Ponnusamy, N. Tahir, S.-H. Kim, C.-D. Dong, Lignin valorisation via enzymes: A sustainable approach, Fuel 311 (2022) 122608. https://doi.org/10.1016/j.fuel.2021.122608.

[38] M. Tien, T.K. Kirk, Lignin-Degrading Enzyme from the Hymenomycete *Phanerochaete chrysosporium* Burds, Science (1979) 221 (1983) 661–663. https://doi.org/10.1126/science.221.4611.661.

[39] C.F. Thurston, The structure and function of fungal laccases, Microbiology (N Y) 140 (1994) 19–26. https://doi.org/10.1099/13500872-140-1-19.

[40] H. Claus, Laccases and their occurrence in prokaryotes, Arch Microbiol 179 (2003) 145–150. https://doi.org/10.1007/s00203-002-0510-7.

[41] G. Janusz, A. Pawlik, J. Sulej, U. Świderska-Burek, A. Jarosz-Wilkołazka, A. Paszczyński, Lignin degradation: microorganisms, enzymes involved, genomes analysis and evolution, FEMS Microbiol Rev 41 (2017) 941–962. https://doi.org/10.1093/femsre/fux049.

[42] P.K. Dikshit, H.-B. Jun, B.S. Kim, Biological conversion of lignin and its derivatives to fuels and chemicals, Korean Journal of Chemical Engineering 37 (2020) 387–401. https://doi.org/10.1007/s11814-019-0458-9.

[43] Z. Antošová, H. Sychrová, Yeast Hosts for the Production of Recombinant Laccases: A Review, Mol Biotechnol 58 (2016) 93–116. https://doi.org/10.1007/s12033-015-9910-1.

[44] C.J. Rodgers, C.F. Blanford, S.R. Giddens, P. Skamnioti, F.A. Armstrong, S.J. Gurr, Designer laccases: a vogue for high-potential fungal enzymes, Trends Biotechnol 28 (2010) 63–72. https://doi.org/10.1016/j.tibtech.2009.11.001.

[45] A. Vieira Gomes, T. Souza Carmo, L. Silva Carvalho, F. Mendonça Bahia, N. Parachin, Comparison of Yeasts as Hosts for Recombinant Protein Production, Microorganisms 6 (2018) 38. https://doi.org/10.3390/microorganisms6020038.

[46] M. Karbalaei, S.A. Rezaee, H. Farsiani, *Pichia pastoris* : A highly successful expression system for optimal synthesis of heterologous proteins, J Cell Physiol 235 (2020) 5867–5881. https://doi.org/10.1002/jcp.29583.

[47] Q. Deparis, A. Claes, M.R. Foulquié-Moreno, J.M. Thevelein, Engineering tolerance to industrially relevant stress factors in yeast cell factories, FEMS Yeast Res 17 (2017). https://doi.org/10.1093/femsyr/fox036.

[48] C.S. Harwood, R.E. Parales, The beta-ketoadipate pathway and the biology of self-identity, Annu Rev Microbiol 50 (1996) 553–590. https://doi.org/10.1146/annurev.micro.50.1.553.

[49] C. Calixto-Campos, T.T. Carvalho, M.S.N. Hohmann, F.A. Pinho-Ribeiro, V. Fattori, M.F. Manchope, A.C. Zarpelon, M.M. Baracat, S.R. Georgetti, R. Casagrande, W.A. Verri, Vanillic Acid Inhibits Inflammatory Pain by Inhibiting Neutrophil Recruitment, Oxidative Stress, Cytokine Production, and NFκB Activation in Mice, J Nat Prod 78 (2015) 1799–1808. https://doi.org/10.1021/acs.jnatprod.5b00246.

[50] I.S. Kim, D.-K. Choi, H.J. Jung, Neuroprotective Effects of Vanillyl Alcohol in Gastrodia elata Blume Through Suppression of Oxidative Stress and Anti-Apoptotic

Activity in Toxin-Induced Dopaminergic MN9D Cells, Molecules 16 (2011) 5349–5361. https://doi.org/10.3390/molecules16075349.

[51] J. Dai, A.F. Patti, K. Saito, Recent developments in chemical degradation of lignin: catalytic oxidation and ionic liquids, Tetrahedron Lett 57 (2016) 4945–4951. https://doi.org/10.1016/j.tetlet.2016.09.084.

[52] X. OUYANG, Y. TAN, X. QIU, Oxidative degradation of lignin for producing monophenolic compounds, Journal of Fuel Chemistry and Technology 42 (2014) 677–682. https://doi.org/10.1016/S1872-5813(14)60030-X.

[53] X. Chen, X. Xi, A. Pizzi, E. Fredon, G. Du, C. Gerardin, S. Amirou, Oxidized demethylated lignin as a bio-based adhesive for wood bonding, J Adhes 97 (2021) 873–890. https://doi.org/10.1080/00218464.2019.1710830.

[54] Y. Mathieu, J.D. Vidal, L. Arribas Martínez, N. Abad Fernández, S. Iborra, A. Corma, Molecular Oxygen Lignin Depolymerization: An Insight into the Stability of Phenolic Monomers, ChemSusChem 13 (2020) 4743–4758. https://doi.org/10.1002/cssc.202001295.

[55] A. Kumar, B. Biswas, K. Saini, A. Kumar, J. Kumar, B.B. Krishna, T. Bhaskar, Effect of hydrogen peroxide on the depolymerization of prot lignin, Ind Crops Prod 150 (2020) 112355. https://doi.org/10.1016/j.indcrop.2020.112355.

[56] J. Gierer, Chemistry of delignification, Wood Sci Technol 20 (1986) 1–33. https://doi.org/10.1007/BF00350692.

[57] N.F. Cymbaluk, T.S. Neudoerffer, A quantitative gas-liquid chromatographic determination of aromatic aldehydes and acids from nitrobenzene oxidation of lignin, J Chromatogr A 51 (1970) 167–174. https://doi.org/10.1016/S0021-9673(01)96851-7.

[58] H. Deng, H. Zhang, Z. Wu, X. Tian, X. Jiang, W. Guo, Rules and mechanism for the oxidation of lignin-based aromatic aldehyde under alkaline wet oxygen, Bioresources 15 (2020) 3487–3503. https://doi.org/10.15376/biores.15.2.3487-3503.

[59] V. Tarabanko, N. Tarabanko, Catalytic Oxidation of Lignins into the Aromatic Aldehydes: General Process Trends and Development Prospects, Int J Mol Sci 18 (2017) 2421. https://doi.org/10.3390/ijms18112421.

[60] P.-L. Tang, O. Hassan, M.Y. Maskat, K. Badri, Production of Monomeric Aromatic Compounds from Oil Palm Empty Fruit Bunch Fiber Lignin by Chemical and Enzymatic Methods, Biomed Res Int 2015 (2015) 1–14. https://doi.org/10.1155/2015/891539.

[61] H. Deng, L. Lin, S. Liu, Catalysis of Cu-Doped Co-Based Perovskite-Type Oxide in Wet Oxidation of Lignin To Produce Aromatic Aldehydes, Energy & Fuels 24 (2010) 4797–4802. https://doi.org/10.1021/ef100768e.

[62] T. Voitl, P. Rudolf von Rohr, Oxidation of Lignin Using Aqueous Polyoxometalates in the Presence of Alcohols, ChemSusChem 1 (2008) 763–769. https://doi.org/10.1002/cssc.200800050.

[63] X. Xi, A. Pizzi, C.R. Frihart, L. Lorenz, C. Gerardin, Tannin plywood bioadhesives with non-volatile aldehydes generation by specific oxidation of mono- and

disaccharides, Int J Adhes Adhes 98 (2020) 102499. https://doi.org/10.1016/j.ijadhadh.2019.102499.

[64] C.R. Frihart, A. Pizzi, X. Xi, L.F. Lorenz, Reactions of Soy Flour and Soy Protein by Non-Volatile Aldehydes Generation by Specific Oxidation, Polymers (Basel) 11 (2019) 1478. https://doi.org/10.3390/polym11091478.

[65] H. Wang, Y. Tang, H. Gao, H. Gao, Q. Zhao, J. Li, F. Xin, W. Zhang, M. Jiang, Microbial co-culturing of *Chlorella* sp. And *Rhodotorula toruloides* for the enhanced microbial lipid production, Fuel 324 (2022) 124609. https://doi.org/10.1016/j.fuel.2022.124609.

[66] S. Lee, P. Kim, Current Status and Applications of Adaptive Laboratory Evolution in Industrial Microorganisms, J Microbiol Biotechnol 30 (2020) 793–803. https://doi.org/10.4014/jmb.2003.03072.

[67] J. Steensels, T. Snoek, E. Meersman, M.P. Nicolino, K. Voordeckers, K.J. Verstrepen, Improving industrial yeast strains: exploiting natural and artificial diversity, FEMS Microbiol Rev 38 (2014) 947–995. https://doi.org/10.1111/1574-6976.12073.

[68] M. Maldini, F. Natella, S. Baima, G. Morelli, C. Scaccini, J. Langridge, G. Astarita, Untargeted Metabolomics Reveals Predominant Alterations in Lipid Metabolism Following Light Exposure in Broccoli Sprouts, Int J Mol Sci 16 (2015) 13678–13691. https://doi.org/10.3390/ijms160613678.

[69] W.A. Laviña, S.S.M. Sakurai, S. Pontrelli, S.P. Putri, E. Fukusaki, Metabolomics Analysis Reveals Global Metabolic Changes in the Evolved E. coli Strain with Improved

Growth and 1-Butanol Production in Minimal Medium, Metabolites 10 (2020) 192. https://doi.org/10.3390/metabo10050192.

[70] S. Qiu, Y. Cai, H. Yao, C. Lin, Y. Xie, S. Tang, A. Zhang, Small molecule metabolites: discovery of biomarkers and therapeutic targets, Signal Transduct Target Ther 8 (2023) 132. https://doi.org/10.1038/s41392-023-01399-3.

[71] F.J.N. Putra, P. Kahar, A. Kondo, C. Ogino, Valorization of Lignin and Its Derivatives Using Yeast, Processes 10 (2022) 2004. https://doi.org/10.3390/pr10102004.

[72] J. Becker, C. Wittmann, A field of dreams: Lignin valorization into chemicals, materials, fuels, and health-care products, Biotechnol Adv 37 (2019) 107360. https://doi.org/10.1016/j.biotechadv.2019.02.016.

[73] P.S. Chauhan, R. Agrawal, A. satlewal, R. Kumar, R.P. Gupta, S.S.V. Ramakumar, Next generation applications of lignin derived commodity products, their life cycle, techno-economics and societal analysis, Int J Biol Macromol 197 (2022) 179–200. https://doi.org/10.1016/j.ijbiomac.2021.12.146.

[74] J. Wenger, V. Haas, T. Stern, Why Can We Make Anything from Lignin Except Money? Towards a Broader Economic Perspective in Lignin Research, Current Forestry Reports 6 (2020) 294–308. https://doi.org/10.1007/s40725-020-00126-3.

[75] D. Chettri, S. Ahmed, A.A. Malik, A.K. Verma, Lignin Depolymerization for Its Valorization, Bioenergy Res (2023). https://doi.org/10.1007/s12155-022-10561-8.

[76] A. Amore, P.N. Ciesielski, C.-Y. Lin, D. Salvachúa, V. Sànchez i Nogué, Development of Lignocellulosic Biorefinery Technologies: Recent Advances and Current Challenges, Aust J Chem 69 (2016) 1201. https://doi.org/10.1071/CH16022.

[77] R. Reshmy, P. Athiyaman Balakumaran, K. Divakar, E. Philip, A. Madhavan, A. Pugazhendhi, R. Sirohi, P. Binod, M. Kumar Awasthi, R. Sindhu, Microbial valorization of lignin: Prospects and challenges, Bioresour Technol 344 (2022) 126240. https://doi.org/10.1016/j.biortech.2021.126240.

[78] B. Jacobs, Y. Yao, I. Van Nieuwenhove, D. Sharma, G.-J. Graulus, K. Bernaerts, A. Verberckmoes, Sustainable lignin modifications and processing methods: green chemistry as the way forward, Green Chemistry 25 (2023) 2042–2086. https://doi.org/10.1039/D2GC04699G.

[79] C. Zhang, F. Wang, Catalytic Lignin Depolymerization to Aromatic Chemicals, Acc Chem Res 53 (2020) 470–484. https://doi.org/10.1021/acs.accounts.9b00573.

[80] J. Ralph, C. Lapierre, W. Boerjan, Lignin structure and its engineering, Curr Opin Biotechnol 56 (2019) 240–249. https://doi.org/10.1016/j.copbio.2019.02.019.

[81] N. Zhou, W.P.D.W. Thilakarathna, Q.S. He, H.P.V. Rupasinghe, A Review: Depolymerization of Lignin to Generate High-Value Bio-Products: Opportunities, Challenges, and Prospects, Front Energy Res 9 (2022). https://doi.org/10.3389/fenrg.2021.758744.

[82] S. Wang, X. Sun, Q. Yuan, Strategies for enhancing microbial tolerance to inhibitors for biofuel production: A review, Bioresour Technol 258 (2018) 302–309. https://doi.org/10.1016/j.biortech.2018.03.064.

[83] J.G. Linger, D.R. Vardon, M.T. Guarnieri, E.M. Karp, G.B. Hunsinger, M.A. Franden, C.W. Johnson, G. Chupka, T.J. Strathmann, P.T. Pienkos, G.T. Beckham, Lignin valorization through integrated biological funneling and chemical catalysis,

Proceedings of the National Academy of Sciences 111 (2014) 12013–12018. https://doi.org/10.1073/pnas.1410657111.

[84] A.J. Ragauskas, G.T. Beckham, M.J. Biddy, R. Chandra, F. Chen, M.F. Davis, B.H. Davison, R.A. Dixon, P. Gilna, M. Keller, P. Langan, A.K. Naskar, J.N. Saddler, T.J. Tschaplinski, G.A. Tuskan, C.E. Wyman, Lignin Valorization: Improving Lignin Processing in the Biorefinery, Science (1979) 344 (2014). https://doi.org/10.1126/science.1246843.

[85] J. Arreola-Vargas, X. Meng, Y. Wang, A.J. Ragauskas, J.S. Yuan, Enhanced medium chain length-polyhydroxyalkanoate production by co-fermentation of lignin and holocellulose hydrolysates, Green Chemistry 23 (2021) 8226–8237. https://doi.org/10.1039/D1GC02725E.

[86] M. Hu, J. Wang, Q. Gao, J. Bao, Converting lignin derived phenolic aldehydes into microbial lipid by *Trichosporon cutaneum*, J Biotechnol 281 (2018) 81–86. https://doi.org/10.1016/j.jbiotec.2018.06.341.

[87] A.A. Fadahunsi, C. Li, M.I. Khan, W. Ding, MXenes: state-of-the-art synthesis, composites and bioapplications, J Mater Chem B 10 (2022) 4331–4345. https://doi.org/10.1039/D2TB00289B.

[88] M.I. Khan, S. Xu, M.M. Ali, R. Ali, A. Kazmi, N. Akhtar, M. Bilal, Y. Hu, F. Li, Assessment of multidrug resistance in bacterial isolates from urinary tract-infected patients, J Radiat Res Appl Sci 13 (2020) 267–275. https://doi.org/10.1080/16878507.2020.1730579.

[89] Y.W. Jang, J.Y. Lee, C.J. Kim, Anti-asthmatic activity of phenolic compounds from the roots of *Gastrodia elata* Bl, Int Immunopharmacol 10 (2010) 147–154. https://doi.org/10.1016/j.intimp.2009.10.009.

[90] H. Zhu, D. Zhang, Q. Zhang, Y. Zhao, Z. He, Y. Gao, L. Zhang, 4-Hydroxybenzyl alcohol derivatives and their sedative–hypnotic activities, RSC Adv 8 (2018) 19539–19550. https://doi.org/10.1039/C8RA01972J.

[91] C. Lu, S. Qu, Z. Zhong, H. Luo, S.S. Lei, H.-J. Zhong, H. Su, Y. Wang, C.-M. Chong, The effects of bioactive components from the rhizome of *Gastrodia elata* blume (Tianma) on the characteristics of Parkinson's disease, Front Pharmacol 13 (2022). https://doi.org/10.3389/fphar.2022.963327.

[92] I.S. Kim, D.-K. Choi, H.J. Jung, Neuroprotective Effects of Vanillyl Alcohol in *Gastrodia elata* Blume Through Suppression of Oxidative Stress and Anti-Apoptotic Activity in Toxin-Induced Dopaminergic MN9D Cells, Molecules 16 (2011) 5349–5361. https://doi.org/10.3390/molecules16075349.

[93] E.S. Caldwell, C. Steelink, Phenoxy radical intermediate in the enzymatic degradation of lignin model compounds, Biochimica et Biophysica Acta (BBA) - General Subjects 184 (1969) 420–431. https://doi.org/10.1016/0304-4165(69)90046-4.

[94] L. Zhang, J.T.E. Lee, Y.S. Ok, Y. Dai, Y.W. Tong, Enhancing microbial lipids yield for biodiesel production by oleaginous yeast *Lipomyces starkeyi* fermentation: A review, Bioresour Technol 344 (2022) 126294. https://doi.org/10.1016/j.biortech.2021.126294.

[95] R.L. Amza, P. Kahar, A.B. Juanssilfero, N. Miyamoto, H. Otsuka, C. Kihira, C. Ogino, A. Kondo, High cell density cultivation of *Lipomyces starkeyi* for achieving highly efficient lipid production from sugar under low C/N ratio, Biochem Eng J 149 (2019) 107236. https://doi.org/10.1016/j.bej.2019.05.013.

[96] F. Al-Rimawi, I. Odeh, Development and Validation of an HPLC-UV Method for Determination of Eight Phenolic Compounds in Date Palms, J AOAC Int 98 (2015) 1335–1339. https://doi.org/10.5740/jaoacint.15-010.

[97] A.B. Juanssilfero, P. Kahar, R.L. Amza, N. Miyamoto, H. Otsuka, H. Matsumoto, C. Kihira, A. Thontowi, Yopi, C. Ogino, B. Prasetya, A. Kondo, Effect of inoculum size on single-cell oil production from glucose and xylose using oleaginous yeast *Lipomyces starkeyi*, J Biosci Bioeng 125 (2018) 695–702. https://doi.org/10.1016/j.jbiosc.2017.12.020.

[98] M. Kanai, T. Yamada, M. Hayashi, S. Mano, M. Nishimura, Soybean (*Glycine max* L.) triacylglycerol lipase GmSDP1 regulates the quality and quantity of seed oil, Sci Rep 9 (2019) 8924. https://doi.org/10.1038/s41598-019-45331-8.

[99] O. Ibraheem, B.K. Ndimba, Molecular Adaptation Mechanisms Employed by Ethanologenic Bacteria in Response to Lignocellulose-derived Inhibitory Compounds, Int J Biol Sci 9 (2013) 598–612. https://doi.org/10.7150/ijbs.6091.

[100] R. Lin, J. Cheng, L. Ding, W. Song, J. Zhou, K. Cen, Inhibitory effects of furan derivatives and phenolic compounds on dark hydrogen fermentation, Bioresour Technol 196 (2015) 250–255. https://doi.org/10.1016/j.biortech.2015.07.097.

[101] Z.L. Liu, J. Moon, A novel NADPH-dependent aldehyde reductase gene from Saccharomyces cerevisiae NRRL Y-12632 involved in the detoxification of aldehyde inhibitors derived from lignocellulosic biomass conversion, Gene 446 (2009) 1–10. https://doi.org/10.1016/j.gene.2009.06.018.

[102] A. Mukhopadhyay, Tolerance engineering in bacteria for the production of advanced biofuels and chemicals, Trends Microbiol 23 (2015) 498–508. https://doi.org/10.1016/j.tim.2015.04.008.

[103] R. Lin, J. Cheng, L. Ding, W. Song, J. Zhou, K. Cen, Inhibitory effects of furan derivatives and phenolic compounds on dark hydrogen fermentation, Bioresour Technol 196 (2015) 250–255. https://doi.org/10.1016/j.biortech.2015.07.097.

[104] X. Chen, Y. Xue, J. Hu, Y.F. Tsang, M.-T. Gao, Release of Polyphenols Is the Major Factor Influencing the Bioconversion of Rice Straw to Lactic Acid, Appl Biochem Biotechnol 183 (2017) 685–698. https://doi.org/10.1007/s12010-017-2457-9.

[105] M.F. Adegboye, O.B. Ojuederie, P.M. Talia, O.O. Babalola, Bioprospecting of microbial strains for biofuel production: metabolic engineering, applications, and challenges, Biotechnol Biofuels 14 (2021) 5. https://doi.org/10.1186/s13068-020-01853-2.

[106] R. Tramontina, J.L. Galman, F. Parmeggiani, S.R. Derrington, T.D.H. Bugg, N.J. Turner, F.M. Squina, N. Dixon, Consolidated production of coniferol and other high-value aromatic alcohols directly from lignocellulosic biomass, Green Chemistry 22 (2020) 144–152. https://doi.org/10.1039/C9GC02359C.

[107] N. Kamimura, T. Goto, K. Takahashi, D. Kasai, Y. Otsuka, M. Nakamura, Y. Katayama, M. Fukuda, E. Masai, A bacterial aromatic aldehyde dehydrogenase critical for the efficient catabolism of syringaldehyde, Sci Rep 7 (2017) 44422. https://doi.org/10.1038/srep44422.

[108] O. de Smidt, J.C. du Preez, J. Albertyn, The alcohol dehydrogenases of *Saccharomyces cerevisiae* : a comprehensive review, FEMS Yeast Res 8 (2008) 967–978. https://doi.org/10.1111/j.1567-1364.2008.00387.x.

[109] H. Zhang, L. Zhang, H. Chen, Y.Q. Chen, C. Ratledge, Y. Song, W. Chen, Regulatory properties of malic enzyme in the oleaginous yeast, *Yarrowia lipolytica*, and its non-involvement in lipid accumulation, Biotechnol Lett 35 (2013) 2091–2098. https://doi.org/10.1007/s10529-013-1302-7.

[110] A. Kamineni, J. Shaw, Engineering triacylglycerol production from sugars in oleaginous yeasts, Curr Opin Biotechnol 62 (2020) 239–247. https://doi.org/10.1016/j.copbio.2019.12.022.

[111] H. Takaku, T. Matsuzawa, K. Yaoi, H. Yamazaki, Lipid metabolism of the oleaginous yeast *Lipomyces starkeyi*, Appl Microbiol Biotechnol 104 (2020) 6141–6148. https://doi.org/10.1007/s00253-020-10695-9.

[112] I.R. Sitepu, L.A. Garay, R. Sestric, D. Levin, D.E. Block, J.B. German, K.L. Boundy-Mills, Oleaginous yeasts for biodiesel: Current and future trends in biology and production, Biotechnol Adv 32 (2014) 1336–1360. https://doi.org/10.1016/j.biotechadv.2014.08.003.

[113] K. V. Probst, P. V. Vadlani, Single cell oil production by *Lipomyces starkeyi*: Biphasic fed-batch fermentation strategy providing glucose for growth and xylose for oil production, Biochem Eng J 121 (2017) 49–58. https://doi.org/10.1016/j.bej.2017.01.015.

[114] S. Sutanto, S. Zullaikah, P.L. Tran-Nguyen, S. Ismadji, Y.-H. Ju, *Lipomyces starkeyi*: Its current status as a potential oil producer, Fuel Processing Technology 177 (2018) 39–55. https://doi.org/10.1016/j.fuproc.2018.04.012.

[115] D. Greetham, A.J. Hart, G.A. Tucker, Presence of low concentrations of acetic acid improves yeast tolerance to hydroxymethylfurfural (HMF) and furfural, Biomass Bioenergy 85 (2016) 53–60. https://doi.org/10.1016/j.biombioe.2015.11.026.

[116] G.T. Tsao, Principles of microbe and cell cultivation, S. John Pirt, Halsted Press, Division of John Wiley and Sons, New York, 274, AIChE Journal 22 (1976) 621–621. https://doi.org/10.1002/aic.690220342.

[117] R. Miah, A. Siddiqa, U. Chakraborty, J.F. Tuli, N.K. Barman, A. Uddin, T. Aziz, N. Sharif, S.K. Dey, M. Yamada, A.A. Talukder, Development of high temperature simultaneous saccharification and fermentation by thermosensitive *Saccharomyces cerevisiae* and *Bacillus amyloliquefaciens*, Sci Rep 12 (2022) 3630. https://doi.org/10.1038/s41598-022-07589-3.

[118] A. Tanimura, T. Sugita, R. Endoh, M. Ohkuma, S. Kishino, J. Ogawa, J. Shima, M. Takashima, Lipid production via simultaneous conversion of glucose and xylose by a novel yeast, *Cystobasidium iriomotense*, PLoS One 13 (2018) e0202164. https://doi.org/10.1371/journal.pone.0202164.

[119] A.B. Juanssilfero, P. Kahar, R.L. Amza, Yopi, K. Sudesh, C. Ogino, B. Prasetya, A. Kondo, Lipid production by *Lipomyces starkeyi* using sap squeezed from felled old oil palm trunks, J Biosci Bioeng 127 (2019) 726–731. https://doi.org/10.1016/j.jbiosc.2018.12.002.

[120] M. Tai, G. Stephanopoulos, Engineering the push and pull of lipid biosynthesis in oleaginous yeast *Yarrowia lipolytica* for biofuel production, Metab Eng 15 (2013) 1–9. https://doi.org/10.1016/j.ymben.2012.08.007.

[121] A. Chattopadhyay, M. Mitra, M.K. Maiti, Recent advances in lipid metabolic engineering of oleaginous yeasts, Biotechnol Adv 53 (2021) 107722. https://doi.org/10.1016/j.biotechadv.2021.107722.

[122] J. Zhang, Y. Wang, Q. Gou, W. Zhou, Y. Liu, J. Xu, Y. Liu, W. Zhou, Z. Gong, Consolidated bioprocessing of cassava starch into microbial lipid for biodiesel production by the amylolytic yeast *Lipomyces starkeyi*, Ind Crops Prod 177 (2022) 114534. https://doi.org/10.1016/j.indcrop.2022.114534.

[123] H. Takaku, S. Ebina, K. Kasuga, R. Sato, S. Ara, H. Kazama, T. Matsuzawa, K. Yaoi, H. Araki, Y. Shida, W. Ogasawara, K. Ishiya, S. Aburatani, H. Yamazaki, Isolation and characterization of *Lipomyces starkeyi* mutants with greatly increased lipid productivity following UV irradiation, J Biosci Bioeng 131 (2021) 613–621. https://doi.org/10.1016/j.jbiosc.2021.01.006.

[124] M. Zhao, W. Zhou, Y. Wang, J. Wang, J. Zhang, Z. Gong, Combination of simultaneous saccharification and fermentation of corn stover with consolidated bioprocessing of cassava starch enhances lipid production by the amylolytic oleaginous

yeast *Lipomyces starkeyi*, Bioresour Technol 364 (2022) 128096. https://doi.org/10.1016/j.biortech.2022.128096.

[125] S.L. Ngan, A.C. Er, P. Yatim, B.S. How, C.H. Lim, W.P.Q. Ng, Y.H. Chan, H.L. Lam, Social Sustainability of Palm Oil Industry: A Review, Frontiers in Sustainability 3 (2022). https://doi.org/10.3389/frsus.2022.855551.

[126] Y. Shigetomi, Y. Ishimura, Y. Yamamoto, Trends in global dependency on the Indonesian palm oil and resultant environmental impacts, Sci Rep 10 (2020) 20624. https://doi.org/10.1038/s41598-020-77458-4.

[127] O. Farobie, E. Hartulistiyoso, Palm Oil Biodiesel as a Renewable Energy Resource in Indonesia: Current Status and Challenges, Bioenergy Res 15 (2022) 93–111. https://doi.org/10.1007/s12155-021-10344-7.

[128] R. Heilmayr, J. Benedict, Indonesia makes progress towards zero palm oil deforestation, Trase Insights (2022). https://doi.org/https://doi.org/10.48650/50NG-RT71.

[129] H. Akita, M.Z.M. Yusoff, S. Fujimoto, Preparation of Oil Palm Empty Fruit Bunch Hydrolysate, Fermentation 7 (2021) 81. https://doi.org/10.3390/fermentation7020081.

[130] S.R. Juliastuti, N. Hendrianie, K.R. Sabar, S. Anggita, Glucose production from oil palm empty fruit bunch (OPEFB) using microwave and fungal treatment method, IOP Conf Ser Earth Environ Sci 963 (2022) 012053. https://doi.org/10.1088/1755-1315/963/1/012053.

[131] P.S. Chauhan, R. Agrawal, A. satlewal, R. Kumar, R.P. Gupta, S.S.V. Ramakumar, Next generation applications of lignin derived commodity products, their life cycle, techno-economics and societal analysis, Int J Biol Macromol 197 (2022) 179–200. https://doi.org/10.1016/j.ijbiomac.2021.12.146.

[132] V.K. Garlapati, A.K. Chandel, S.P.J. Kumar, S. Sharma, S. Sevda, A.P. Ingle, D. Pant, Circular economy aspects of lignin: Towards a lignocellulose biorefinery, Renewable and Sustainable Energy Reviews 130 (2020) 109977. https://doi.org/10.1016/j.rser.2020.109977.

[133] A. Amore, P.N. Ciesielski, C.-Y. Lin, D. Salvachúa, V. Sànchez i Nogué, Development of Lignocellulosic Biorefinery Technologies: Recent Advances and Current Challenges, Aust J Chem 69 (2016) 1201. https://doi.org/10.1071/CH16022.

[134] B. Jacobs, Y. Yao, I. Van Nieuwenhove, D. Sharma, G.-J. Graulus, K. Bernaerts, A. Verberckmoes, Sustainable lignin modifications and processing methods: green chemistry as the way forward, Green Chemistry 25 (2023) 2042–2086. https://doi.org/10.1039/D2GC04699G.

[135] C. Zhang, F. Wang, Catalytic Lignin Depolymerization to Aromatic Chemicals, Acc Chem Res 53 (2020) 470–484. https://doi.org/10.1021/acs.accounts.9b00573.

[136] A.A. Shah, T.H. Seehar, K. Sharma, S.S. Toor, Biomass pretreatment technologies, in: Hydrocarbon Biorefinery, Elsevier, 2022: pp. 203–228. https://doi.org/10.1016/B978-0-12-823306-1.00014-5.

[137] H. Wang, X. Peng, H. Li, A. Giannis, C. He, Recent Biotechnology Advances in Bio-Conversion of Lignin to Lipids by Bacterial Cultures, Front Chem 10 (2022). https://doi.org/10.3389/fchem.2022.894593.

[138] W. Zhang, C. Diao, L. Wang, Degradation of lignin in different lignocellulosic biomass by steam explosion combined with microbial consortium treatment, Biotechnology for Biofuels and Bioproducts 16 (2023) 55. https://doi.org/10.1186/s13068-023-02306-2.

[139] F.J.N. Putra, P. Kahar, A. Kondo, C. Ogino, The bioconversion of lignin derivative aldehydes into high-value aromatic alcohols and lipids via *Lipomyces starkeyi*, Biochem Eng J 200 (2023) 109065. https://doi.org/10.1016/j.bej.2023.109065.

[140] P. Kahar, A. Itomi, H. Tsuboi, M. Ishizaki, M. Yasuda, C. Kihira, H. Otsuka, N. binti Azmi, H. Matsumoto, C. Ogino, A. Kondo, The flocculant *Saccharomyces cerevisiae* strain gains robustness via alteration of the cell wall hydrophobicity, Metab Eng 72 (2022) 82–96. https://doi.org/10.1016/j.ymben.2022.03.001.

[141] R. Sun, J.M. Lawther, W.B. Banks, The effect of alkaline nitrobenzene oxidation conditions on the yield and components of phenolic monomers in wheat straw lignin and compared to cupric(II) oxidation, Ind Crops Prod 4 (1995) 241–254. https://doi.org/10.1016/0926-6690(95)00038-0.

[142] W. Schutyser, J.S. Kruger, A.M. Robinson, R. Katahira, D.G. Brandner, N.S. Cleveland, A. Mittal, D.J. Peterson, R. Meilan, Y. Román-Leshkov, G.T. Beckham, Revisiting alkaline aerobic lignin oxidation, Green Chemistry 20 (2018) 3828–3844. https://doi.org/10.1039/C8GC00502H.

[143] M.N.M. Ibrahim, M.Y.N. Nadiah, M.S. Norliyana, S. Shuib, Separation and Characterization of the Vanillin Compound from Soda Lignin, in: Innovations in Chemical Biology, Springer Netherlands, Dordrecht, 2009: pp. 103–110. https://doi.org/10.1007/978-1-4020-6955-0_9.

[144] V. Tarabanko, N. Tarabanko, Catalytic Oxidation of Lignins into the Aromatic Aldehydes: General Process Trends and Development Prospects, Int J Mol Sci 18 (2017) 2421. https://doi.org/10.3390/ijms18112421.

[145] M. Yamamura, T. Hattori, S. Suzuki, D. Shibata, T. Umezawa, Microscale alkaline nitrobenzene oxidation method for high-throughput determination of lignin aromatic components, Plant Biotechnology 27 (2010) 305–310. https://doi.org/10.5511/plantbiotechnology.27.305.

[146] K. Ninomiya, K. Ochiai, M. Eguchi, K. Kuroda, Y. Tsuge, C. Ogino, T. Taima, K. Takahashi, Oxidative depolymerization potential of biorefinery lignin obtained by ionic liquid pretreatment and subsequent enzymatic saccharification of eucalyptus, Ind Crops Prod 111 (2018) 457–461. https://doi.org/10.1016/j.indcrop.2017.10.056.

[147] M.N. Mohamad Ibrahim, S.B. Chuah, W.D. Wan Rosli, Characterization of Lignin Precipitated From The Soda Black Liquor of Oil Palm Empty Fruit Bunch Fibers by Various Mineral Acids, ASEAN Journal on Science and Technology for Development 21 (2017) 57. https://doi.org/10.29037/ajstd.92.

[148] Sun, J.M. Fang, J. Tomkinson, J. Bolton, Physicochemical and Structural Characterization of Alkali Soluble Lignins from Oil Palm Trunk and Empty Fruit-Bunch Fibers, J Agric Food Chem 47 (1999) 2930–2936. https://doi.org/10.1021/jf9810463.

[149] M. Yamamura, S. Wada, N. Sakakibara, T. Nakatsubo, S. Suzuki, T. Hattori, M. Takeda, N. Sakurai, H. Suzuki, D. Shibata, T. Umezawa, Occurrence of guaiacyl/p-hydroxyphenyl lignin in *Arabidopsis thaliana* T87 cells, Plant Biotechnology 28 (2011) 1–8. https://doi.org/10.5511/plantbiotechnology.10.0823c.

[150] W. Zhou, Y. Wang, J. Zhang, M. Zhao, M. Tang, W. Zhou, Z. Gong, A metabolic model of *Lipomyces starkeyi* for predicting lipogenesis potential from diverse low-cost substrates, Biotechnol Biofuels 14 (2021) 148. https://doi.org/10.1186/s13068-021-01997-9.

[151] A. Yaguchi, N. Franaszek, K. O'Neill, S. Lee, I. Sitepu, K. Boundy-Mills, M. Blenner, Identification of oleaginous yeasts that metabolize aromatic compounds, J Ind Microbiol Biotechnol 47 (2020) 801–813. https://doi.org/10.1007/s10295-020-02269-5.

[152] H. Zhang, L. Zhang, H. Chen, Y.Q. Chen, C. Ratledge, Y. Song, W. Chen, Regulatory properties of malic enzyme in the oleaginous yeast, *Yarrowia lipolytica*, and its non-involvement in lipid accumulation, Biotechnol Lett 35 (2013) 2091–2098. https://doi.org/10.1007/s10529-013-1302-7.

[153] Z.-Y. Wang, Y. Yin, D.-N. Li, D.-Y. Zhao, J.-Q. Huang, Biological Activities of p-Hydroxycinnamic Acids in Maintaining Gut Barrier Integrity and Function, Foods 12 (2023) 2636. https://doi.org/10.3390/foods12132636.

[154] F. Abeln, C.J. Chuck, The history, state of the art and future prospects for oleaginous yeast research, Microb Cell Fact 20 (2021) 221. https://doi.org/10.1186/s12934-021-01712-1.

[155] J.T. Mindrebo, A. Patel, W.E. Kim, T.D. Davis, A. Chen, T.G. Bartholow, J.J. La Clair, J.A. McCammon, J.P. Noel, M.D. Burkart, Gating mechanism of elongating β-ketoacyl-ACP synthases, Nat Commun 11 (2020) 1727. https://doi.org/10.1038/s41467-020-15455-x.

[156] M. Sun, Z. Shi, C. Zhang, Y. Zhang, S. Zhang, G. Luo, Novel Long-Chain Fatty Acid (LCFA)-Degrading Bacteria and Pathways in Anaerobic Digestion Promoted by Hydrochar as Revealed by Genome-Centric Metatranscriptomics Analysis, Appl Environ Microbiol 88 (2022). https://doi.org/10.1128/aem.01042-22.

[157] J. Wenger, V. Haas, T. Stern, Why Can We Make Anything from Lignin Except Money? Towards a Broader Economic Perspective in Lignin Research, Current Forestry Reports 6 (2020) 294–308. https://doi.org/10.1007/s40725-020-00126-3.

[158] D. Chettri, S. Ahmed, A.A. Malik, A.K. Verma, Lignin Depolymerization for Its Valorization, Bioenergy Res (2023). https://doi.org/10.1007/s12155-022-10561-8.

[159] L. Lyu, Y. Chu, S. Zhang, Y. Zhang, Q. Huang, S. Wang, Z.K. Zhao, Engineering the Oleaginous Yeast *Rhodosporidium toruloides* for Improved Resistance Against Inhibitors in Biomass Hydrolysates, Front Bioeng Biotechnol 9 (2021). https://doi.org/10.3389/fbioe.2021.768934.

[160] M. Postaru, A. Tucaliuc, D. Cascaval, A.-I. Galaction, Cellular Stress Impact on Yeast Activity in Biotechnological Processes—A Short Overview, Microorganisms 11 (2023) 2522. https://doi.org/10.3390/microorganisms11102522.

[161] O. V. Zalomaeva, O.Yu. Podyacheva, A.N. Suboch, L.S. Kibis, O.A. Kholdeeva, Aerobic oxidation of syringyl alcohol over N-doped carbon nanotubes, Appl Catal A Gen 629 (2022) 118424. https://doi.org/10.1016/j.apcata.2021.118424.

[162] E. Tapia V, A. Anschau, A.L. Coradini, T. T Franco, A.C. Deckmann, Optimization of lipid production by the oleaginous yeast *Lipomyces starkeyi* by random mutagenesis coupled to cerulenin screening, AMB Express 2 (2012) 64. https://doi.org/10.1186/2191-0855-2-64.

[163] F.J. Nusantara Putra, S.P. Putri, E. Fukusaki, Metabolomics-based profiling of three terminal alkene-producing *Jeotgalicoccus* spp. during different growth phase, J Biosci Bioeng 127 (2019) 52–58. https://doi.org/10.1016/j.jbiosc.2018.06.014.

[164] Q. Wu, N. Su, X. Huang, J. Cui, L. Shabala, M. Zhou, M. Yu, S. Shabala, Hypoxia-induced increase in GABA content is essential for restoration of membrane potential and preventing ROS-induced disturbance to ion homeostasis, Plant Commun 2 (2021) 100188. https://doi.org/10.1016/j.xplc.2021.100188.

[165] Md.R.H. Raihan, M. Rahman, A. Rastogi, M. Fujita, M. Hasanuzzaman, Exogenous Allantoin Confers Rapeseed (Brassica campestris) Tolerance to Simulated Drought by Improving Antioxidant Metabolism and Physiology, Antioxidants 12 (2023) 1508. https://doi.org/10.3390/antiox12081508.

[166] R. Bernini, I. Carastro, F. Santoni, M. Clemente, Synthesis of Lipophilic Esters of Tyrosol, Homovanillyl Alcohol and Hydroxytyrosol, Antioxidants 8 (2019) 174. https://doi.org/10.3390/antiox8060174.

[167] I. Belda, J. Ruiz, A. Esteban-Fernández, E. Navascués, D. Marquina, A. Santos, M. Moreno-Arribas, Microbial Contribution to Wine Aroma and Its Intended Use for Wine Quality Improvement, Molecules 22 (2017) 189. https://doi.org/10.3390/molecules22020189.

[168] S. Krysenko, W. Wohlleben, Polyamine and Ethanolamine Metabolism in Bacteria as an Important Component of Nitrogen Assimilation for Survival and Pathogenicity, Medical Sciences 10 (2022) 40. https://doi.org/10.3390/medsci10030040.

[169] C. Shaw, M. Hess, B.C. Weimer, Microbial-Derived Tryptophan Metabolites and Their Role in Neurological Disease: Anthranilic Acid and Anthranilic Acid Derivatives, Microorganisms 11 (2023) 1825. https://doi.org/10.3390/microorganisms11071825.

[170] K. Sasikumar, S. Hannibal, V.F. Wendisch, K.M. Nampoothiri, Production of Biopolyamide Precursors 5-Amino Valeric Acid and Putrescine From Rice Straw Hydrolysate by Engineered *Corynebacterium glutamicum*, Front Bioeng Biotechnol 9 (2021). https://doi.org/10.3389/fbioe.2021.635509.

## List of publications

**F.J.N. Putra**, P. Kahar, A. Kondo, C. Ogino, Valorization of Lignin and Its Derivatives Using Yeast, Processes 10 (2022) 2004, Review article, (Published).

**F.J.N. Putra**, P. Kahar, A. Kondo, C. Ogino, Advanced lignin valorization for biorefinery application, Advanced Lignin Technologies, Intech Open, London, UK (2024), Book chapter, (Published).

**F.J.N. Putra**, P. Kahar, A. Kondo, C. Ogino, The bioconversion of lignin derivative aldehydes into high-value aromatic alcohols and lipids via *Lipomyces starkeyi*, Biochemical Engineering Journal 200 (2023), Research article, (Published).

**F.J.N. Putra**, P. Kahar, A. Kondo, C. Ogino, Production of lignin monomeric alcohols and lipids from oil palm empty fruit bunch by a combination of alkaline nitrobenzene depolymerization and *Lipomyces starkeyi* bioconversion, Biochemical Engineering Journal 208 (2024), Research article, (Published).

**F.J.N. Putra**, P. Kahar, A. Kondo, C. Ogino, Adaptive laboratory evolution of *Lipomyces starkeyi* for high production of lignin derivative alcohols and lipids with comparative untargeted metabolomics-based analysis, Research article, (Manuscript submitted).

## Supplementary information

Primer list for qPCR of *Lipomyces starkeyi* NBRC 10381 (Chapter 2)

| No. | Genes | Forwards (F), 5`→3` | Reverse (R), 5`→3` |
|---|---|---|---|
| 1 | TUB1 | CTACGGCAAGAAGTCCAAGTT | GCGTGCTCCAATGTAGTATGA |
| 2 | ADH | ACGAGCGAGAATGGATGG | TGAGACTTGCCTGATTGAACA |
| 3 | ALDH | CGGACTGGAAGGCTATCG | CCTCGTGTTGTATGCTATTGGA |
| 4 | AKR | GCAGTATCCAAGTGACGGTATC | TGGCAATGGCTCAAGAAGG |

TUB1: Alpha-tubulin, ADH: Alcohol dehydrogenase, ALDH: Aldehyde dehydrogenase, AKR: Aldehyde-ketone reductase